THE
PHYSICAL REVIEW
A Journal of Experimental and Theoretical Physics
VOL. 44, No. 5 SEPTEMBER 1, 1933 SECOND SERIES

An Effect of Positive Space Charge in Collector Analysis of Discharges

R. H. SLOANE, *Queen's University, Belfast*
AND
K. G. EMELEUS, *University of Michigan*
(Received March 23, 1933)

By use of a collector with mutually insulated sections to which different potentials could be applied, it has been shown, with a low voltage arc in argon, that under the special conditions of short collector and small electron concentration the positive ion sheath which forms on insulating surfaces near a collector in a plasma may lead to serious misinterpretation of the characteristics of the collector. The effect is twofold, first, a general diminution in the apparent concentration of electrons in the plasma, and, second, an apparent preferential suppression of the slowest electrons. Under most working conditions, these are probably inconsiderable at low pressure but perhaps important at a pressure of a few mm and higher. The collector characteristics obtained have been analyzed for Maxwellian distributions and by a method in which no initial assumption is made concerning the energy distribution other than that it is isotropic. A formula is given to facilitate double differentiation in the latter case.

SEELIGER and Hirchert[1] have found that the results obtained with collectors in positive columns at a pressure of a few mm depend on the length of collector used. In particular, a collector characteristic which can be taken to reveal the presence of two Maxwellian groups of electrons and is obtained with fairly long collectors may degenerate with short collectors into the simple form indicating the presence of one group only. It was thought desirable to investigate this effect at lower pressures and to see if it could be accounted for through action of the positive ion sheath which forms on the glass near the collector, since it has been shown that considerable modification of the usual characteristic is produced if part of a collector is exposed to a positive space charge.[2] With this aim a collector, in a low-voltage arc in argon, has been designed which permitted variations of a nearby positive ion sheath with or without change in length of the collector. It has been found that at low pressures distortion of the characteristic through positive ions congregating on insulated surfaces is usually small but that it may be serious with an abnormally short collector.

DETAILS OF EXPERIMENTS

The collector is shown in Fig. 1. A molybdenum wire *A* (0.11 mm diameter) was arranged so that the length projecting beyond the end of a copper shield could be adjusted by moving an iron slug with a magnet. A glass shield *B* insulated the

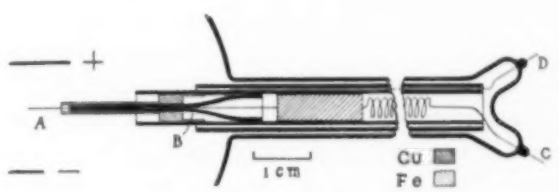

FIG. 1. Double collector.

[1] Seeliger and Hirchert, Ann. d. Physik **11**, 817 (1931).
[2] Emeleus and Sloane, Phil. Mag. **14**, 355 (1932).

Mo collector from the Cu. The latter could be held at any desired potential by the connecting wire *D*, which passed out as shown between two coaxial Pyrex tubes. Contact was made with the Mo through the iron by the lead *C*. *B* was slightly tapered so that it did not come into contact with the Cu at the exposed end of the latter. The insulation resistance between *C* and *D* was better than 6×10^{11} ohms. The collector was mounted in a low voltage arc tube about halfway between an oxide coated platinum filament cathode (−) and a nickel disk anode (+) (2 cm in diameter, 1.8 cm from the cathode). The tip of the Cu extended a little under the anode. It was found immaterial whether the argon contained 0.5 percent nitrogen or not. The circuits employed were of the usual type for collector analysis of discharges.

The problem can be approached in two ways. (a) The length of Mo projecting from the Cu can be kept constant and the characteristic curve of the former taken for several potentials of the latter; in this method the extent of the positive ion sheath on the Cu is varied. (b) The Cu can be held at a fixed potential and characteristics taken with various lengths of Mo projecting; the Mo then passes to a varying extent through an almost fixed positive ion sheath on the Cu.

In analyzing the characteristics the positive ions have first to be taken into account at small negative potentials. This has been done by making a large scale plot of either the current or the square of the current, to the Mo as a function of voltage, from about −70 to −25 volts. One or other of these plots has invariably been nearly straight and it has been assumed that the extrapolation of this straight line to smaller negative voltages gives the contribution of positive ions to the current there. The electron currents can then be obtained from the differences between this and the total observed current at any potential. In a few cases the positive ion line, when so extrapolated, gave an electron current at the space-potential; this usually occurred only when the Mo was short, with a considerable negative potential on the Cu. The resulting semi-logarithmic electron plots, a good example of which appears in Fig. 3, I*a*, can be analyzed in two ways. In the first, the fall of the plot for the highest negative voltages is ignored and the more negative straight part of the remainder taken to be due to a fast Maxwellian group. From the extrapolation of this straight portion to low negative voltages a difference curve is constructed (I*b*) which is taken to represent a slow Maxwellian group. Electron temperatures and concentrations are calculated from the two straight lines.[3] In the second way, no assumption is made about the electron velocity distribution in the plasma other than that it is isotropic.[4] The distribution is deduced from the second differential coefficient of the electron current *vs.* voltage curve for the same retarding potentials for electrons as before.

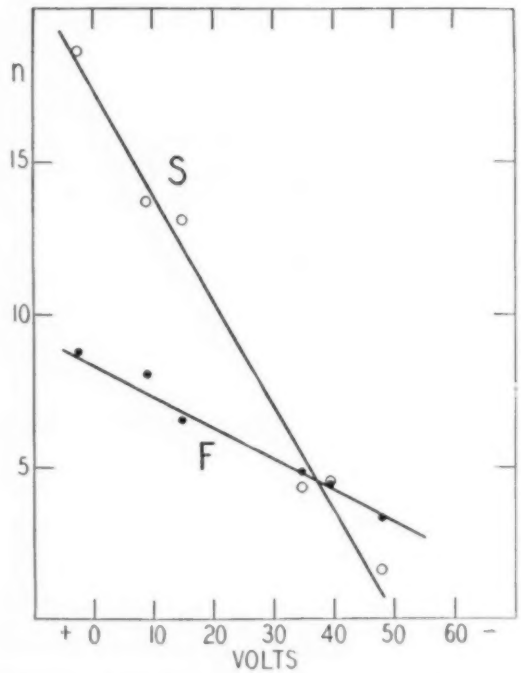

FIG. 2. Electron concentration *vs.* potential of copper (Table I).

RESULTS OF EXPERIMENTS

1. Temperature analysis

Table I shows a set of results obtained by method (a). Discharge conditions were: projecting length of Mo 1 mm, tube voltage about 30, tube current 35 milliamp., argon pressure 0.09 mm Hg. Concentrations have been calculated as if the whole length of Mo projecting were effective. It is difficult to obtain more consistent

[3] Langmuir and Mott-Smith, Gen. Elec. Rev. **27**, 449 ff. (1924).

[4] Electron reflection is however neglected.

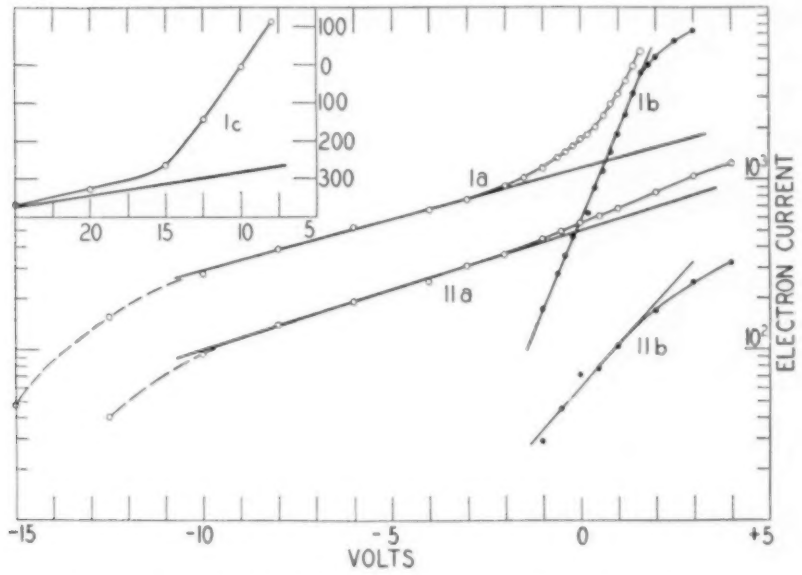

FIG. 3. Part of original characteristic and semi-logarithmic plots.

values for the electron temperatures without more elaborate precautions than the present investigation warranted.[1] Fig. 2 is a plot of the concentration data of Table I. In 1 the Mo ap-

TABLE I. *Results obtained by method (a).*

Run	Potential of Cu relative to anode (volts)	*Fast Group* Temperature (volts)	*Fast Group* Concentration per cc	*Slow Group* Temperature (volts)	*Slow Group* Concentration per cc
1	−48	9.6	$3.35\ 10^9$	0.91	$1.66\ 10^9$
2	−39	9.9	4.43	0.78	4.53
3	−35	11.5	4.87	0.84	4.33
4	−15	11.6	6.55	1.13	13.1
5	− 9	10.5	8.04	0.88	13.7
6	2.5	9.5	8.78	0.92	18.6

peared entirely covered by the positive ion sheath on the Cu, and in 2 was just projecting. The Cu was at its floating potential in 5. The apparent concentration of the slow group *S* falls off much more rapidly with increase in the negative potential applied to the Cu and hence with increase in the region occupied by the positive ion sheath on the latter, than does that of the fast group *F*, a result confirmed by other runs and in this example deliberately exaggerated by use of a short projecting length of Mo.

Two examples from another set, one showing the slow group on the point of complete suppression, are shown in Fig. 3. I*a* and I*b* represent data obtained with the Cu connected to anode, I*b* giving the slow group and space-potential. II*a* shows the effect of applying −60 volts to the Cu relative to the anode. An attempt has been made to analyze the low voltage rise in II*a* for a slow group, II*b*.

The results of method (b) need not be presented since they confirm those obtained by method (a).

2. Differential analysis

By modifying slightly a result due to Druyvesteyn,[5] the energy distribution ($N_v dV$) for electrons in unit volume of the plasma can be obtained from the current-voltage characteristic of the collector for electrons received in a retarding field, from the relation

$$N_v = K V^{\frac{1}{2}} (d^2 i / d V_s^2),$$

where V_s is the potential of the collector, V the difference between the space potential and that of the collector and K a constant, involving numerical and atomic constants, which is of no interest here except that it is inversely proportional to the area of the collector. Double differentiation of slightly erratic experimental data presents difficulty. In the present case the opera-

[5] Druyvesteyn, Zeits. f. Physik **64**, 781 (1930).

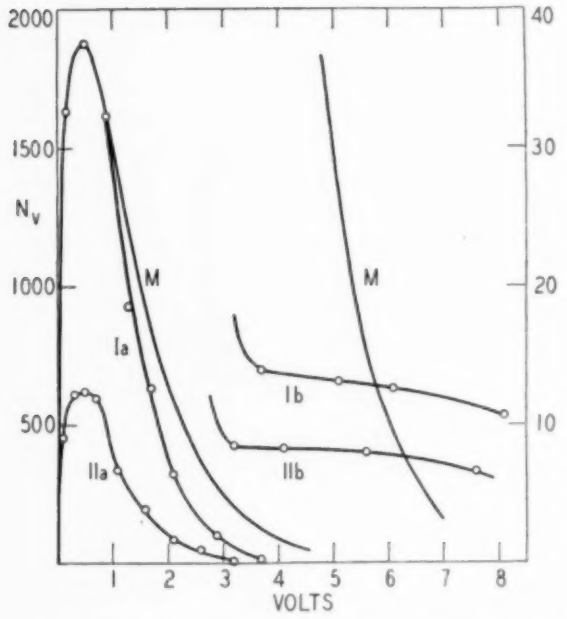

FIG. 4. Electron energy distributions compared with Maxwellian distribution.

tion is simplified by the fact that considerable stretches of the characteristic are straight in a semi-log plot. From the identity

$$y^{-1}(d^2y/dx^2) = (d \ln y/dx)^2 + d^2 \ln y/dx^2.$$

N_v is then readily evaluated, since the second term on the right vanishes. Even when the second term does not vanish determination of the second differential is often facilitated and it has been used except for the rapidly falling semi-log curve for the highest negative voltages.

Some results are shown in Figs. 4 and 5. In Fig. 4, I and II give the distributions for runs 5 and 2 of Table I. The characteristics were generally similar to those of Fig. 3. The ordinates are in the same arbitrary units for I and II. The low voltage Maxwellian groups of the temperature analysis correspond roughly to I*a* and II*a*, and the high voltage groups to the large scale sections I*b* and II*b*. These results again show an apparent preferential suppression of low speed electrons produced by surrounding part of the Mo with a positive ion sheath on the Cu. Curve *M* in Fig. 4 is the Maxwellian distribution corresponding to the linear portion of the original semi-logarithmic plot I*a* near the space potential. The right-hand part of *M* is on the larger scale of I*b* and II*b*. As pointed out by Druyvesteyn in a similar case,[5] there is a deficiency of medium speed electrons, relative to *M*.

The electron currents for high retarding potentials cannot now be ignored. Fig. 5 shows the complete distribution curve derived from the data used for curve I*a*, Fig. 3, Curve I*c* being a portion of the original current voltage characteristic, which was closely linear for larger negative potentials and extrapolates as shown. Compared with the Maxwellian curves a new high voltage peak in N_v appears, although accurate determination of its position and height is difficult. This peak might be due to electrons, accelerated through the cathode fall in potential, which have made a single resonance collision with argon atoms. The electron energies are of the right order for this explanation to be tenable but the exact fall in potential across the tube was not measured. Presence of such groups is important in the interpretation of the spectrum of the discharge.

Discussion of Results

From both methods of analysis the effect of application of increasing negative potentials to

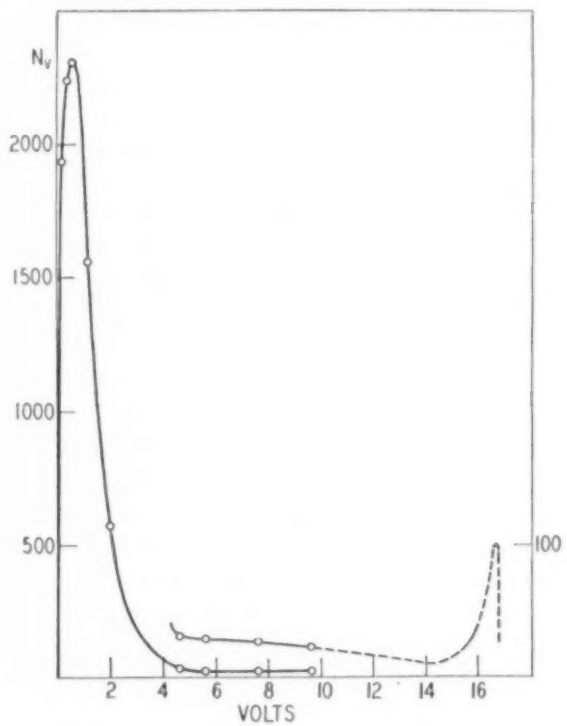

FIG. 5. Electron energy distribution with high voltage peak.

the Cu, with increase in the size of the positive ion sheath on it, is to cause a greater apparent decrease in the slower electrons in the plasma than of the faster. In other words, the effective length of the Mo decreases more rapidly for the slow electrons than for the fast.

A full theory of the effect is impracticable on account of the necessarily complicated conditions of collector geometry and space-charge. An approximate account may be given as follows. Suppose the plasma contains two full Maxwellian groups, with temperatures T_1, T_2, random currents I_1, I_2. To a rough approximation the Mo may be considered to be in two sections. That more remote from the copper will receive electrons when negative to the plasma through a region of positive space-charge in which the potential varies monotonically between that of the plasma and that of the Mo. For this, conditions for the original theory of Langmuir[3] obtain and the currents received at the Mo will be

$$lpI_1 \exp(-eV_{Mo}/kT_1)$$

and

$$lpI_2 \exp(-eV_{Mo}/kT_2),$$

where l is the length of this section of the Mo, p the perimeter of the Mo, and zero and V_{Mo} the potentials of the plasma and Mo. The other section of Mo, nearer the Cu, will receive electrons through a positive space-charge region in which they pass through a potential minimum V_{min} lower than V_{Mo}. The magnitude of V_{min} will increase from the end of the first region—absent for sufficient negative potential on the Cu—towards the inner end of the Mo at the Cu base. Between this minimum and the Mo the concentration of the electrons will not be governed by the Boltzmann relation on account of the drain of electrons to the Mo from it in the local accelerating field but the flux of electrons to the Mo is more nearly determined by the electrons reaching the potential minimum from the plasma, and the two components are nearer

$$pI_1 \int \exp(-eV_{min}/kT_1)dl$$

and

$$pI_2 \int \exp(-eV_{min}/kT_2)dl$$

along this inner section of Mo. On account of the entry of the electron temperatures through the exponential there will thus be an excess reception of the fast electrons relative to the slow compared with what would have been received had there been no potential minimum. Similar reasoning is applicable to the Druyvesteyn distributions. The approximate linearity of the lines in Fig. 2 must be regarded as fortuitous, although the sense of the changes is that predicted and the approximate constancy of the electron temperatures in the table may be regarded as in part due to the insensitiveness of the semi-log method of analysis.

The arc tube used did not function well for the higher pressures used by Seeliger and Hirchert.[1] It is believed, however, for two reasons, that the effect studied now at low pressures may have been important in their tubes. The first is that with increase in pressure the ionization in the positive column becomes more concentrated towards the axis of a tube; it is thus likely that the ionization near the wall would be small, and the wall sheaths thick. The second is the observation made in the course of the present work that the sheaths which formed on the floating Cu at the higher pressures could be seen to be abnormally thick, which, whether due to an effect of collisions in the sheath, or to the first effect, would tend to lead to conditions similar to those which we have studied.

Our thanks are due to Professor W. B. Morton for the facilities provided for this work and to Professor O. S. Duffendack for discussion of it.

A Test of the Classical "Momentum Transfer" Theory of Accommodation Coefficients of Ions at Cathodes

K. T. COMPTON AND E. S. LAMAR, *George Eastman Research Laboratories, Massachusetts Institute of Technology*

(Received July 7, 1933)

On the classical theory of momentum transfer at impact of a moving particle with a stationary particle, one of us suggested that the accommodation coefficient for positive gas ions striking a metal cathode should be less than unity only if the mass of the metal atom exceeds that of the gas ion. To test this hypothesis, momentum experiments of the type already reported for helium ions striking a molybdenum cathode have been continued for argon ions striking molybdenum and aluminum, respectively. The transfer of momentum was measured by the deflection of a delicate pendulum, whose bob consisted of the metal cathode under investigation, the surrounding argon atmosphere being strongly ionized by a discharge between supplementary electrons. The experimental data made possible the computation of the accommodation coefficient for the positive ions and also the fraction of the current carried by electrons at the cathode. The accommodation coefficient for argon ions on molybdenum was 0.8, in good agreement with the value obtained by Compton and Van Voorhis by thermal measurements, while for argon ions on aluminum the accommodation coefficient was unity, in accordance with the above prediction. The classical theory would be expected to hold in such cases where the energy of the impinging particle greatly exceeds the thermal energy of the cathode. Three cases are analyzed: first, impact by large ions which do not penetrate into the cathode; second, impact by smaller ions which may penetrate only a few layers into the cathode; and third, impact of very small high speed ions which may penetrate many layers of atoms in the cathode. The experimental values of accommodation coefficients are shown to conform sufficiently closely to the predictions of this analysis to indicate that the phenomena of loss of energy and momentum are at least approximately described by the postulates of this analysis.

INTRODUCTION

IN a recent paper by one of us[1] experiments were reported which measured the momentum transferred to a molybdenum cathode by impinging helium positive ions of known speed. These experiments, although subject to some uncertainties as a result of the many complicating factors in the electric arc, gave a measure of the accommodation coefficient for the ions at the cathode. In a paper[2] presented before the National Academy of Sciences and following the arguments of Baule,[3] reasons were given for expecting that the accommodation coefficient should be less than unity only if the mass of the metal atom composing the cathode exceeds that of the ion. It seemed of interest, therefore, to repeat the experiments referred to above for two different cathode metals, one of greater and the other of less atomic weight than the ions. The present paper is a report of these experiments for argon ions at cathodes of molybdenum and of aluminum.

APPARATUS AND EXPERIMENTAL PROCEDURE

Since a detailed description of the apparatus and experimental procedure has been given in an earlier paper,[1] a brief description only will be given here. A low voltage arc between a hot cathode and an anode was maintained in argon gas at pressures ranging between 0.004 and 0.02 mm. In the ionized atmosphere thus created was suspended the auxiliary cathode C to be studied, which was the bob of a glass pendulum whose deflection gave a measure of the force acting on the cathode. The deflection was measured by observing on a scale the position of the image of a cross-hair, the light beam having been reflected from a mirror attached to the pendulum.

The experimental procedure consisted in taking first a blank run, by way of correction for possible complicating effects, as described in the previous paper.[1] Then, with constant arc current, the deflections resulting from a change in voltage

[1] Lamar, Phys. Rev. **43**, 169 (1933).
[2] Compton, Proc. Nat. Acad. Sci. **18**, 705 (1932).
[3] Baule, Ann. de Physique **44**, 145 (1914).

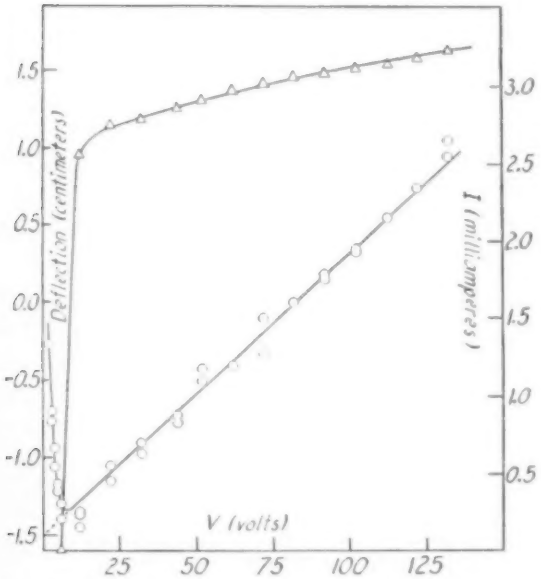

FIG. 1. Pressure per unit measured current and measured current *vs.* negative potential of the auxiliary cathode with respect to the surrounding space (argon ions on molybdenum).

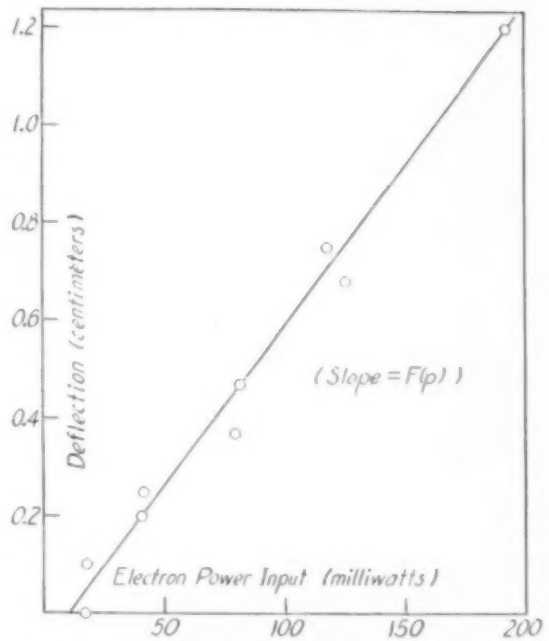

FIG. 2. Pressure resulting from electron bombardment as a function of electron power input (argon ions on molybdenum).

of the auxiliary cathode were measured. A typical set of observations is shown in Fig. 1 in which the deflection in centimeters is plotted against the negative voltage of the auxiliary cathode with respect to the surrounding space. The measured currents to the auxiliary cathode are shown on the same diagram. As the auxiliary cathode voltage is made less and less negative, a sudden change is seen to occur in both curves. This occurs when the potential of the auxiliary cathode approaches the potential of the surrounding space. The current curve indicates a large increase in electron current reaching the cathode and the deflection curve shows a correspondingly large increase in pressure on the cathode. This increase in pressure is evidently a radiometric pressure resulting from heating of the cathode by electron bombardment.

Fig. 2 shows a plot of the deflections resulting from electron bombardment *vs.* the electron power input. The slope of this curve $F(p)$ gives the radiometric pressure per unit power input when the gas pressure has the value p.

Figs. 3 and 4 show the deflections per unit measured current (positive ion current plus current of outgoing secondary electrons) *vs.* $F(p)$ for molybdenum and aluminum as determined from a series of curves of the type of Fig. 1 taken at different gas pressures.

CALCULATIONS AND DISCUSSION OF RESULTS

The pressure on the cathode resulting from ion bombardment is expressible in two terms, designated by P_1 and P_2, P_1 being an equal opposite momentum to that retained by the ions after neutralization and P_2, a radiometric pressure resulting from heating of the cathode by ion bombardment. Therefore

$$P/I = P_1/I + P_2/I$$
$$= (1-f)[C\{(1-\alpha)V\}^{\frac{1}{2}} + F(p)\alpha(V+\varphi_+)] \quad (1)$$

where f is the fraction of the current at the auxiliary cathode carried by electrons; C is a constant involving a number of known physical constants and the sensitivity of the pendulum; V is the kinetic energy, in electron-volts, of the incoming positive ions; $F(p)$ is the radiometric pressure per unit power input; α is the accommodation coefficient, and φ_+ is the work function of the cathode for positive ions. φ_+ is included in P_2 but not in P_1 since it is improbable that any energy of excitation would appear as kinetic energy of the neutralized ions.

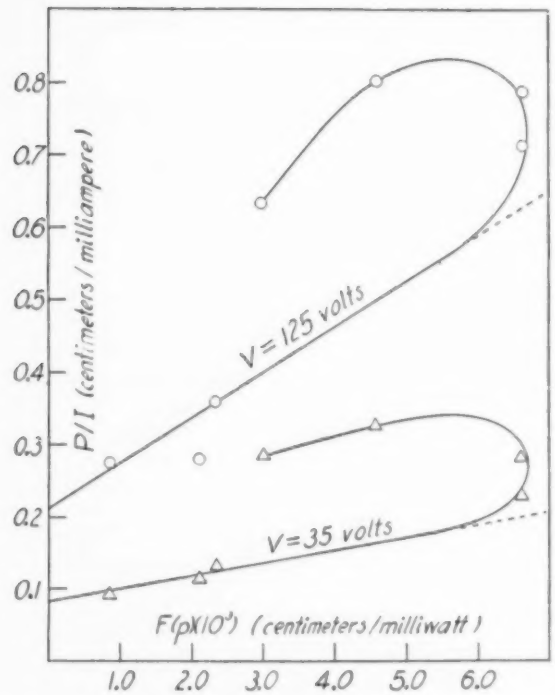

FIG. 3. Pressure per unit measured current resulting from ion bombardment *vs.* $F(p)$, the radiometric pressure per unit power input (argon ions on molybdenum).

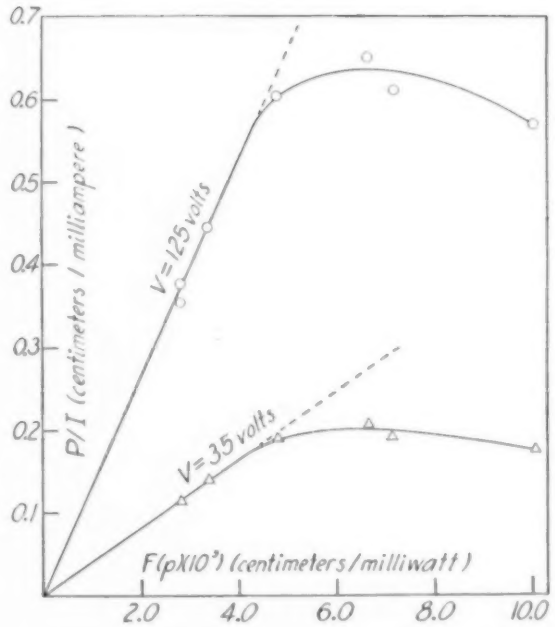

FIG. 4. Pressure per unit measured current resulting from ion bombardment *vs.* $F(p)$, the radiometric pressure per unit power input (argon ions on aluminum).

If P/I and $F(p)$ were the only variables in Eq. (1), plots of Eq. (1) under different conditions (as shown in Figs. 3 and 4) should be straight lines from the slopes and intercepts of which values of α and of f could be obtained. Since $F(p)$ has a maximum when plotted against gas pressure, there should be two sets of points on each curve, one for data obtained below and the other for data above the maximum. The rather sharp departure of these curves from linearity is believed to be due to the formation of an adsorbed layer of gas (probably argon) on the surface of the cathode. Since such a gas layer changes the nature of the surface, it may change any quantity in Eq. (1) whose value depends upon the nature of the surface. It is therefore difficult to predict the direction of deviation from linearity of the curves of Figs. 3 and 4 and it is not surprising that they should be different for the two metals investigated.

The linear portions shown in Figs. 3 and 4 were taken at low pressures where it is most justifiable to assume that the surface of the metal under investigation was free from adsorbed gas layers. Calculations of α and of f were made from the slopes and intercepts of these curves and the basis of two limiting values of φ_+, namely, 0 and $V_i-\varphi_-$ where V_i is the ionization potential of the gas and φ_- is the work function of the cathode for electrons.* The values are given in Table I. The assumption of $\varphi_+=0$ led to impossible values of f in the case of aluminum.

TABLE I.

V = negative potential of cathode with respect to space; α = accommodation coefficient; f = fraction of current carried by electrons; φ_+ = work function of cathode for positive ions; V_i = ionization potential of the gas; φ_- = work function of cathode for electrons.

	α		f	
V	$\varphi_+=0$	$\varphi_+=V_i-\varphi_-$	$\varphi_+=0$	$\varphi_+=V_i-\varphi_-$
Argon ions on molybdenum				
35	0.90	0.84	0.42	0.43
125	.83	.81	.40	.43
Argon ions on aluminum				
35	1.0	1.0	—	.031
125	1.0	1.0	—	.034

* These limiting values are set by the energy principle. If all of the energy available from the process of neutralization of a positive ion is retained by the cathode, then

Theoretical Interpretation and Conclusions

(1) Case of ions which do not penetrate the surface layer of atoms on the cathode (large and slow moving ions)

In the paper mentioned above,[2] by treating the case of single impact between elastic sphere atoms from a classical point of view, the following expression for the accommodation coefficient was given, $\alpha = 2MM_s/(M+M_s)^2$ subject to $M_s > M$, where M is the mass of the impinging ion and M_s that of the metallic atom struck. In the actual case of an ion striking a metal surface it is believed that α should be more nearly double this value as will be seen from the following argument.

In the first place, this expression with the factor 2 was derived for the impact of molecules moving under thermal motion and consequently incident at all possible angles to the surface. In dealing with ions, however, drawn in through a space charge sheath by an applied field, the ions all strike the surface perpendicularly. If they all rebound perpendicularly from head-on collisions with surface atoms, the accommodation coefficient would be

$$\alpha = 4MM_s/(M+M_s)^2, \quad M_s > M$$

$$\alpha = 1.0, \quad M_s < M.$$

Actually, however, the neutralized ion may rebound at any angle between 0 and 90° with the normal to the surface. If it rebounds at an angle near 90°, it will collide a second time with a neighboring atom of the surface layer and it leaves the surface after having made two collisions, each of them involving some loss in kinetic energy through transfer of momentum. If it strikes a surface atom more nearly head-on, it will rebound at some small angle with the normal to the surface and will strike only one atom. What we measure experimentally is, of course, a weighted mean of these possibilities.

Considering first the case of a single impact with rebound between 0 and 90° with the normal, Compton and Langmuir[4] have shown that the fraction of the kinetic energy of an impinging spherical particle which is transferred on a collision specified by the angle θ is

$$f_\theta = 4MM_s/(M+M_s)^2 \cos^2\theta,$$

where θ is the angle made by the original trajectory of the impinging particle and the radius vector from the center of the particle struck to the point of impact. The following relationship holds between θ and φ.

$$M[\sin(\varphi-\theta)\sin(\varphi+\theta)+\sin^2\theta] = M_s[\sin^2(\varphi-\theta)-\sin^2\theta]$$

where φ is the angle made by the original and final trajectories of the impinging particle.

On substituting the masses of argon and molybdenum atoms, respectively, for M and M_s, it is found that the rebound at $\varphi = 90°$ is given when $\theta = 32°\,42'$. Multiplying f_θ by the probability of a collision specified by θ, integrating between the limits imposed by the condition $\varphi \leqslant \pi/2$, and substituting the values of M_s and M, we have,

$$\alpha = \frac{4MM_s}{(M+M_s)^2} \frac{\int_0^{32°\,42'} 2\pi \sin\theta\cos^3\theta d\theta}{\int_0^{32°\,42'} 2\pi \sin\theta\cos\theta d\theta} \qquad (2)$$

$$= 0.830 \times 0.854 = 0.709.$$

We see, therefore, that the accommodation coefficient would be 0.830 if all collisions of ions were of the "head-on" type with metal atoms but would be 0.709 if all angles of rebound between 0 and 90° are considered as the result of *single* collisions only.

As has been pointed out above, however, those collisions which are relatively far from the "head-on" type involve another collision with a second surface atom. The effect of the second collisions is to increase the total energy loss and bring the accommodation coefficient nearer to

$\varphi_+ = V_i - \varphi_-$. If, however, all of this energy leaves the cathode as radiation and/or as excitation energy of the departing neutralized ion, then $\varphi_+ = 0$. There is some evidence that the true intermediate value may depend somewhat on angle of incidence. It must also depend on the extent to which this residual energy is adequate for an excited or metastable state. In all measurements which have been made of accommodation coefficient the value calculated from $\varphi_+ = V_i - \varphi_-$ gives somewhat the more consistent results.

[4] Compton and Langmuir, Rev. Mod. Phys. **2**, 210 (1930).

unity. It is easily shown, for example, that the average case of a double collision, namely, a first deflection at 90° and a second deflection back again perpendicularly to the surface, involves a total loss of energy by the impinging particle which is almost exactly the same as that which would have occurred by a single head-on collision. Thus we see that the actual accommodation coefficient is the weighted mean of one group which have collided nearly head-on and which contribute to the accommodation coefficient values between 0.830 and some lower value intermediate between 0.83 and 0.709, and a second group which have collided twice with a net contribution of about 0.830. Consequently, it is evident that the actual value of the accommodation coefficient should be much closer to 0.830 than to 0.709 and to a close approximation the value 0.830 for head-on collisions may be taken to represent the predictions of the theory.

(The further refinement of these considerations depends upon more accurate knowledge than we now have of the relation of the effective sizes of the atoms and ions and the spacing between atoms in the surface layer of the cathode.)

The experimental values of this accommodation coefficient are reported by Compton and Van Voorhis[5] as 0.75 and are found in the present investigation to be very close to 0.83. Consequently the results are in excellent agreement with the theoretical expectations.

(2) Case of slight penetration of impinging ions into cathode (small ions at moderate speeds or moderate sized ions at high speed)

In these cases the spacing between atoms of the metal may roughly be considered as greater than the diameter of the impinging ion, so that there will be a certain probability that the ion will collide in any particular layer. If α_0 is the fraction of the energy of an impinging particle which is transferred at a single collision, it is easily shown that

$$\alpha=\alpha_0\sum_{n=1}^{\infty}(1-\alpha_0)^{n-1}P_n,$$

where P_n is the probability that an impinging particle will make n collisions before its escape from the metal.

The collision probabilities in this equation can be calculated roughly if one resorts to what amounts to a crude system of averaging. Let us assume that in any layer of the metal lattice an impinging particle either makes a head-on collision with an atom of the lattice, or passes through the layer without having suffered any collision at all. If the metal is considered as of infinite thickness, obviously each impinging particle will eventually suffer one collision and therefore $P_1=1$. After the first collision the impinging particle reverses its direction and may escape from the metal without a second collision. Let σ be the probability of collision in a particular layer. The probability that an impinging particle will collide first in the ath layer and second in the bth $(b<a)$ is obviously

$$P_{ab}=\sigma^2(1-\sigma)^{a-1}(1-\sigma)^{a-b-1};$$

$$\therefore\qquad P_2=\sigma^2\sum_{a=2}^{\infty}\sum_{b=1}^{a-1}(1-\sigma)^{a-1}(1-\sigma)^{b-1}$$

or changing variable

$$P_2=\sigma^2\sum_{p=1}^{\infty}\sum_{q=0}^{p-1}(1-\sigma)^p(1-\sigma)^q.$$

The summations can be carried out as a system of geometric progressions yielding

$$P_2=(1-\sigma)/(2-\sigma)$$

as the probability of two collisions within the metal.

Since after an even numbered collision the impinging particle is travelling back into the body of the metal and will thus make another collision, the probability of any odd numbered collision is equal to that of the preceding even numbered collisions.

$$P_3=P_2,\quad P_5=P_4,\quad \text{etc.}$$

In a similar way to that described above, the probability of four collisions can be written down as

$$P_4=\sigma^4\sum_{a=2}^{\infty}\sum_{b=1}^{a-1}\sum_{c=b+1}^{\infty}\sum_{d=1}^{c-1}(1-\sigma)^{a-1}\times(1-\sigma)^{a-b-1}(1-\sigma)^{c-b-1}(1-\sigma)^{c-d-1}$$

[5] C. C. Van Voorhis and K. T. Compton, Phys. Rev. **35**, 1438 (1930); Phys. Rev. **37**, 1596 (1931).

or, changing variables

$$P_4=\sigma^4\sum_{p=1}^{\infty}\sum_{q=0}^{p-1}\sum_{r=0}^{\infty}\sum_{s=0}^{r+p-q-1}\times(1-\sigma)^p(1-\sigma)^q(1-\sigma)^r(1-\sigma)^s.$$

This expression can be reduced since each step in the reduction involves a known summation. The final result is

$$P_4=(1-\sigma)/(2-\sigma)\{1-(1-\sigma)^3/(2-\sigma)^2\}.$$

The calculation of these collision probabilities becomes increasingly laborious for each successive collision and in the present paper the calculations have not been carried beyond five collisions. Substitution of these in the expression for α yields

$$\alpha=\alpha_0[1+(1-\alpha_0)(2-\alpha_0)\{(1-\sigma)/(2-\sigma)\}\times\{\alpha_0(2-\alpha_0)-(1-\alpha_0)^2(1-\sigma)^3/(2-\sigma)^2\}]+\cdots.$$

The experimental value of α given by Compton and Van Voorhis[5] for neon ions on molybdenum is 0.65. This is greater than the value of α (slightly less than 0.57) to be expected from a single collision by Eq. (2), which fact indicates some possible penetration of the ions beyond the first layer of atoms of the metal, i.e., multiple collisions. The above expression for α gives good agreement with the experimental value if we assume that $\sigma=0.64$. This is equivalent to saying that the process is equivalent to head-on collisions by 64 percent of the incoming ions in the first layer of the metal; the remaining 36 percent go on to the second layer where 64 percent of them collide, and so on.

Attempts to apply the above theory to the case of helium ions on molybdenum have been unsuccessful probably for the reason that there may be so much penetration of the ions into the metal that five collisions are by no means sufficient to account for the energy transferred. That this penetration does occur was proven by experiments of Langmuir and his colleagues, who showed that metal cathodes will absorb relatively large quantities of helium incident in the form of bombarding ions and that this helium may subsequently be driven out by heating the cathode. The amounts of helium thus absorbed may be equivalent to many layers deep of atoms over the surface, which indicates that the ions may penetrate considerable distances. Under these circumstances the following argument appears to be a more satisfactory approximation than the one preceding.

(3) Case of ions which penetrate deeply into the cathode (helium or hydrogen ions at high speed)

If, as a first approximation, the ions are scattered like elastic spheres, there should be a high degree of randomness of motion after the first collision, approaching a completely random distribution if the mass of the ion is very small in comparison with that of the metal atoms. We will therefore assume a completely random direction of motion in the metal after the first collision. The probability that an ion will travel into the metal a distance x and collide in dx at x is

$$P_1=\mu_1 e^{-\mu_1 x}dx.$$

Then, after the first collision, the ions will be divided into two groups; those which are travelling toward the surface of the metal and those which are travelling toward the interior. Although an ion may on collision change from one of the above groups to the other, there should be an equal probability of a reverse change for one of the other group, so that, on the average, the grouping will remain unaltered. Those ions which travel into the metal will lose all of their energy before their ultimate escape. Those ions which travel out from the metal after the first collision will travel a distance greater than x in going the perpendicular distance x. The probability that an ion, which has made its first collision in dx at x, will make n collisions before escaping from the metal is

$$P_2=[(\mu_2 x)^n/n!]e^{-\mu_2 x},$$

where μ_2 is the reciprocal of the normal component of mean free path as the ion moves toward the surface.

If an ion retains a fraction f of its energy at a collision, then the total fraction of the initial energy of all the incoming ions which escapes from the metal with those ions which have made their first collision in the layer dx at x is

$$dF=c_1 f\mu_1 e^{-\mu_1 x}\sum_{n=1}^{\infty}f^n\frac{(\mu_2 x)^n}{n!}e^{-\mu_2 x}dx,$$

whence the fraction of all the energy of the incoming ions which escapes from the metal, is given by

$$F=c_1 f\mu_1 \sum_{n=1}^{\infty} \frac{f^n}{n!} \int_0^{\infty} (\mu_2 x)^n e^{-(\mu_1+\mu_2)x} dx$$

$$=\frac{c_1 f^2 \mu_1 \mu_2}{(\mu_1+\mu_2)(\mu_1+\mu_2-f\mu_2)}.$$

$$\therefore \quad \alpha=1-F=1-\frac{c_1 f^2 \mu_1 \mu_2}{(\mu_1+\mu_2)(\mu_1+\mu_2-f\mu_2)}.$$

The constant c is the grouping constant, i.e., the fraction of the ions which travel toward the surface of the metal after the first collision. If the scattering were completely random, c_1 would be $\frac{1}{2}$. (This would be accurate for the particles of infinitesimal weight colliding with elastic spheres but would be progressively less accurate as the mass of the ion approaches that of the metal atoms. It is, however, a fair assumption to make for the case of small penetrating particles like hydrogen or helium.)

With the same degree of approximation as leads to $c_1=\frac{1}{2}$, we may assume that the average particle moving toward the surface moves twice as far as if it escaped normally, so that we may take the ratio μ_2/μ_1 to be approximately 2. With these rough approximations and taking

$$f=1-2MM_s/(M+M_s)^2$$

we have for helium on molybdenum

$$\alpha=1-0.852\times 2/[2\times 3(3-1.845)]=0.754.$$

This value should be an upper limit to the accommodation coefficient and would be appropriate for very high speed ions, since the collision radius becomes small at very high velocities.

Actually we have a variety of values reported for helium. For helium atoms thermally incident on a clean tungsten surface, Roberts[6] gives a value 0.06, while Michaels[7] reports 0.17. Getting, in some unpublished work very recently performed in this laboratory, has checked closely the value given by Roberts. These values are in excellent agreement with the value 0.067 which would be calculated by the methods of Eq. 2 for the impact of nonpenetrating particles.

On the other hand, the accommodation coefficient of helium ions incident on molybdenum has been found to range between 0.35 and 0.55, with indication that the larger values are characteristic of ions of higher velocities (this is in accordance with the values of Van Voorhis and Compton[5] and also the values of Lamar,[1] where an indication of a reversed variation at higher velocities is probably attributable to the effect of collisions within the space charge sheath at the larger voltages).

We thus find in the case of helium, values of accommodation coefficient which are of the order of magnitude of those to be expected for nonpenetrating or penetrating conditions under just those circumstances in which it is known experimentally that the helium does not or does penetrate into the metal.

Just as in specific heats at high temperatures the classical picture of collisions appears to be adequate to explain momentum and energy transfers when high speed particles like ions strike a surface. For large ions there appears to be no appreciable penetration beyond the first layer of surface atoms but there is some evidence of scattering at various angles and double collisions at the rebound. For small ions like neon, and much more with helium, there is evidence of penetration into the cathode in the process of neutralization and rebound.

---

[6] Roberts, Proc. Roy. Soc. **A135**, 192 (1932).

[7] Michaels, Phys. Rev. **40**, 472 (1932).

A New Method for Determining the Thermionic Work Functions of Metals and Its Application to Nickel

GERALD W. FOX AND ROBERT M. BOWIE, *Physics Laboratory, Iowa State College*

(Received April 12, 1933)

A new procedure for determining thermionic work functions of metals has been developed. The metal sample is in the form of an approximate sphere and is heated by electron bombardment from an auxiliary filament which is disconnected when measurements are made. Electron emission from the cooling sample charges a condenser which, at predetermined times, is discharged through a ballistic galvanometer. Temperatures are determined by a Pt, Pt+10 percent Rh thermocouple spot-welded to the sample. The thermionic constants are obtained from the equation: $\log_{10}(T^2/SQ)=\log_{10}(2.3/aA)+\Phi/(1.988\times10^{-4}T)$ where Q is the quantity of charge yet to flow upon cooling the sample from a given temperature to absolute zero and $-S$ is the slope of the $\log Q$ *vs.* time curve. This equation is derived from Richardson's. The values of the thermionic constants obtained by applying this method to the case of thoroughly outgassed nickel are found to be $\Phi=5.03\pm0.05$ volts and $A=1.38\times10^3$ amp./cm^2 deg.^{2}.

INTRODUCTION

THE usual method for determining the thermionic constants of a metal depends upon heating the sample by passing an electric current through it. Generally, the specimen is in wire or strip form and, since a uniform temperature of the emitting surface is essential, it is necessary that the cross section of the sample be uniform at the start and remain so throughout the experiment. It is not possible to treat many substances by this method, due, in some instances, to their rapid evaporation during the outgassing process and, in others, to the fact that they cannot conveniently be made into a wire or strip form. The method here described eliminates these difficulties by using a sample in the form of an approximate sphere which is heated by electron bombardment from an auxiliary filament. The required data are obtained as the specimen cools. This necessitates measuring the charge accumulated over a period of time rather than measuring a current so that a modification of the Richardson equation must be made. The method has been applied so far to nickel.

EXPERIMENTAL

The tube and vacuum system

The tube, Fig. 1, was connected through two liquid air traps in series to a single stage Hg diffusion pump backed by a Cenco oil pump. A General Electric Pliotron FP-62, sealed to the tube, served to measure the pressure in the system. The complete high vacuum system was of Pyrex and 702p glasses with no waxed or greased joints. All the metal parts within the tube were of molybdenum, tungsten, or nickel, spot-welded together and previously outgassed by an induction furnace. The molybdenum collector surrounding the emitter was cylindrical in shape, open at the top but closed at the bottom except for a $\frac{1}{4}$ inch hole through which the auxiliary filament leads passed.

The nickel emitter

Before machining, the emitter was cast in a vacuum tungsten resistance furnace from electrolytic nickel obtained from the International Nickel Company. It was nearly spherical in shape and weighed approximately 15 grams. The 20 mil tungsten wire supporting the emitter and the wires to the thermocouple junction, spot-welded to the upper part of the emitter, were inclosed by fine quartz tubes to prevent contamination by evaporated nickel. The evaporated nickel coat deposited on the quartz prevented the quartz from emitting.

Outgassing

Before placing the sample in the tube of Fig. 1, it was heated by electron bombardment for a preliminary period of 1000 hours in another tube.

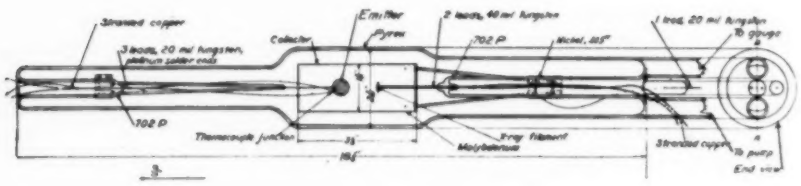

FIG. 1. Longitudinal section through and end view of thermionic emission tube.

Then it was mounted as described and its temperature maintained at 1375°K for 575 hours after which it was removed, measured, weighed, photographed, and replaced. No data used in determining the final values of the constants were taken until after a further period of heating at about 1440°K for 375 hours, followed by a 72-hour period, during which the temperature of the sample varied from 1500°K to 1650°K. After replacing the sample, the tube, ionization gauge and first air trap were baked for 10 hours at temperatures ranging from 415°C to 460°C. These glass parts had been baked previously for 53 hours.

Taking data

The method of heating and taking data can be explained by referring to the wiring diagram, Fig. 2. During the heating process, the switches

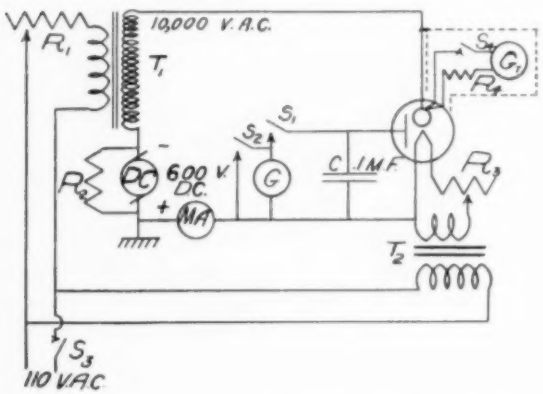

FIG. 2. Circuit diagram for thermionic emission tube.

S_1, S_2 and S_3 were closed. After maintaining the temperature of the emitter at some chosen value for five minutes, S_3 was opened simultaneously with the starting of a stopwatch. Opening this switch, shut off both the filament current and the high potential, thus allowing the voltage produced by d.c. to accelerate the thermoelectrons from the cooling emitter to the collecting cylinder. At the end of a predetermined time, S_1 was opened, thereby allowing the emission current to charge a condenser C which was discharged through the ballistic galvanometer G at the end of another time interval. This accumulation of charge and subsequent discharge was repeated several times until the nickel became too cold to emit appreciably. No charge data were taken during the first interval of about 30 seconds, to allow heat conduction to eliminate temperature gradients in the specimen. An empirical relation between time and temperature was determined in the form of a cooling curve.

Theoretical

If we denote by dq the quantity of charge emitted by the metal in a time dt, then

$$dq/dt = I = aAT^2 \exp(-\Phi e/kT) \qquad (1)$$

in which the current is given by Richardson's equation multiplied by the area of the emitter a. Although it is theoretically possible to determine various values of the current from the slopes taken at different points upon the q *vs.* t curve practically it is impossible to draw the required tangents with sufficient accuracy.

Here q is the quantity of charge which has been accumulated since the starting of the cooling process. If Q is defined as the quantity of charge yet to flow upon cooling the emitter from any variable, intermediate temperature to absolute zero, then $q+Q$ is a constant for any starting temperature and $dq = -dQ$. Also

$$dQ/dt = -aAT^2 \exp(-\Phi e/kT). \qquad (2)$$

A logarithmic curve, from which the slope may

be determined with sufficient accuracy, is obtained from (2) by dividing by $2.3Q$.

$$dQ/2.3Qdt = -(aAT^2/2.3Q)\exp(-\Phi e/kT)$$

$$d(\log_{10} Q)/dt = -S = \tag{3}$$

Here $-S$ is the slope of the $\log Q$ *vs.* t curve. This relation can be expressed in logarithmic form as follows:

$$\log_{10}(T^2/SQ) = \log_{10}(2.3/aA) + \Phi e/2.3kT = \log_{10}(2.3/aA) + \Phi/(1.988\times10^{-4}T). \tag{4}$$

A straight line should result from plotting $\log(T^2/SQ)$ against $1/T$, from the slope of which Φ can be determined.

The theoretical shape of the $\log Q$ *vs.* t curve can be derived from the integrated form of (2) and is given by

$$S = K\Phi eT^2/2.3k.$$

The constant K contains the thermal emissivity of the emitter and its heat capacity. As the percentage variation of T in the experimental range is not great the resulting curve is nearly straight. Although at first q appears to be the more logical quantity to use in the derivation of Eq. (4), intuition shows that the shape of the $\log q$ *vs.* t curve would eliminate this method. At the initial temperature q is zero; it rises rapidly at first as time increases and then asymptotically approaches a constant value. The $\log q$ *vs.* t curve would, therefore, start at $-\infty$, rise rapidly and then asymptotically approach a constant value while S would start at ∞ and go nearly to zero within the experimental range.

Results

Curves

In all, 48 sets of charge-time data were taken, of which 24 were used in computing the final values of the thermionic constants. These data were divided into three arbitrary groups depending upon when they were taken and each group was analyzed separately. The resulting curves from one set of data as required by Eq. (4) are shown in Figs. 3 and 4.

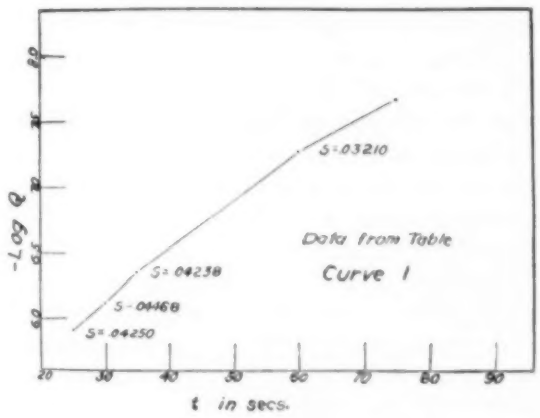

FIG. 3. Log Q *vs.* t curve for nickel.

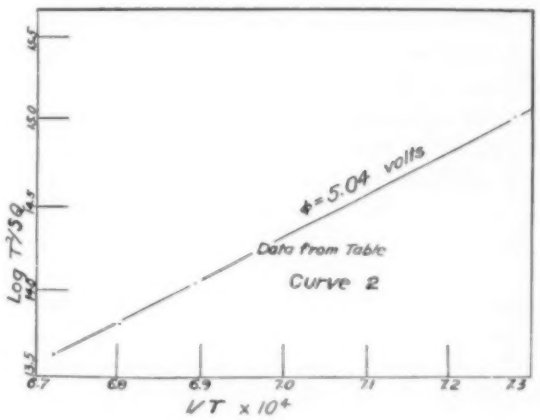

FIG. 4. Log T^2/SQ *vs.* $1/T$ curve for nickel.

Pressure in the tube

While the data used in computing the final values of the thermionic constants were being taken, the pressure as measured by the Pliotron FP-62 ranged from 1.7 to 2.9×10^{-6} mm of Hg. Upon allowing the emitter to cool nearly to room temperature, the pressure dropped to and remained at 1×10^{-7} mm of Hg as long as the emitter remained cold. It is interesting to note that the approximate vapor pressure of nickel as computed from the loss of 2.365 g during the last 475 hours of heating was about 2×10^{-8} mm of Hg, which was ten times the pressure of the residual gas in the tube.

Area of the emitter

Before it was possible to determine the constant A from Eq. (4), it was necessary to know

the area of the emitter. As the emitter was made by turning on a lathe, it was a figure of revolution, the area of which could, therefore, be computed by use of the first theorem of Pappus. The length of the generating arc was obtained from the length of a uniform copper strip bent to coincide with half of the perimeter of an enlarged photograph of the emitter. Its centroid was obtained by the use of an analytical balance and the elementary theory of moments as applied to the same copper strip. The area so obtained was for a similar enlarged solid, which, when divided by the square of the magnification, yielded the area desired (6.11 cm^2).

Values of constants

The final values of the thermionic constants for nickel were obtained by taking the weighted averages of the values from the last three groups of data analyzed and are $\Phi = 5.03 \pm 0.05$ volts and $A = 1.38 \times 10^3$ amp./$cm^2 deg.^2$. This value of Φ agrees with that of 5.01 ± 0.02 volts obtained photoelectrically by Glasoe.[1] The only other thermionic determination for nickel was made by Schlichter[2] in 1915 and yielded the anomalous value 2.77 volts. Although A does not agree with the universal value derived by Dushman,[3] this deviation might be expected from the position of nickel in the periodic table. The value for platinum in the same periodic group was found by DuBridge[4] to be 1.7×10^4 amp./$cm^2 deg.^2$.

Conclusion

The authors feel that the agreement furnished by this method with the photoelectric method in the case of nickel recommends it for use with other metals which are too hard, or, like nickel, are too volatile to be treated by the conventional method. Work on other metals is continuing in this laboratory.

[1] G. N. Glasoe, Phys. Rev. **38**, 1490 (1931).
[2] W. Schlichter, Ann. d. Physik [4] **47**, 573 (1915).
[3] S. Dushman, Phys. Rev. **21**, 623 (1923).
[4] L. A. DuBridge, Phys. Rev. **32**, 961 (1928).

Fine Structure in the *K* X-Ray Absorption Spectrum of Bromine*

SEYMOUR TOWN STEPHENSON, *Sloane Physics Laboratory, Yale University*

(Received June 26, 1933)

The existence of an extended Kronig type fine structure in the *K* absorption edge of bromine is established by the double crystal ionization spectrometer method. This fine structure as obtained with partially polarized x-rays and a single crystal absorber is very pronounced and some evidence has been found of a smoothing out and shifting of the structure for orientations of the crystal absorber in which the most probable direction of ejection of electrons is not perpendicular to an important plane in the crystal. There is some indication that the structure is less pronounced for unpolarized x-rays. The results follow from Kronig's theory of extended fine structure and quantitative agreement with the theory is obtained when comparison is made with results obtained (photographically) by others. A value for the side of a unit cube of KBr is given.

INTRODUCTION

A MORE or less complicated fine structure has often been observed on the short wavelength side of x-ray absorption edges. This structure has been found to extend only a few volts from the main edge in the case of monatomic gases and vapors. Polyatomic gases and solids exhibit, in addition to this close in structure, a fine structure extending several hundred volts from the main edge. The fine structure in and close to the edge has been explained by Kossel.[1] Recently Kronig[2, 3, 4] has given a theoretical explanation of the extended fine structure and much evidence has been accumulated in favor of the theory.

In a preliminary report[5] some experimental work on fine structure was presented. It is desired to give a brief description of the work and to give some additional results. The purpose of the present investigation is twofold. All the experiments on extended fine structure appearing in the literature reviewed were performed by the photographic method. The ionization method has been used with the double crystal spectrometer in investigations on the width and structure of the main absorption edges and some fine structure in the edge itself has been observed. The first part of the present problem, then, is to obtain the extended fine structure by the ionization method and to compare these ionization results with the photographic results of others in checking some aspects of Kronig's theory.

It occurred to Professor C. D. Cooksey that, by the use of polarized x-rays and a single crystal acting both as absorber and grating, one should obtain very pronounced fine structure. In addition one would expect from Kronig's[3] theory a variation in intensity and a shift in position for each discontinuity, with change of orientation of the electric vector with respect to the crystal axes of the absorber. The second part of the present problem is to look for such effects. The variations and shifts observed will be small because of (1) the large number of planes concerned, (2) incomplete polarization and the fact that all the electrons are not ejected in the direction of the electric vector and (3) the finite resolving power of the crystal grating.

APPARATUS

A double crystal spectrometer of the precision type designed by Compton[6] and made by the *Societe Genevoise* was used. The first crystal, C_1, acted both as polarizer and grating. A calcite crystal was used having its reflecting face ground

* Part of a dissertation presented for the degree of Doctor of Philosophy in Yale University.

[1] W. Kossel, Zeits. f. Physik **1**, 119 (1920).

[2] R. de L. Kronig, Zeits. f. Physik **70**, 317 (1931).

[3] R. de L. Kronig, Zeits. f. Physik **75**, 191 (1932).

[4] R. de L. Kronig, Zeits. f. Physik **75**, 468 (1932).

[5] C. D. Cooksey and S. T. Stephenson, Phys. Rev. **43**, 670 (1933).

[6] A. H. Compton, R.S.I. **2**, 365 (1931).

parallel to a set of (110) planes, thus giving a high degree of polarization. (In the third order, for this face, the Bragg angle for the wavelength of the bromine K edge is 46°.) The second crystal, C_2, contained the absorbing element. A large crystal of artificial KBr kindly sent to us by Professor G. A. Lindsay of the University of Michigan was used, with reflection taking place from a cleavage (100) face. By rotating C_2 about an axis normal to its reflecting face, the angle between the normal to a set of (100) planes and the principal direction of ejection of electrons could be altered. Very pronounced extended fine structure should be observed when this angle is zero. For other angles it should be shifted and somewhat smoothed out.

A sensitive quadrant electrometer measured the ionization currents in a small copper ionization chamber. About every two minutes small kicks of 1 or 2 divisions due to α-particles were noted and these formed the most serious source of error.

Results

Because of the low intensity with C_1 reflecting in the third order, no satisfactory curves could be obtained for this position most closely approximating complete polarization. (Work is now in progress in the third order with a metal x-ray tube capable of giving greater intensity.) C_1 was set for the second order reflection of a small region near and including the Br K edge. The total deviation produced by C_1 was about 57°30″, giving about 75 percent polarization of the rays incident on C_2. Therefore, the fine structure was expected to be less pronounced and the variations with the change of orientation of C_2 less noticeable than for the case of completely polarized x-rays but the effects, though smaller, were easier to detect because the intensity in the second order was some three or four times that in the third order.

The figure in the preliminary report[5] showed a pronounced extended fine structure obtained by the double crystal ionization method. After the completion of runs for this curve, work was started on the effects of polarization and crystal orientation. C_2 was set with a cube edge accurately parallel to its axis of rotation. Most of the electrons, with C_2 in this position, were ejected normal to the (100) planes of the crystal. The

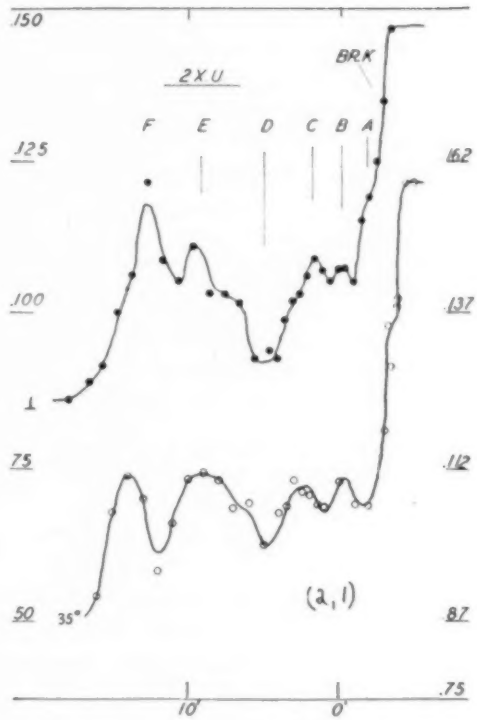

Fig. 1. Fine structure observed when the most probable direction of ejection of electrons is perpendicular (⊥) and at an angle of 35° with the normal to a set of (100) planes. Mo target.

curve shown at the top of Fig. 1 was taken with C_2 in this position at an electrometer sensitivity of 2500 divisions per volt using the Mo target tube at 50 kv and 25 m.a. The fine structure A in the edge itself is of the Kossel type. The peaks B, C, E, and F represent extended fine structure caused by forbidden zones in the KBr crystal lattice. The minima, of which D is the most pronounced, correspond to the permitted zones.

The curve just described is to be compared with the curve appearing below it in Fig. 1. This curve (marked 35°) was taken with C_2 rotated about an axis normal to its reflecting cleavage face some 35°. The main direction of ejection of electrons for this orientation was perpendicular to no very important plane in the crystal. The main features of the structure A, B, C, D, E and F repeat in their general shape and appearance in the lower curve. This proves the fine structure to be independent of any imperfections in C_2. The valley D is more pronounced in the top curve than in the lower curve and the peaks E and F

appear more pronounced. It should be noted, however, that peaks B and C do not smooth out in the lower curve as do E and F. It may be that B and C being closer to the main edge are in a region where Kronig's approximations do not hold so well as they do for higher energy values.

The fact that E and F are two peaks on a broader fine structure peak lends some weight to Kronig's assumption that the structure usually observed is an aggregate of the discontinuities due to individual planes. Apparently E and F are due to two important individual planes. E and F are slightly more separated in the lower curve than in the upper. This shift is small but is as large as one might expect. The shift according to the theory should be towards the main edge for some planes and away from it for others which would account for the broadening observed.

In order to obtain more intensity, a W target tube was used at 50 kv and 25 m.a. Fig. 2 shows the results for normal ($\perp$) ejection (top curve) and 35° ejection (lower curve). The electrometer sensitivity was 1900 divisions per volt. The main edge is less pronounced than in Fig. 1 because

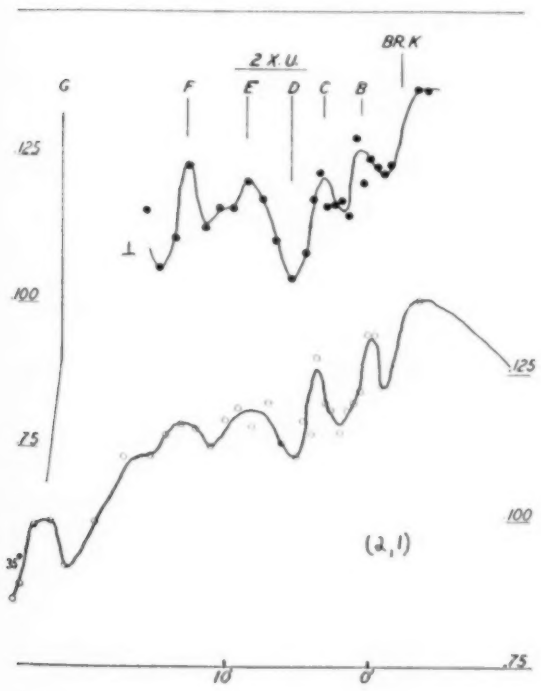

FIG. 2. Fine structure as in Fig. 1. W target.

of a more curved distribution of background intensity. No attempt was made to run over the structure A accurately.

C_1 was not in exactly the same position for these curves as for the previous curves, also a broader focal spot gave a different distribution of intensity on C_1. The fact that these curves are so nearly identical with those of Fig. 1 proves that the fine structure observed is not due to imperfections in C_1 or to the structure of the focal spot.

In Fig. 2 as in Fig. 1, we notice a more pronounced minimum D in the upper curve than in the lower and the structure E and F appears slightly smoothed over and broadened in the lower curve. Again B and C do not show such effects.

Thus, we have obtained with the ionization method very pronounced fine structure with partially polarized x-rays and a single crystal absorber. The top curves in Figs. 1 and 2 and the previously reported curve[5] show a more pronounced fine structure compared to the main edge than any structure appearing in the literature reviewed. It is interesting to note that the most pronounced fine structure referred to in the journals is that obtained with a single crystal as absorber and no appreciable polarization, polycrystalline absorbing screens giving a much less pronounced structure. There is some evidence of a smoothing over and shifting of the structure as one changes the orientation of C_2. It is well to mention here three objections to this evidence on the smoothing and shifting of the structure. (1) The scattering of the points (necessarily present because of the weak intensity), the effects observed being within a possible scattering of the points. (2) Crystal imperfections, which may cause slight variations in the structure for different positions, although the structure in general has been shown to be independent of such imperfections. (3) Peaks B and C do not behave as do peaks E and F but the strictest application of the theory may not be permissible so close to the edge.

In a search for further fine structure discontinuities the peak G was found. Its presence was later verified with C_1 reflecting in the first order.

Runs in the (1, 1) position (no appreciable polarization and lower dispersion) gave the fine

structure again. Here it is still quite pronounced since the absorption is in a single crystal but possibly not quite so pronounced as for the (2, 1) position where the polarization is appreciable. However, the change due to polarization is small.

TABLE I. *Fine structure positions relative to the main edge. (2, 1)*

Units	*A*	*B*	*C*	*D*	*E*	*F*	*G*
Minutes	0.8	2.6	5.2	7.8	11.8	16.1	24.7
X. U.	0.3	1.0	2.0	3.0	4.5	6.2	9.7
Volts	4.4	14.9	28.9	43.7	65.8	90	140

Table I shows the positions of the fine structure peaks relative to the center of the main edge, the values being averages of the values obtained from all the (2, 1) curves.

TABLE II. *Fine structure positions relative to the main edge. (X.U.)*

Position	*A*	*B*	*C*	*D*	*E*	*G*
(2, 1)	0.3	1.0	2.0	3.0	4.5	9.7
(1, 1)	0.3	1.0	1.85	3.0	4.7	10.2

Table II shows a comparison of the positions of the fine structure distances relative to the main edge with C_1 in second and first orders. (Because of low dispersion in first order F was not separated from E.) It is obvious from this table that the fine structure is independent of crystal imperfections, line-up and source of x-rays.

TABLE III. *Distances from center of main edge in volts.*

Author		*B*	*C*	$\frac{1}{2}(E-D)$
Lindsay[7]	(K in KBr)	14.2	24.9	
Nuttall[8]	(K in KCl)	14.2	24.9	62
Hanawalt[9]	(Br in NaBr)	5.5–13	28.0	54
Present	(Br in KBr)	14.9	28.9	55

Table III shows a comparison of the present results with those obtained photographically by other authors. The values given by Lindsay[7] are for the K edge of potassium in a KBr crystal. On Kronig's theory bromine and potassium should show the same fine structure absorption in KBr. The agreement shown is well within experimental error. Following Kronig's theory Nuttall's[8] values for the absorption of potassium in KCl were corrected for the difference in grating space between KBr and KCl and the values thus obtained agree well with those obtained here for bromine. Finally Hanawalt's[9] results for bromine in NaBr are shown corrected and the agreement is excellent although Hanawalt's data for the first peak leaves the exact position of the maximum in doubt. (In this table the values given by the other authors were with respect to the bottom of the main edge. The values here given have been corrected for half the width of the edge as estimated from the curves which were published. The first two columns give the positions of maxima. The third column shows the beginning of the secondary structure hump E and represents a point about half way between D and E in the present work, i.e., 55 volts. Nuttall's and Lindsay's B and C are given as the same because Lindsay remeasured Nuttall's plates and remarks that the values are the same within experimental error.)

The results are in striking agreement with Kronig's fundamental postulate that the extended fine structure depends on the crystal structure and not on the elements in the crystal.

The side of a unit cube of KBr has been given by various observers as 6.59,[10] 6.57,[11] and 6.5904A.[12] There is some discrepancy in these results. Taking the value of the wave-length of the Br edge to be 918.1 X.U.,[13] runs in the (2, 1), (2, −1), (1, 2) and (1, −2) positions gave for $2d$ the value 6.574 ± 0.006A. Though not a precision measurement, it is felt that this value is more accurate than those previously obtained.

In conclusion, the author wishes to express his thanks to Professor C. D. Cooksey for suggesting the problem and for his help and advice while directing the experimental work and to Dr. Donald Cooksey for the loan of precision instruments and for suggestions. The author is indebted to Professor L. W. McKeehan for making the necessary apparatus available.

[7] G. A. Lindsay, Zeits. f. Physik **71**, 735 (1931).

[8] J. M. Nuttall, Phys. Rev. **31**, 742 (1928).

[9] J. D. Hanawalt, Phys. Rev. **37**, 715 (1931).

[10] R. W. G. Wyckoff, J. Wash. Acad. Sci. **11**, 429 (1921).

[11] W. P. Davey, Phys. Rev. **21**, 143 (1923).

[12] F. Oberlies, Ann. d. Physik **87**, 238 (1928).

[13] J. Stenman, Zeits. f. Physik **48**, 349 (1928).

Remarkable Optical Properties of the Alkali Metals

R. W. Wood, *Johns Hopkins University*

(Received June 23, 1933)

Thin films of alkali metals opaque to visible light are highly transparent in the ultraviolet region. The point in the spectrum at which transparency commences moves toward shorter wave-lengths with decreasing atomic number as follows: Cs 4400; Rb 3600; K 3150; Na 2100; Li 2050A. The transparency continues as far down the spectrum as the investigations have gone (1860A). In this region the phenomenon of plane polarization by reflection is observed. The reflecting powers of these metals for different wave-lengths have been measured. From these measurements and also from the Brewsterian angles for plane polarization, the refractive index of a potassium film has been calculated. The values range from 0.90 at 2147A to 0.50 at 3100A. Since the refractive index is less than unity total reflection takes place, although the critical angle is not sharply defined. Interference maxima and minima in the spectrum of light reflected from a metal film permit a rough determination of the film thickness.

THE optical properties of the metals of the alkali group have been investigated chiefly with reference to the photoelectric effect, their optical constants having been studied in only a few instances and then only in the visible region of the spectrum. Extension of this study into the region of shorter wave-lengths has brought to light the very remarkable fact that, at a certain point in the spectrum, they cease to exhibit the optical properties of metals and acquire those of transparent media, yielding plane polarized light by reflection of ordinary light at a Brewsterian angle, from which their refractive index (and dispersion) can be calculated. A preliminary report of these results was published in *Nature* for April 22, 1933.

As was shown by the writer[1] over fifteen years ago, films of sodium and potassium, deposited on the inner walls of highly exhausted quartz bulbs at liquid air temperature, while completely opaque to visible, were highly transparent to the ultraviolet. The entire spectrum from wave-length 3000 to the limit reached by the quartz spectrograph was freely transmitted in the case of potassium. No additional observations of importance appear to have been made since these experiments and the investigation was taken up again with a view to studying the optical properties of all the alkali metals in a more quantitative manner and over a wider spectral range than in the earlier investigation. Their high transparency indicated that other interesting phenomena were to be expected.

It is necessary to deposit the films at liquid air temperature, for at higher temperatures a colloidal deposit is obtained, the optical properties of which are quite different from those of homogeneous films.

The films deposited in this way, in the earlier investigation, survived exposure to room temperature for only a few minutes. Minute holes appeared which increased in size rapidly and acquired arborescent forms. The metal finally gathered into invisible drops and the bulb became almost completely transparent. In the present work it soon developed that a certain degree of permanency at room temperature was acquired if before the introduction of the metal, the bulbs were thoroughly degassed by prolonged pumping at high temperature. A potassium film formed under these conditions, of such thickness that the sun's disk was barely visible through it, lasted several days before developing small pinhole leaks. Such a film forms a most useful filter for spectroscopic work as it transmits everything below 3000, reducing the intensity to about one-fourth, while the entire visible and upper ultraviolet is certainly reduced several hundred thousand times.

In some of the bulbs, probably because of imperfect degassing, a potassium film, deposited in the form of a circular disk 2 cm in diameter, when warmed to room temperature contracted

[1] R. W. Wood, Phil. Mag. **38**, 98 (1918).

to a single flattened globule about 1.5 mm in diameter at the center of the circle. It seems surprising that surface tension can draw in a metal having a rigidity of a moderately hard wax. Further investigations along these lines are contemplated.

The bulbs are prepared in the following way. A quartz bulb is blown of the form and size shown in Fig. 1*a*, with very thin walls, and the

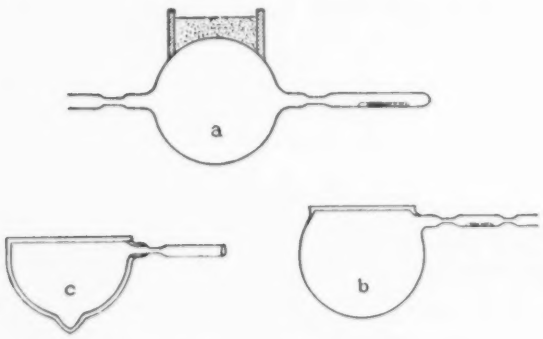

FIG. 1. Forms of bulbs used.

metal introduced into the side chamber either by distillation from a mixture of the chloride with calcium turnings or from the metal contained in a very thin walled tube of about 1 mm bore. A small fragment of the metal should be melted in a tube of about 8 mm bore, closed at the bottom, and a small amount sucked up into a long capillary tube made by drawing out a short piece of thin walled tubing. It is advisable to use a rubber tube for this operation as it is easier to watch the rise of the metal. A number of such tubes can be prepared at one time, closing one end by fusion near the metal and the other by a small lump of soft wax. A piece of the desired length is then cut off with scissors and quickly slipped into the side tube, which should be immediately sealed and the pump started. The exhaustion is best done with a mercury vapor pump with liquid air trap, the bulb being heated up to the constricted portions over a Bunsen flame or in an electric furnace. After a thorough exhaustion the bulb is allowed to cool, the metal distilled into it and the side tube sealed off. The metal should now be driven back and forth from one side of the bulb to the other with a small flame to remove occluded hydrogen. After sealing off the bulb from the pump a spot is cleaned by a small pointed gas flame and this spot covered by a short piece of fiber tube half filled with infusorial earth (shown in Fig. 1), or other similar incombustible power, covered with a disk of filter paper and then thoroughly saturated with liquid air. The metal is then deposited by local heating of other parts of the bulb with the flame. The thickness of the film is regulated by the area cleaned off. During the operation the capsule can be removed for a few seconds and the opacity observed by viewing a small electric lamp mounted below the bulb.

The point in the spectrum at which transparency commences moves towards shorter wave-lengths with decreasing atomic number, as follows: caesium 4400, rubidium 3600, potassium 3150, sodium 2100, lithium 2050. A little uncertainty is felt about lithium, as some plates indicated that its transparency commenced at about the same point as in the case of sodium, while others indicated a shift towards shorter wave-lengths. Interference introduces an uncertainty as will appear presently.

The transmission spectra of the five metals are shown by Fig. 2, the source of light being an end-on hydrogen tube with its inner wall silvered to suppress the line spectrum by catalyzing the atomic hydrogen. The upper spectrum shows the distribution of intensity with the spectrograph employed, a small quartz instrument with its prism replaced by one of fluorite. The great intensity recorded in the region of longer wave-lengths makes the efficiency of the metal filters in suppressing this part of the spectrum all the more striking. The absorption bands below 1900 are the oxygen bands of the air. A comparison spectrum of the Cd-Al spark is at the bottom of the figure.

Because of underexposure the transparency of the last three metals in the region of shortest wave-lengths is not apparent in these photographs. It is brought out to better advantage in Fig. 3 made with the Cd-Al spark. Here rubidium and potassium show commencement of transmission at the same point, but the point of highest transparency for potassium is shifted to the right. The failure of the last aluminum line, 1860, to appear in the case of lithium has not

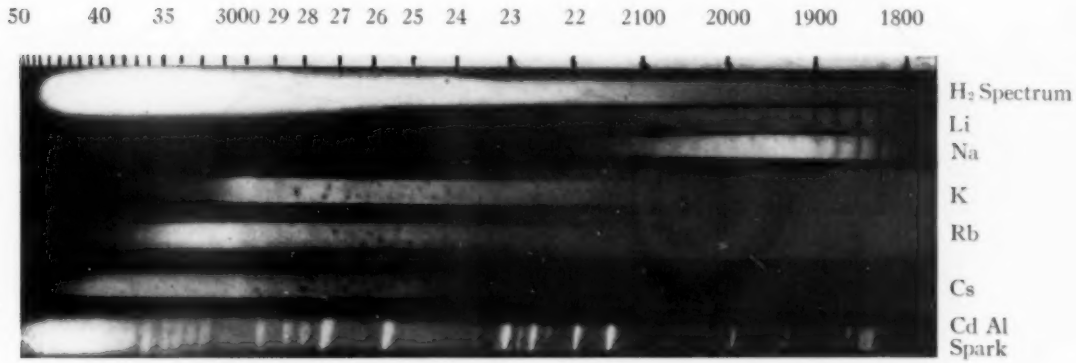

FIG. 2. Transmission by the alkali metals of light from a hydrogen tube.

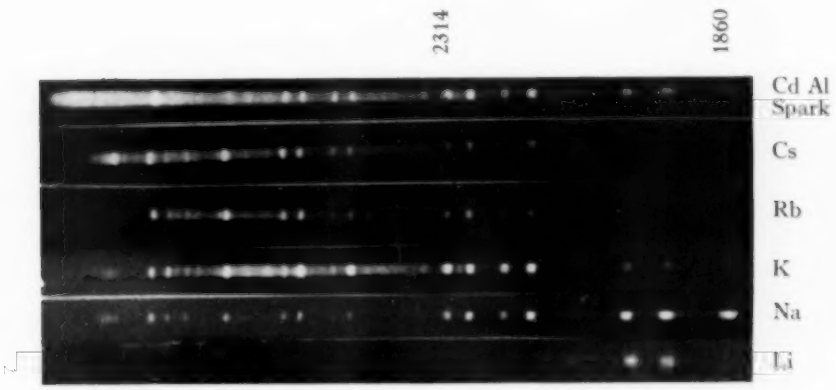

FIG. 3. Transmission by the alkali metals of light from a Cd-Al spark.

been explained but it is certainly not due to absorption by the metal as it appears in other spectrograms. The transparency continues from the points indicated as far down the spectrum as the investigations have gone at the present time, i.e., to about 1860. In the case of caesium there appeared to be indications of a slight increase of absorption at the extreme end of the spectrum. It is clear that we have in these cases a very wide gap between the absorptions due to the free and bound electrons. A somewhat similar but very narrow gap occurs in the case of silver at $\lambda = 3160$, but the transparency in the case of the alkali metals is of a different order of magnitude from that of silver. A film of potassium through which the sun's disk is barely visible (which means a reduction of intensity of perhaps half a million) transmits 25 percent of everything below 3000.

The case of caesium is especially interesting as its region of high transparency begins in the visible violet and films of the proper thickness transmit light of a rich violet color as deep and pure as that transmitted by a strong solution of cuprammonium or dense cobalt glass.

The transmission of potassium is illustrated by Fig. 4*a* for a film of increasing thickness, the upper spectrum of two seconds exposure made with no film, the following spectra with eight seconds exposure, a candle flame easily visible through the film in the first case and the sun's disk absolutely invisible in the last. It is to be noticed that only a very slight increase in the ultraviolet absorption accompanies this enormous increment in the absorption of visible light. It seemed probable that the high transparency would be accompanied by a very low reflecting power and this was found to be the case, the reflection of potassium, for example, at wave-length 2147 being only 0.003, or 1/10th that of a single surface of fused quartz.

The reflecting powers for different wave-lengths for these metals, with the exception of lithium, are shown by the curves in Fig. 5.

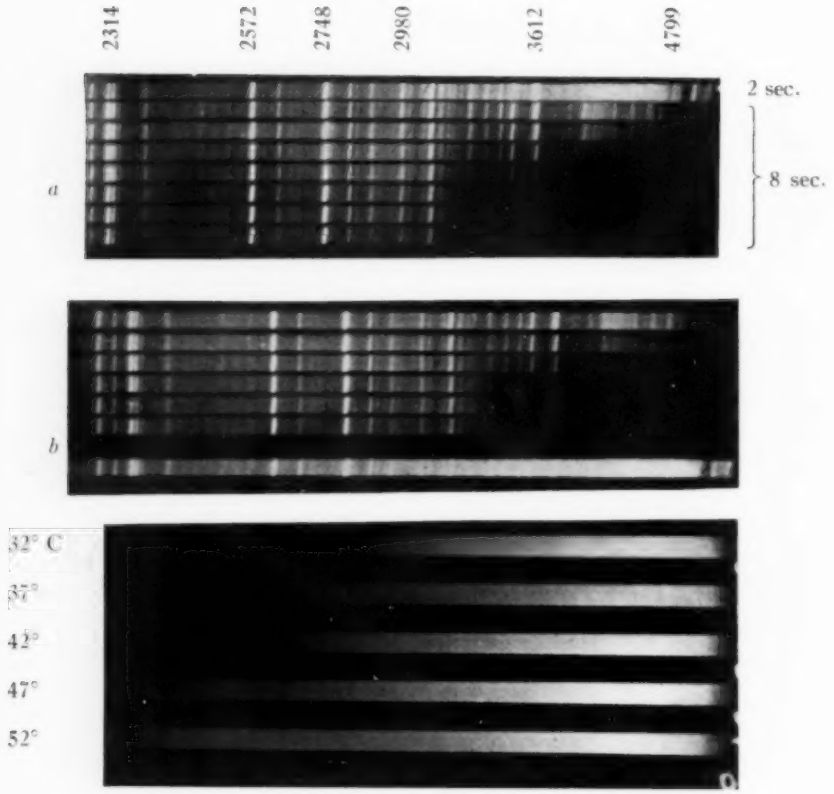

FIG. 4. Transmission of light by various thicknesses of potassium film.

Values higher than 30 percent are not given, as only determinations in the region of low reflectivity were made. This very low reflecting power, combined with high transparency, raised the question as to why the intensity was reduced to one-quarter by transmission through a moderately thin film, while a further considerable increment of thickness produced very little change in the intensity of the transmitted light. The loss evidently occurred at the surface and the only plausible hypothesis appeared to be that there was a surface scattering. The metal surface sometimes showed slight traces of granularity, a faint halo appearing around the reflected image of the spark. A film was accordingly built up with especial care to avoid this condition, the capsule being wet with liquid air every half minute. A series of photographs for increasing thicknesses, with exposures of five seconds each and a final exposure, also of five seconds, with the film cleaned off, is reproduced in Fig. 4*b*. Comparison of the first spectrum with the last shows very little difference in intensity in the short wave-length region, certainly not a 1 : 4 ratio, as in the case of Fig. 4*a* where equality was secured with exposures in this ratio.

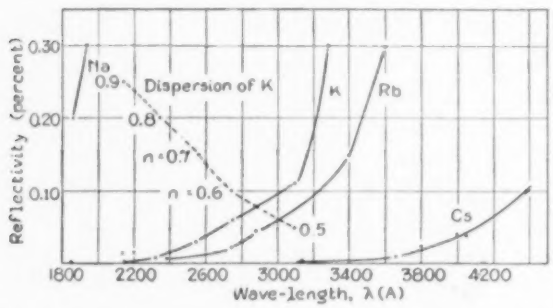

FIG. 5. Reflecting power of films of alkali metals and the dispersion curve for potassium.

The reflecting powers for different wave-lengths were determined by forming a very thick film on the inner surface of the quartz bulb, cleaning off the front surface with a small flame and pointing a quartz spectrograph at the image of a Cd-Al spark reflected in the concave metal

mirror, the spark being close to the slit. A number of exposures of different times were made, after which the film was removed by the flame and the outer surface of the quartz painted with black Duco. A second set of exposures was now made of the reflection from the single surface of quartz. By comparison of these plates the reflecting power of the metal in comparison to that of quartz was determined. After the reflecting power of quartz for the different spectral lines had been computed from the table of its refractive indices, it was easy to determine R for the metal.

From the reflecting powers thus determined, the refractive index of the metal can be determined, as in the case of transparent substances, from the formula $(n-1)^2/(n+1)^2=R$ in which R is expressed in percent. The rigorous formula could not be used as no measurements of the absorption coefficient have been made as yet. The dispersion curve for potassium obtained in this way is shown (dotted) in Fig. 5.

Certain anomalies, observed at first in the measurements of the reflecting power for different wave-lengths, were suspected to be due to interference between rays reflected from the front and back surface of the metal film, which would be almost certain to occur in the case of a film of such high transparency.

It should then be possible to photograph maxima and minima in the spectrum of the light from a continuous source, as in the case of thin films of glass. Substitution of the end-on hydrogen tube as a source proved the presence of very distinct maxima and minima and a series of spectra were then taken in coincidence, the thickness of the potassium film being slightly increased between each exposure. The cell of infusorial earth was attached to the bulb with a wire and liquid air introduced through a small thistle tube every few minutes as shown in Fig. 6, in which case a bulb with a flat plate as the reflecting surface is represented.

The spectrograms are reproduced in Fig. 7 which shows in a very graphic manner how the interference minima enter the spectrum at the short wave-length end and move gradually along the spectrum as the film thickness increases. As the reflection minima move up the spectrum they become less well defined, because of increased loss by reflection at the first surface. They cannot be pushed beyond wave-length 3000.

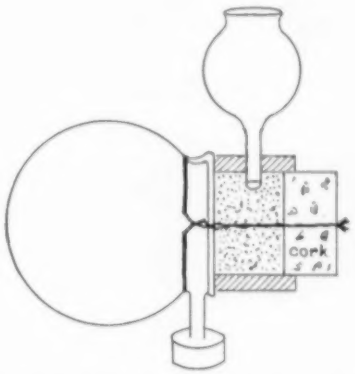

FIG. 6. Arrangement of bulb for interference measurements.

The prediction was now made that these metals would show a Brewsterian angle in the ultraviolet, giving plane polarization by reflection of ordinary light. This was found to be the case, the angle varying with the wave-length, so that it became at once possible to calculate the dispersion from the formula $n=\tan i$, in which i is the polarizing angle.

For the experiments on polarization a quartz bulb of the form shown in Fig. 1*b* was made by fusing an optically worked circular disk on the end of a tube, inserting a small side tube for exhaustion and introduction of the metal, drawing down (Fig. 1*c*) and then blowing out, a thin walled bulb as shown. This bulb was mounted on a divided circle with the reflecting inner surface parallel to and over the axis of rotation, Fig. 6. The rays from the image of the spark in the metal mirror were passed through a double image Wollaston prism and focussed on the slit by a short focus fluorite lens. From the relative intensities of the cadmium lines in the two images the completeness of the polarization could be determined, the ratio of exposure times to secure equality being in some cases as 1 : 400.

The Brewsterian angle, in the case of potassium was found to vary with the wave-length, making it possible to determine the dispersion of the metal in the ultraviolet. Considerable trouble was experienced at first due to the fog on the plate caused by the high reflecting power of the metal films in the violet and upper ultraviolet.

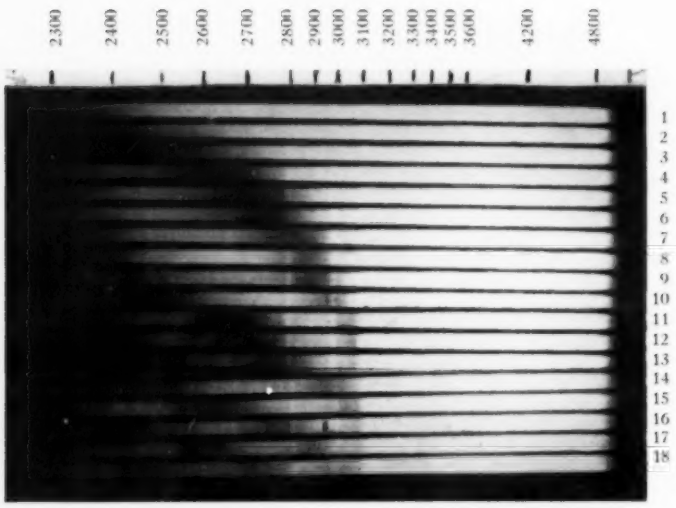

FIG. 7. Interference minima by reflection from potassium film of increasing thickness.

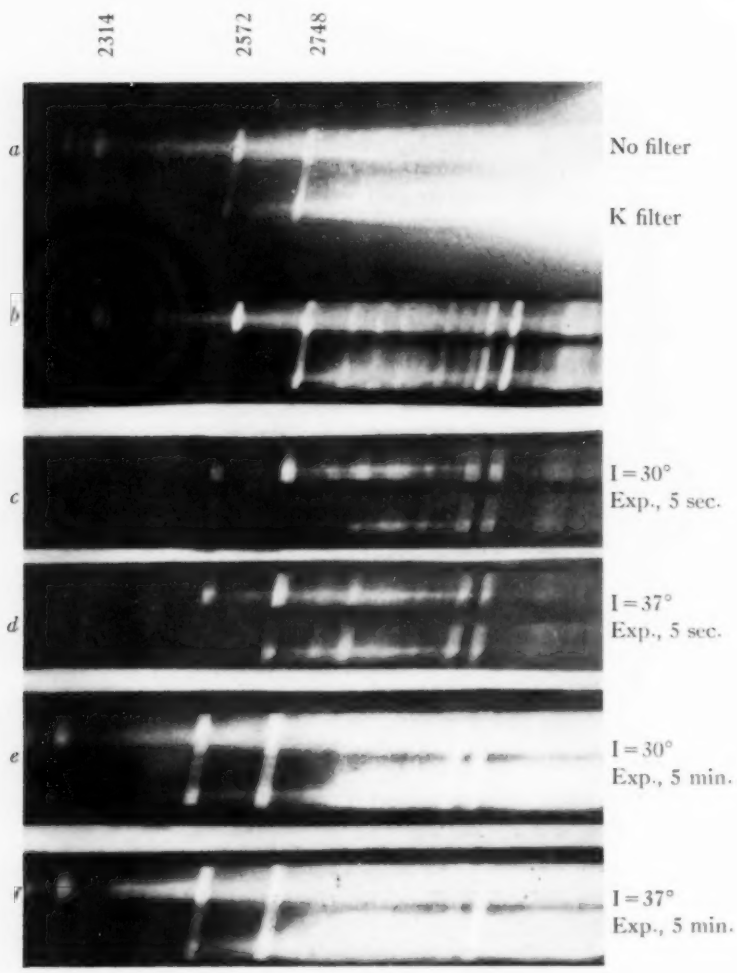

FIG. 8. Plane polarization by reflection from potassium.

This was overcome by inserting a second quartz bulb with a fairly thick potassium film in front of the spark as an ultraviolet filter. The advantage gained by the use of this filter is illustrated in Fig. 8, the upper pair of polarized spectra (*a*) having been made without the filter, the second pair (*b*) with the filter inserted. The two polarized spectra have equal intensity above 2748 while the lower spectrum is practically absent below this point. The dispersion is illustrated by Fig. 8*c* and *e*, which show that the polarizing angle for 2748 is 30°, the intensity of this line in the lower spectrum being about 1/40 of that in the upper. An exposure of five seconds was given for *c* and five minutes for *e* to bring out the 2314 line, for which the intensity ratio is 1/10. Figs. *d* and *f* show a polarization angle of 37° for 2314, the measured intensity ratio in this case being 1 : 240.

The intensity ratios were measured by giving, say, a five minute exposure to the two spectra, and then making a series of exposures of the brighter spectrum (covering the image of the fainter on the slit) of 1, 2, 4, 8, . . . etc., seconds, picking out the one which matched the fainter spectrum made with the five minute exposure. The results obtained in this way are, of course, not very accurate but the dispersion calculated from the values of the angle i of maximum polarization by the formula $n = \tan i$ agreed surprisingly well with the values obtained from the reflecting power, as shown by Table I.

TABLE I. *Refractive index of potassium film as measured by reflection and by polarizing angle.*

λ	n (from R)	n (from Pol)
2147	0.895	—
2200	.877	0.86
2314	.83	.80
2572	.70	.69
2748	.60	.58
3100	.50?	—

DETERMINATION OF FILM THICKNESS FROM INTERFERENCE BANDS

We can determine the thickness of the metal film from the interference bands shown in Fig. 6 and obtain as well a check on the values of n for the different wave-lengths.

A preliminary calculation showed that the interference bands could not be reconciled with the calculated values of n if reflection from the two surfaces of the metal involved no relative phase change. Since n is less than unity, in every case we are dealing with a reflection from "dense to rare" at the vacuum-metal interface and from "rare to dense" at metal quartz surface. Assuming a phase change of 180° such as we have in the case of a transparent film we have for e the thickness for a minimum $e = 2(n-1)\lambda/4$ in which n is the order of interference, or thicknesses corresponding to 0, $\lambda/2$, λ, $3\lambda/2$, etc., and λ is the wave-length in the metal which can be calculated from the dispersion curve.

If the values of the refractive indices are correctly given, the values of e, the thickness calculated from, say, three interference bands, should agree. For spectrum No. 4, Fig. 5, the minimum comes at 2650, for which $n = 0.65$ giving $\lambda = 4100$ or $e = 2050$A.

For spectrum 6 we have two minima available, at 2200 ($n = 0.87$) and 2750 ($n = 0.6$), the former giving $e = 2530$A, the latter 2300A, a fair agreement under the circumstances.

For spectrum 11, Fig. 7, we have minima at 2300 ($n = 0.83$), 2600 ($n = 0.65$) and a third in the vicinity of 3100, the position of which cannot be accurately determined as it falls in the region of strong reflection and the interference is incomplete. The values for the thickness in this case were 4150 and 4100.

For spectrum 16, $e = 4620$ calculated from the band at 2750 ($n = 0.60$) and $e = 4830$ from the band at 2450 ($n = 0.76$). This last case shows us that with a film of thickness equal to twice the wave-length in air, we have sufficient intensity, after two transmissions, to produce strong interference. In the case of silver a single transmission through a film one-tenth of a wave-length in thickness reduces the intensity to less than 1 percent.

ANGLE OF TOTAL REFLECTION

As the alkali metals function for ultraviolet light as the rarer medium with respect to vacuum, an angle of total reflection is to be expected which can be calculated from the refractive index. Calculations showed that total reflection should occur at an incidence angle of

about 30° for wave-length 2750, at 45° for 2570 and 52° for 2350. A series of spectra of the light of the hydrogen tube reflected at incidence angles included in this range are reproduced in Fig. 4*c* showing the gradual extension of the spectrum towards shorter wave-lengths with increasing incidence angle. There is, however, no sudden transition in the intensity at a definite wave-length as is to be expected for an imperfectly transparent medium.

The results obtained up to the present time are to be regarded as preliminary only. No determinations have been made as yet of the coefficient of absorption and it is obvious that it is extremely important to investigate the optical constants in the transition region where the extreme opacity passes over into comparative transparency. This investigation will require the development of a technique for the determination of the angles of principal incidence and azimuth in the visible and upper ultraviolet region and preparations for this work are now under way.

Nuclear Moments and Their Dependence upon Atomic Number and Mass Number

NORMAN S. GRACE,* *Department of Physics, University of California*
(Received June 27, 1933)

Nuclei are grouped into four classes depending upon whether Z and M (atomic number and mass number, respectively) are even or odd. A summary of the nuclear mechanical and magnetic moments which have been experimentally observed is given. This summary indicates similarities within each nuclear class and definite differences between classes both as to mechanical and magnetic moments and to nuclear g-factors. These results suggest a correlation between nuclear moments and the periodic table; namely, that nearly all nuclei which have large magnetic and mechanical moments lie in columns of the periodic table with Z odd, while nuclei occurring in columns for which Z is even generally have zero, or small magnetic moments and zero, or small mechanical moments. The incompleteness of the present data is emphasized.

RAPID progress has been made recently in the determination of nuclear moments from spectroscopic data, particularly so regarding the calculation of nuclear magnetic moments.[1, 2, 3] In this connection Goudsmit's paper merits particular mention for it is the first extensive attempt to calculate nuclear magnetic moments from hyperfine structure data. A still more recent paper by Fermi and Segrè[3] on nuclear magnetic moments is in excellent general agreement with Goudsmit's calculations. Other recent progress has included the determination of nuclear mechanical moments for a number of additional nuclei. Since nuclear moments are of especial interest in connection with the development of nuclear theory, it has seemed profitable at this time to attempt some organization of the data, even though these data are as yet far from complete.

All nuclei fall into four classes, depending upon whether Z (the atomic number) and M (the mass number) are even or odd. For the present it seems to be safest to adopt this system of nuclear classification since it is quite independent of any particular nuclear model. These four nuclear classes, together with a summary of the nuclear magnetic and mechanical moments which have been observed for each class, are given in Table I. The results for a number of nuclei of each class are also given. It does not seem worth while to include an exhaustive list at this time, for many of our present values are somewhat uncertain and additional results are being obtained so rapidly that no such table would long have any claim to completeness. *The experimental results that have been obtained to date indicate definite similarities within each nuclear class and differences between classes both as to nuclear mechanical and magnetic moments and to nuclear g-factors.* These similarities and differences, because of the incompleteness of the data, must not be over-emphasized; however, they may well serve as a guide in the development of certain phases of nuclear theory.

Nuclei of class I (Z even, M even) have integral mechanical moments (only zero observed) and zero (or very small) magnetic moments. From band spectra, a number of the lighter nuclei of this class up to $Z=16$ have been studied and all definitely have $I=0$. The line spectra of a number of elements up to $Z=82$ have been examined under high resolving power and in no case has any hyperfine structure for members of this class been observed. This lack of structure is particularly striking in such cases as the even isotopes of cadmium, mercury and lead where the odd isotopes (members of class III) *do* show definite structure. This lack of hyperfine structure for nuclei of class I must mean then that either $I=0$ (in keeping with the results from

* Commonwealth Fellow.

[1] Goudsmit, Phys. Rev. **43**, 638 (1933).

[2] Breit and Wills, Bull. Am. Phys. Soc. **8**, No. 2, paper 21.

[3] Fermi and Segrè, Zeits. f. Physik **82**, 729 (1933).

TABLE I. *Classification of nuclei and nuclear moments.*

Element	Atomic number Z	Mass number M	Mechanical moments ($X\ h/2$)	Magnetic moments (proton magnetons)	Nuclear g-factors
Class I	even	even	0 (band spectra)	—	—
He	2	4	0 (band spectra)	—	—
C	6	12	0 (band spectra)	—	—
O	8	16	0 (band spectra)	—	—
S	16	32	0 (band spectra)	—	—
even isotopes of Cd, Hg, Pb, Mo, W, etc.			0 from h.f.s.	—	—
Class II	odd	odd	half integral (from 1/2 to 9/2 observed)	positive varied magnitude	positive-varying from nearly zero to 4.2; I small, g large; I large, g small
Al	13	27	1/2	2.1	4.2
Tl	81	203, 205	1/2	1.8	3.6
Cu	29	63, 65	3/2	2.5	1.7
Sb	51	121	5/2	2.7	1.1
		123	7/2	2.1	0.6
Bi	83	209	9/2	4.0	0.89
Class III	even	odd	half integral (from 1/2 to 5/2 observed)	positive and negative, smaller values than class II	positive and negative—small (from +1.2 to −1.33 obs.)
Pb	82	207	1/2	0.60	1.20
Hg	80	199	1/2	0.55	1.1
		201	3/2	−0.62	−0.41
Cd	48	111, 113	1/2	−0.67	−1.33
Ba	56	137	5/2	1.0	0.4
Class IV	odd	even	integral	small	small
N	7	14	2/2	0.2 or less	$+0.2>g>-0.2$
H	1	2	2/2	—	—

band spectra) or that if $I\neq 0$, then the nuclear magnetic moments can be very little different from zero. It is quite important to settle this question definitely for to date there appears to be no adequate reason why all nuclei of class I should have zero mechanical moments, nor indeed is there adequate proof that such is actually the case.

Nuclei of class II (Z odd, M odd) have half-integral mechanical moments, positive magnetic moments of varied magnitude and positive nuclear g-factors. Mechanical moments from 1/2 to 9/2 have been observed and g-factors from about 4 down nearly to zero. It is interesting and possibly significant that highest g-factors have been found for nuclei where I is small (e.g., Al and Tl, where $I=1/2$), whereas for those nuclei in which I is large (9/2), g is small (e.g., Bi and In). It is also interesting that a number of nuclei in this class have large I values. We[4] have recently investigated four nuclei of this class, Co^{59}, Cb^{93}, La^{139} and Ta^{181} and have found each to have an I value of at least 7/2, while for Co and Cb, I may well be larger.

Nuclei of class III (Z even, M odd) have half integral I values and positive and negative g-factors. In nearly every case examined to date the I values are small (1/2 or 3/2), and the g-factors are also rather small (ranging from +1.2 to −1.3), which means that the nuclear magnetic moments are small. We[4] have recently carried out experiments on some other nuclei of this class Cr^{53}, Mo^{95}, Mo^{97} and W^{183} and have found that their nuclear magnetic moments are all small. It is interesting to note that the only negative nuclear g-factors that have been found occur in this class. Nuclear g-factors in class III (as in class II) are somewhat larger in magnitude for small I values than for large I values.

Nuclei of class IV (Z odd, M even) have integral spins and small magnetic moments. According to Krönig[5] and others, N^{14}, and

[4] Grace, Phys. Rev. **43**, 762 (1933); Grace and Ballard, Grace and More, White and Anderson, Bull. Am. Phys. Soc. **8**, No. 3, papers 2, 3 and 4; Grace and McMillan, Bull. Am. Phys. Soc. **8**, No. 4, paper 54; Grace and White, Phys. Rev. **43**, 1039 (1933).

[5] Krönig, Naturwiss. **16**, 335 (1928).

according to Lewis and Ashley,[6] H^2, have spins of $(2/2)(h/2\pi)$ from band spectra. From the absence of hyperfine structure Bacher[7] has found N^{14} to have an extremely small nuclear magnetic moment. The relative abundance of the homonuclear molecule Li^6Li^6 in lithium vapor is so small that the spin of Li^6 has not yet been determined from band spectra. Li^6 shows no hyperfine structure in the spectrum of Li II where Li^7 shows very wide structure. This means for Li^6 that either $I=0$, or that if $I\neq 0$, then the magnetic moment of Li^6 can differ only very slightly from zero.

In Fig. 1 nuclear magnetic moments are plotted against mechanical moments. Most of the results are taken from Goudsmit's paper[1] in which he states that the data are only prelim-

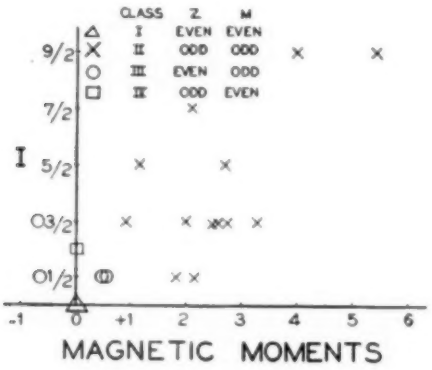

FIG. 1.

inary in nature. There may, therefore, be a considerable change in the numerical values of some of the magnetic moments; it seems improbable, however, that any such change will be sufficient to alter completely the general arrangement shown in Fig. 1, where the magnetic moments of classes II and III group themselves rather separately.

Table II is a rather complete summary of the results that have been obtained on nuclear mechanical moments to date. It shows that there are relatively many more nuclei in class II that have large I values than there are in class III. In class II four of the nuclei with $I=1/2$ have $Z\leq 15$, while ten of those with $I=3/2$ have $Z\leq 37$. Thus most of the small I values in class

[6] Lewis and Ashley, Phys. Rev. **43**, 837 (1933).

[7] Bacher, Bull. Am. Phys. Soc. **8**, No. 2, paper 22.

TABLE II. *Summary of experimental I values.*

I values	1/2	3/2	5/2	7/2	9/2
No. of nuclei in class II	6	11	9	6	3
No. of nuclei in class III	6	2	2 (?)		

II are found for elements of rather low atomic number. This is somewhat analogous to the normal states of extranuclear electrons where elements with low atomic number generally have rather low J values. In class III most of the I values have been determined for nuclei of moderately large atomic number, making the difference between classes II and III even more pronounced. Since nuclear magnetic moments depend directly upon the values of I, the smaller I values found for nuclei of class III will in part explain their smaller magnetic moments. If, however, we compare nuclei with the same I value (e.g., $I=1/2$ or $3/2$ in Fig. 1) we find that nuclei of class II have the larger magnetic moments and consequently the larger g-factors.

The results in Tables I and II and in Fig. 1 suggest a correlation between nuclear properties and the periodic table; namely that *nearly all nuclei which have large magnetic and mechanical moments lie in those columns of the periodic table for which Z is odd, while nuclei found in columns with Z even generally have small, positive or negative (or zero) magnetic moments and rather small (or zero) mechanical moments.* There is, then, more or less of an alternation of nuclear moments throughout the periodic table as Z alternates from odd to even. While it is not our intention at this time to attempt an explanation of these suggested generalizations, yet it seems probable that their true explanation does depend upon whether the total numbers of constituent particles (such as protons and neutrons) within nuclei are odd or even.

The results on N^{14} have been interpreted by Heisenberg and others as indicating that neutrons as well as protons, within complex nuclei, may possess a mechanical moment of $(1/2)(h/2\pi)$. This suggestion may be supported by $I=2/2$ for H^2 and by the half integral I values of nuclei of class III. The small magnetic moment of N^{14} (coupled with the fact that $I=2/2$) has been interpreted by Bacher[7] on the assumption that the neutron possesses a magnetic moment of

magnitude comparable with that of a proton but opposite in sign. This suggestion may find some support from the experimental result that negative nuclear g-factors have been observed only for certain members of class III (nuclei which present nuclear models would indicate contain an odd number of neutrons). If the neutron resembles the electron in having a magnetic moment which is anti-parallel to its mechanical moment, then obviously if the mechanical moments of a neutron and proton add, their magnetic moments oppose (e.g., N^{14}), while if their mechanical moments oppose, then their magnetic moments add. This possibility may explain, at least in part, the results observed in class II, where highest g-factors are observed when I is small and nuclei with high I values generally have rather small g-factors.

Landé,[8] Venkatesachar and Subbaraya[9] and others have considered the possibility of neutron shells within complex nuclei, while Venkatesachar[9] has attempted some correlation between I values and the numbers of neutrons present in incomplete outer shells. It is hoped that such a correlation might permit one to decide whether particles possess orbital angular momentum within nuclei or whether the observed I values can be quantitatively accounted for merely on the basis of their spin moments. It would, however, seem to the writer that for such a correlation we need more complete and more accurate data, for in a number of cases the present uncertainty in I amounts to as much as $2/2$ and sometimes even more.

It is a great pleasure to thank Mr. A. C. Nixon of the Chemistry Department and Professor H. E. White, Mr. S. S. Ballard and Dr. E. M. McMillan of the Department of Physics for their help in the organization and presentation of the material included in this paper.

[8] Landé, Phys. Rev. **43**, 620 and 624 (1933).

[9] Venkatesachar and Subbaraya, Cur. Sci. **1**, 120 (1932).

The Absorption Spectrum of Diatomic Bismuth

G. M. Almy and F. M. Sparks, *University of Illinois*

(Received July 6, 1933)

The absorption spectrum of diatomic bismuth, previously observed but not analyzed, has been obtained by heating pure bismuth in an atmosphere of nitrogen in a carbon-tube furnace at temperatures from 850 to 1500°C and also by heating in an evacuated quartz tube up to 1200°C. Four systems of bands have been photographed and analyzed: (1) the visible system, 4500A to 7900A, which consists of over 300 bands which have been arranged in square array extending to $v'=59$ and $v''=55$. (2) The ultraviolet system of 40 bands, 2600A to 2900A, which has its lower state in common with (1). (3) The far ultraviolet system, below 2250A, which is very difficult to obtain and measure but almost certainly has the same lower state as (1) and (2). (4) The violet system, appearing only at temperatures greater than 1000°C ((1), (2) and (3) appear below 900°C), which consists of 15 sharp band heads, 9 "continuous bands" and a series of closely spaced diffuse bands. Its lower state is the upper state of (1) and its upper state is presumably crossed by a repulsive state which accounts for the diffuse and continuous bands. There is also an extended continuum in the neighborhood of 3100A. Assuming that the lowest state dissociates into two normal $^4S_{3/2}$ bismuth atoms, a set of potential energy curves for the molecular states has been drawn with satisfactory extrapolation into atomic states in all cases. The estimated heat of dissociation of the lowest state is 1.71 volts.

THERE have been a number of observations[1, 2, 3, 4, 5, 6] on the absorption spectrum of molecular bismuth but no analysis of any of the band systems has been published.

There have been two studies of the fluorescence of Bi vapor with Hg radiation excitation. The first, by McLennan, Walerstein, and Smith[7] showed a group of lines excited by λ4358 which can be arranged in three series, each with an interval of about 300 cm^{-1}. The second, recently reported by Parys,[8] shows a series of triplets excited by λ4358 with an interval (from triplet to triplet) running from 309 cm^{-1} down and a series of doublets excited by λ5461 in which the interval from doublet to doublet is 173 cm^{-1} at the beginning of the series. The correlation between fluorescence and absorption spectra will be discussed later but it may be remarked here that the interval 173 is exactly that found in absorption for the normal state of Bi_2 whereas the interval 309 is nowhere to be found in the absorption spectrum.

[1] W. Grotrian, Zeits. f. Physik **18**, 169 (1923).
[2] R. K. Rao, Proc. Roy. Soc. **A107**, 760 (1925).
[3] A. L. Narayan and R. K. Rao, Phil. Mag. **50**, 645 (1925).
[4] A. L. Narayan and R. K. Rao, Proc. Phys. Soc. **A38**, 321 (1926).
[5] J. G. Frayne and A. W. Smith, Phil. Mag. **1**, 732 (1926).
[6] S. Barratt and A. R. Bonar, Phil. Mag. **9**, 515 (1930).
[7] McLennan, Walerstein and Smith, Phil. Mag. **3**, 390 (1927).
[8] J. Parys, Zeits. f. Physik **71**, 807 (1931).

Experimental Methods

The absorption spectrum was obtained with the use of a carbon-tube resistance furnace. The tube was 127 cm long, had an inside diameter of 2.54 cm and 0.64 cm walls. It was heated electrically over a length of 92 cm by a stepdown transformer with induction-regulator control. The tube was supported inside, but insulated from, a 15.2 cm steel tube which was filled with carborundum for heat insulation. This tube was in turn supported in the center of a 9.1 cm steel tube fitted with end plates on which were mounted quartz windows. These end plates were kept cool by circulating water through coils wrapped around the ends of the 9.1 cm tube. The current was led through water-cooled brass conductors through insulating plugs in the end plates and into the tube by large cylindrical blocks of carbon clamped to the heating tube.

Temperatures were measured with an optical pyrometer. A temperature of 2000°C could be

TABLE I. *The visible system.*

v′	v″	Int.	Observed frequency (cm^{-1})	Obs.-Calc.
28	54	0	13055.6	−4.5
27	53	0	13068.7	−3.0
26	52	0	13080.6	−2.2
25	51	0	13093.9	−1.7
24	50	0	13106.6	−1.4
23	49	0	13116.4	−4.3
22	48	0	13131.5	−2.2
30	55	0	13158.0	−3.6
29	54	0	13170.9	−2.8
28	53	0	13182.1	−3.9
27	52	0	13196.1	−1.6
26	51	0	13207.8	−3.5
25	50	0	13221.4	−2.9
24	49	0	13234.5	−3.2
23	48	0	13247.3	−4.0
22	47	0	13262.5	−3.7
21	46	0	13277.8	−1.7
20	45	0	13291.5	−2.4
19	44	0	13307.6	−1.1
18	43	0	13322.1	−1.7
27	51			−4.1
17	42	0	13336.8	−2.3
26	50			−3.2
25	49	0	13350.7	−3.2
24	48	0	13365.1	−3.1
23	47	00	13380.6	−2.2
22	46	0	13395.3	−2.4
21	45	0	13410.7	−2.2
20	44	0	13426.5	−1.8
19	43	0	13442.3	−1.8
18	42	0	13459.2	−0.9
17	41	0	13477.0	0.6
16	40	0	13493.8	0.8
15	39	0	13510.6	0.7
14	38	0	13527.2	0.1
13	37	0	13545.9	1.3
21	44			−1.3
20	43	0	13562.2	−1.5
19	42	0	13579.9	−0.4
18	41	0	13597.6	0.3
17	40	0	13614.1	−0.4
16	39	0	13632.1	−0.1
15	38	0	13650.1	0.1
14	37	0	13669.3	1.2
17	39	0	13754.2	0.5
16	38	0	13772.7	0.5
15	37	0	13790.5	−0.5
14	36	1	13810.0	−0.2
13	35	1	13830.2	0.7
12	34	1	13850.0	0.8
11	33	0	13872.6	0.7
17	38	0	13891.5	−2.2
10	32			2.0
16	37	0	13912.2	−1.0
9	31			2.1
15	36	0	13932.8	−0.3
8	30			1.8
14	35	1	13953.9	0.9
7	29			1.7
13	34	1	13974.5	1.1
12	33	1	13995.0	1.0
11	32	1	14016.8	−0.8
10	31	1	14037.5	1.4
9	30	0	14060.1	2.4
8	29	1	14081.8	2.3
12	32	0	14141.8	2.1
11	31	1	14164.0	−0.2
10	30	0	14185.3	1.5
9	29	1	14209.0	2.8
8	28	1	14231.8	2.8
7	27	1	14254.6	2.6
6	26	0	14277.1	1.8
10	29	0	14333.6	1.3
9	28	1	14357.6	2.0
8	27	2	14381.5	2.2
7	26	2	14405.4	2.1
6	25	1	14430.1	2.6
5	24	0	14453.5	1.5
4	23	0	14478.9	2.2
9	27	0	14510.1	4.1
8	26	1	14532.9	2.3
7	25	2	14558.6	3.2
6	24	2	14582.8	2.3
5	23	2	14607.8	1.9
4	22	1	14633.5	1.9
3	21	0	14659.0	1.5
9	26			1.8
2	20	0	14685.5	1.8
8	25			2.8
7	24	2	14710.5	2.1
6	23	2	14736.1	1.6
5	22	2	14762.6	1.9
4	21	2	14789.2	1.9
3	20	1	14816.3	0.3
2	19	0	14843.8	2.7
7	23	00	14865.2	2.8
6	22	0	14892.3	3.0
5	21	1	14918.2	1.8
4	20	1	14945.8	2.0
3	19	0	14973.6	2.1
2	18	00	15004.1	4.7
5	20	0	15074.9	1.9
4	19	1	15102.7	1.4
3	18	1	15132.2	2.4
2	17	1	15160.0	1.5
1	16	0	15188.1	0.6
4	18	0	15263.1	3.5
3	17	1	15291.0	2.1
2	16	1	15319.4	0.9
1	15	0	15348.6	0.2
3	16	0	15450.7	1.8
2	15	1	15479.5	0.1
1	14	1	15510.7	0.7
0	13	1	15541.7	0.9
4	0	1	18243.3	−1.5
2	14	0	15641.0	0.0
1	13	2	15673.1	0.7
0	12	2	15703 9	−0.2
2	13	1	15803.2	−0.2
1	12	2	15834.9	−0.8
0	11	1	15868.6	0.5
4	14	1	15901.8	0.7
1	11	1	15998.7	−1.0
0	10	2	16031.7	−1.3
4	13	0	16064.9	1.3
3	12	1	16097.2	0.1
0	9	2	16196.8	−1.8
3	11	0	16262.0	0.9
2	10	1	16295.2	−0.4
0	8	2	16363.3	−1.7
2	9	1	16460.3	−0.9
0	7	2	16530.9	−1.2
2	8	0	16627.2	−0.4
1	7	1	16662.1	−1.6
0	6	2	16697.7	−2.3
3	8	1	16756.6	−1.4
1	6	2	16829.1	−2.5
0	5	2	16866.5	−2.1
3	7	0	16924.0	−1.1
1	5	2	16997.5	−2.7
0	4	1	17036.0	−1.9
4	7	00	17053.2	−1.6
2	5	2	17129.1	−2.1
6	8	0	17145.8	0.4
1	4	2	17167.4	−2.1
4	6	1	17221.8	−0.9
2	4	2	17298.9	−1.6
1	3	2	17337.5	−2.0
3	4	1	17429.8	−1.1
2	3	2	17469.1	−1.4
5	5	1	17519.0	−1.5
4	4	00	17555.4	−5.2
3	3	3	17599.6	−1.3
2	2	2	17639.9	−1.3
4	3	1	17729.5	−1.2
3	2	2	17770.2	−1.4
6	4	1	17816.6	−1.7
–	–	00	17846.2	–
4	2	2	17900.1	−1.3
3	1	2	17944.6	1.6
5	2	2	18029.4	−1.1
4	1	3	18071.9	−0.8
3	0	0	18114.7	−0.3
6	2	1	18157.0	−2.1
5	1	3	18200.4	−1.5
6	1	3	18329.4	−1.0
5	0	1	18373.6	−0.4
7	1	2	18457.0	−1.4
6	0	2	18501.4	−1.1
8	1	2	18585.2	−0.5
7	0	2	18630.0	−0.4
10	2	0	18665.9	−1.1
–	–	0	18699.8	–
8	0	2	18757.2	−0.5
11	2	1	18791.9	−3.2
9	0	3	18884.0	−0.4
12	2	1	18916.9	−0.3
10	0	3	19010.0	−0.4
11	0	3	19135.6	−2.9
12	0	2	19260.0	−0.6
14	1	0	19336.2	0.0
13	0	2	19384.6	−0.2
15	1	00	19458.6	−0.5
18	3	0	19480.6	−1.1
14	0	2	19507.9	−0.4
16	1	1	19580.3	−1.0
15	0	2	19631.0	−0.1
17	1	1	19703.0	0.2
16	0	1	19753.0	−0.3
18	1	2	19823.0	−0.8
17	0	2	19874.6	−0.3
19	1	1	19943.6	−0.4
18	0	0	19995.4	−0.4
21	2	0	20010.7	−0.5
20	1	0	20063.2	−0.4
23	3	0	20075.9	−0.3
19	0	0	20115.5	−0.6
22	2	1	20129.4	0.0
21	1	1	20182.4	−0.1
24	3	00	20193.8	0.6
23	2	1	20246.7	−0.3
22	1	0	20300.6	−0.1
25	3	0	20309.5	0.0
24	2	1	20363.7	−0.2
23	1	0	20418.7	0.4
26	3	0	20425.6	0.4
25	2	0	20479.7	−0.5
28	4	1	20483.6	−0.7
30	5	1	20539.6	−1.8
27	3			−0.5
26	2	1	20596.6	0.7
29	4			−1.3
28	3	1	20654.0	−0.3
27	2	1	20709.9	−0.9
30	4			−0.8
29	3	2	20767.6	−0.3
34	6	00	20811.0	−5.1
28	2	1	20823.7	−1.3
31	4			0.8
30	3	1	20880.2	−0.5
32	4	0	20934.0	−0.4
34	5	0	20985.6	0.9
31	3	0	20991.9	−1.0
28	1	00	20997.0	0.6
36	6	0	21035.8	0.3
33	4	0	21043.9	−1.3
35	5	0	21094.9	−0.5
32	3	0	21105.0	0.6
34	4	0	21154.8	0.8
31	2	0	21162.8	−0.8
42	9	0	21171.0	−0.4
39	7	0	21190.0	0.5
36	5	1	21203.6	−0.5
33	3	0	21214.4	−0.8
30	1	0	21224.0	1.2
41	8	0	21235.5	2.2
38	6	0	21250.7	−0.1
35	4	0	21264.2	−0.5
32	2	0	21275.7	0.6
43	9			0.6
40	7	0	21296.0	0.7
37	5	0	21311.6	−0.9
34	3	0	21324.4	0.4
39	6	1	21358.1	0.8
36	4	1	21373.7	0.3
41	7	1	21401.1	0.7
38	5	1	21418.6	−0.7
46	10			2.4
43	8	0	21442.5	1.1
40	6	0	21463.7	0.5
37	4	1	21481.7	−0.6
45	9			1.4
42	7	1	21504.6	−0.3
39	5	1	21526.5	0.6
44	8	0	21547.0	2.6
41	6	0	21568.2	−0.1
46	9	00	21583.2	1.4
38	4	0	21588.7	0.0
43	7	0	21610.1	1.5
48	10	00	21618.5	1.5
40	5	0	21632.2	0.4
45	8	0	21649.7	3.0
42	6	0	21673.3	0.6
47	9	1	21683.5	0.9
39	4	00	21695.0	−0.2
44	7	1	21712.9	1.4
41	5	00	21736.3	−0.6
46	8	1	21750.4	2.2
43	6	0	21777.6	1.2
48	9	1	21781.8	−0.8
40	4	00	21801.2	0.1
45	7	1	21816.0	2.2
50	10			1.1
47	8	1	21850.1	1.2
44	6	1	21881.6	2.2
49	9			−0.3
46	7	1	21914.9	−0.4
51	10			2.2
43	5	00	21945.0	0.0
48	8	00	21950.5	1.5
50	9	1	21982.1	1.6
47	7	0	22014.8	−1.3
54	11	00	22039.7	2.9
49	8	00	22047.4	−0.9
56	12	00	22057.4	−4.2
51	9	1	22081.3	3.0
53	10	0	22108.5	2.4
48	7	00	22118.0	1.9
55	11	00	22134.3	2.7
50	8	1	22148.5	1.6
52	9	1	22177.3	1.9
54	10	00	22204.5	2.9
56	11	0	22225.2	−0.4
51	8	1	22247.7	3.0
53	9	0	22271.4	−0.3
55	10	0	22298.1	1.7
57	11	0	22318.0	−0.9
52	8	0	22342.2	0.4
54	9	0	22370.0	2.8
56	10	0	22389.4	−1.1
58	11	0	22410.0	−1.4
57	10	0	22481.2	−2.6
59	11	0	22503.7	0.5
56	9	0	22555.5	−0.6
57	9	0	22645.4	−4.0
56	8	0	22724.0	1.5
–	–	0	22806.4	–
–	–	0	22887.3	–
–	–	00	22968.0	–
–	–	00	23041.8	–

maintained indefinitely and a temperature of 2200°C for an hour or more. The maximum temperature used with bismuth was 1500°C. To reduce the oxidation of the tube nitrogen was flowed slowly through the furnace. To test the possibility that some of the spectra obtained were due to compounds of bismuth and carbon, nitrogen, or other impurities, some exposures, were taken in which the bismuth was placed in an evacuated quartz tube which was inserted in the carbon tube. Temperatures up to 1100°C could be used. No essential difference appeared in the spectrum. With the quartz absorption tube the bands were somewhat sharper and there were therefore rather more of them than could be seen on the plates at atmospheric pressure.

The bismuth used contained, according to the analysis of the manufacturers, Coleman and Bell Company, less than 0.01 percent iron, 0.04 percent silver, 0.01 percent zinc, as impurities. This analysis was checked by photographing with a vacuum arc, containing argon at various pressures, the emission spectrum of a sample of the bismuth. Examination showed silver to be the only impurity detectable.

As sources of continuous radiation, a Point-o-lite lamp and a tungsten ribbon filament lamp were used in the infrared and visible regions. In the near ultraviolet, a tungsten electrode of a Corex-glass "sun lamp" supplied a continuous background which was satisfactory though crossed by strong Hg lines. Through the ultraviolet a water-cooled, quartz, hydrogen discharge tube of a special, compact type, constructed by Kistiakowsky, provided an excellent source of continuous radiation.

For most of the work an E1 Hilger spectrograph with interchangeable glass and quartz parts was used. This instrument was supplemented with a smaller Bausch and Lomb quartz spectrograph and an E185 Hilger (10 foot Littrow mount). Two to four plates of each region were measured. Every plate was measured by each of two observers.

Observed Band Systems of Bi_2

The absorption spectrum of Bi_2 consists of four systems of bands with discrete structure and two regions of continuous absorption. Reproductions of three systems showing discrete bands and a region of narrow continuous bands appear in Fig. 1. The fourth discrete system, the far ultraviolet, is not reproduced. These various spectra and their analysis will be discussed in order in this section and in the following section a composite picture of the molecular states will be given by means of a potential energy diagram.

The visible system

The visible-infrared system extends from about 4500A to 7910A in which range 304 bands were measured. The visible part of the system appears first at a temperature of about 850°C and can be extended to the infrared by increasing the temperature, as shown in the first 6 photographs in Fig. 1. At the highest temperatures used, about 1500°C, the "red edge" of the system appears. It is, in fact, a double red edge at 7850A and 7910A and the separation is that to be expected if each edge is due to a sequence of bands (see Fig. 2). At high temperatures (above 1000°C) the bismuth vapor becomes luminous and a part of this system appears in emission in the red.

The wave numbers of the band edges are listed in Table I. The estimates of intensity are not of much significance except in a narrow range of wave numbers since no attempt was made to compare intensities in widely different regions. Vibrational quantum numbers, also in Table I, were assigned by fitting the observed wave numbers into a square array, testing continually for constant differences. The square array, extending to $v'=59$ and $v''=55$, is shown in Fig. 2. The assignments were easily made except near the violet end where there is some doubt. However, all but 6 bands, each of which was found on only one plate, fitted into the array. The bands fall into the usual parabolic order. The width of each branch of the parabola is quite small, indicating a close adherence to the Franck principle that the internuclear distance does not change much in a transition.

The mean values of the vibrational differences, $\Delta G(v+\frac{1}{2})$, for the various states are shown in Fig. 3. Curves A and B represent the lower and upper states, respectively, of the visible system. The data from which these curves were plotted

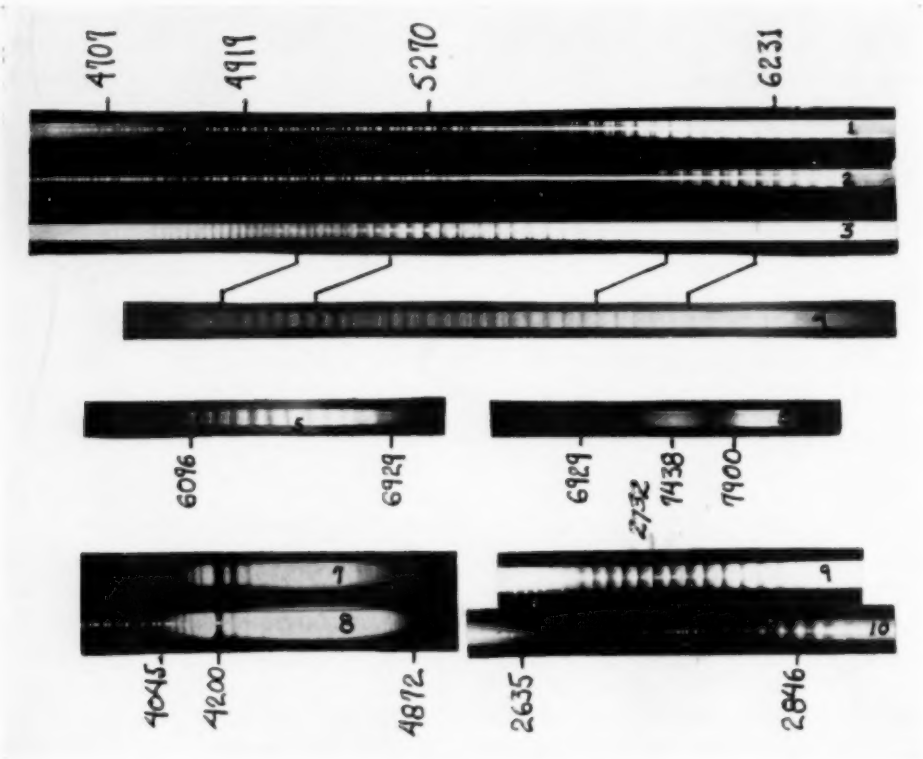

FIG. 1. Reproductions of photographs of Bi_2 band systems.

Exposure number	System	Temperature (°C)	Time of exposure	Exposure number	System	Temperature (°C)	Time of exposure
1	Visible	1075	40 sec.	6	Visible	1500	80 sec.
2	Visible	1155	15 sec.	7	Violet	1215	5 min.
3	Visible	1155	60 sec.	8	Violet	1215	2 min.
4	Visible	1250	16 min.	9	Ultraviolet	925	60 min.
5	Visible	1350	30 min.	10	Ultraviolet	900	4 min.

were used to obtain the molecular constants. Least squares calculations of $\Delta G'$ and $\Delta G''$ in powers of v' and v'', respectively, were transformed into the following expression for the wave number of the edge of the (v', v'') band of the system·

$$\nu = 17{,}742.3 + [132.205(v'+\tfrac{1}{2}) - 0.30090(v'+\tfrac{1}{2})^2 - 0.000{,}473{,}9(v'+\tfrac{1}{2})^3] - [172.708(v''+\tfrac{1}{2}) - 0.322{,}72(v''+\tfrac{1}{2})^2 - 0.002{,}320{,}9(v''+\tfrac{1}{2})^3 + 0.000{,}013{,}18(v''+\tfrac{1}{2})^4]. \quad (1)$$

As a check on the calculations and on the assignments of v' and v'', the wave numbers of all the bands were calculated by means of Eq. (1). The last column of Table I gives the difference of the observed and the calculated values. Following down the "obs.-calc." column one sees that this difference moves slowly up and down through a variation greater than the average fluctuation from band to band. The fluctuation is due to errors of measurement. The reduction of the slow variation is a matter of using more terms in the power series. (A fourth power equation was necessary to represent state A as accurately as the cubic represents state B.) There is no wide departure, however, and the fit is good enough at the extreme wave numbers so that Eq. (1) is considered adequate to represent the visible system.

It is interesting to compare the expression for the energy of the lower state with the fluorescence

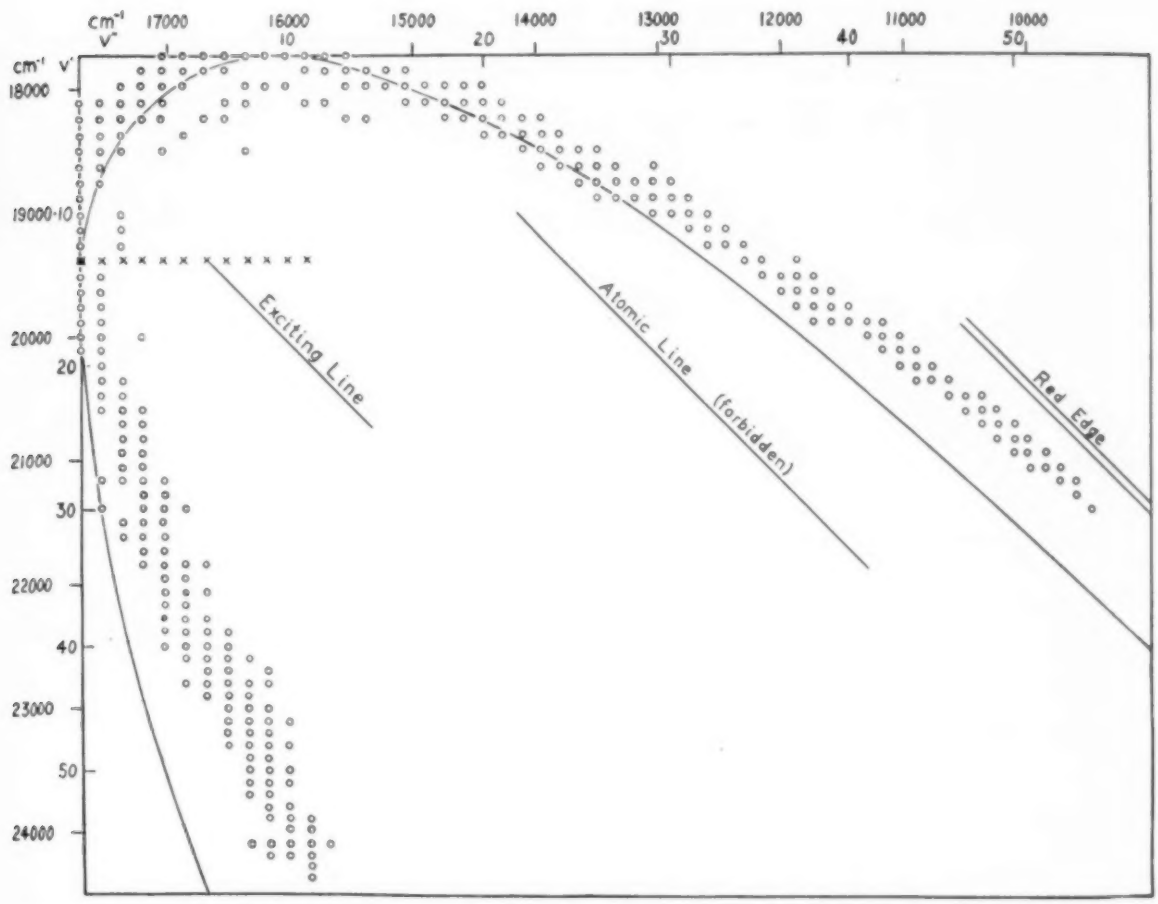

FIG. 2. Square array for the visible system. The circles represent measured band heads, plotted according to wave number. Projection to the upper, or left, axis at 45° gives the wave number of any band head. The red branch of the parabola shows a red edge, that is to say, it turns back on itself (on the wave number scale) beyond the point where measurements were obtained and leads almost certainly to dissociation with an atomic energy difference between upper and lower states of 15,437 cm^{-1}. The next eligible atomic energy is 21,600 cm^{-1}. The red edge appears to be double with a separation approximately equal to $\Delta G''$ ($=\Delta G'$ at the red edge) indicating that each edge is formed by a sequence. The solid curve is the Franck-Condon parabola constructed from the potential energy curves in Fig. 4. The crosses indicate the bands in which Parys observed fluorescence. It is rather remarkable that the progression is so much longer than that readily observed in absorption.

series formula given by Parys[8]:

$$\nu = 19{,}422.4 - 173.30(v''+\tfrac{1}{2}) + 0.324(v''+\tfrac{1}{2})^2 - 0.0074(v''+\tfrac{1}{2})^3.$$

The agreement is satisfactory. The constant 19,422.4 is not to be compared with the electronic frequency given in Eq. (1) but is the wave number of $v''=-\frac{1}{2}$ level for a higher v'' progression, probably the one for which $v'=13$. This probable correlation of the fluorescence series and the absorption bands is indicated by the series of crosses in Fig. 2.

The ultraviolet system

The ultraviolet system extends from 2600A to 2900A. It appears at about the same temperature as the visible system but the absorption is much more intense. The system is not greatly extended with increasing temperatures as is the visible system. Table II gives in square array the wave numbers, intensities and differences of the bands to which quantum numbers could be assigned. *s* indicates a band with a sharp edge, *d* a diffuse edge. The vibrational differences are plotted as crosses in Fig. 3. It is obvious that the lower state is state *A*, also the lower state of the

TABLE II. *The ultraviolet system.*

v' \ v''	0		1		2		3		4		5		6		7	
0	36447.0 d3	171.9	36275.1 d4	171.0	36104.1 d7	172.5	35931.6 d4	171.6	35760.0 d1							
	150.1		149.9				151.0		152.8							
1	36597.1 s9	172.1	36425.0 s6				36082.6 s1	169.8	35912.8 s5	169.2	35743.6 s7	169.0	35574.6 s5	167.0	35407.6 s3	165.5
	146.8						144.2						142.9		142.0	
2	36743.9 d7						36226.8 d2						35717.5 d3	167.9	35549.6 d3	166.0
	141.5															
3	36885.4 d5															
	141.1															
4	37026.5 d4															
Mean $\Delta G''$		172.0		171.0		172.5		170.7		169.2		169.0		167.4		165.7

v' \ v''	8		9		10		11		12		13	Mean $\Delta G'$
0												
1	35242.1 s0	170.2	35071.9 d0									150.9
	141.5		143.8									143.5
2	35383.6 d1	167.9	35215.7 d0									
			141.3									141.4
3			35357.0 d1	163.6	35193.4 d1	168.2	35025.2 d0					
					(125.0)		132.6					136.8
4					35318.4? d1	(160.6)	35157.8 s1	160.8	34997.0 s1	162.7	34834.3 s0	
Mean $\Delta G''$		169.0		163.6		168.2		160.8		162.7		

visible system. The upper state, marked C in Fig. 3, behaves in an erratic manner. Five vibrational levels are fairly definite, whereupon the bands become diffuse and their positions indefinite. Farther to the violet there are some fairly definite edges, listed in Table III, to which no satisfactory assignments could be made. It seems likely that some form of predissociation is occurring in this state but exposures under a wide variety of conditions of pressure, temperature and exposure time did not give enough data to disclose the process in detail. It may be noted that all bands with $v'=0$ are diffuse, those with $v'=1$ are sharp and most of those with v' greater than 1 are diffuse. From the graph in Fig. 3 the constants of state C were estimated as $\omega_e=157$ cm^{-1}, $x_e\omega_e=4.6$ cm^{-1}.

TABLE III. *Unassigned bands of the ultraviolet system. Wave-number (cm^{-1}), with intensity in parentheses.*

ν (cm^{-1})	ν (cm^{-1})
37167.1 (s5)	37300.0 (d2)
37340.0 (d3)	37446.2 (d0)
37611.0 (00)	37682.0 (00)
37789.0 (00)	37867.0 (00)

The far ultraviolet system

The far ultraviolet system extends from about 2250A to the violet and appears at a temperature of about 825°C. The bands are diffuse and accurate measurements were impossible. The mean of several measurements of the wave numbers is given in Table IV. What appears to be a v'' progression with the same vibrational interval as state A is fairly well developed as

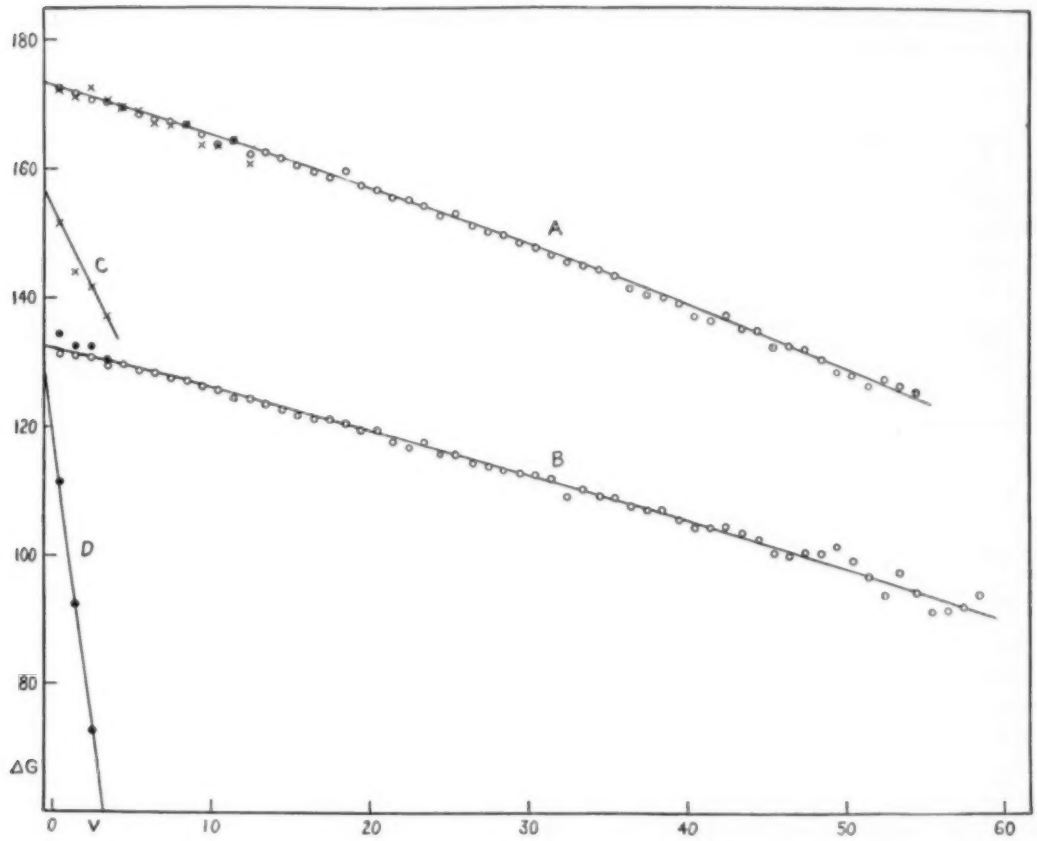

FIG. 3. Mean vibrational level differences of all observed states. Open circles are data from the visible system, crosses from the ultraviolet system, solid circles from the violet system. The intersection at the vertical axis gives ω_e. The areas under the curves, extrapolated to $\Delta G=0$, give the heats of dissociation.

TABLE IV. *The far ultraviolet system.*

Int.	ν (cm^{-1})	$\Delta\nu$	Int.	ν (cm^{-1})	$\Delta\nu$
0	44941		0	46176	164
0	45104	163	1	46522	2×173
0	45164		1	46650	
1	45330	166	1	46806	
1	45498	168	0	46932	
2	45673	175	0	47022	
1	45847	174	0	47090	
1	46012	165	0	47192	

indicated by the column of differences. This, together with the fact that the system appears at low temperatures, indicates that it has the same lower state as the visible and ultraviolet systems. The data are insufficient to justify any statement about the upper vibrational level.

The violet system

The violet system, which appears only at temperatures greater than 1000°C, consists of three parts, (1) a group of sharp-edged bands extending from 4050A to 4200A, (2) a series of diffuse "continuous bands" from 4200A to 4500A and (3) a group of closely spaced bands from 4000A to 4050A so weak and diffuse that no adequate measurements could be made. The wave numbers of the discrete bands are arranged in square array in Table V. The lower state of this system is state B, the upper state of the visible system. This is shown by the close agreement of the vibrational interval (see the solid circles on Fig. 3, state B). It is clearly possible, moreover, to put many molecules into state B by thermal excitation since the visible bands ($B\rightarrow A$) appear in emission at temperatures greater than 1000°C. The upper state of this system appears to be a very rapidly converging series of vibrational levels with $\omega_e=129$ cm^{-1}, $x_e\omega_e=9.7$ cm^{-1} as shown by curve D in Fig. 3.

TABLE V. *The violet system.*

v''	0		1		2		3		4	Mean $\Delta G'$
0	24485.3	134.6	24350.7	132.7	24218.0	132.6	24085.4	130.4	23955.0	
	s1		s4		s5		s4		s1	
	110.8		111.7		109.2		111.7			110.9
1	24596.1	133.7	24462.4	135.2	24327.2	130.1	24197.1			
	s2		s1		00		d0			
	92.5		90.3				94.1			92.3
2	24688.6	135.9	24552.7				24291.2			
	s1		d0				d0			
	72.2		74.8				71.0			72.7
3	24760.8	133.3	24627.5				24362.2			
	00		00				00			
Mean $\Delta G''$		134.4		134.0		131.4		130.4		
				Continuous Bands						
			22069		22654		23350			
			22246		22877		23578			
			22440		23104		23797			

Moreover, it breaks off rather suddenly, indicating predissociation into some perturbing state lying near. The existence of such a state is also suggested by the series of continuous bands (wave numbers in Table V) lying to the red of the discrete bands. These continuous bands are intense, rather narrow, symmetrical, regions of continuous absorption (see reproductions 7 and 8, Fig. 1). The intensity decreases rapidly as the series progresses to the red. An explanation of the origin of these bands will be given in the section on potential energy curves.

Continuous absorption

In the ultraviolet is a short series of continuous bands whose appearance is similar to that of the continuous bands of the violet system just described. Only 3 bands are observed, with wave numbers 40115, 40275 and 40467 cm^{-1}.

In addition to the continuous bands just described there is a region of continuous absorption which appears to be independent of any of the band systems. It appears, quite faint, at about 900°C with a maximum absorption at 3120A. At 1000°C it extends roughly from 2950 to 3350A. At 1050°C it overlaps the ultraviolet system and complete absorption occurs from 2600A to 3400A. At 1215°C it extends almost to the violet system as can be seen in reproductions 7 and 8 in Fig. 1.

POTENTIAL ENERGY CURVES AND HEATS OF DISSOCIATION

Although there are not enough data available to plot accurately the potential energy curves, it is worth while to go as far as possible in obtaining such a picture of the collection of molecular states. For this purpose the Morse expression for potential energy has been used. It may be stated

$$U(r) = E_e + D_e[1 - e^{-a(r-r_e)}]^2,$$

where E_e is the electronic energy, D_e the heat of dissociation, r_e the equilibrium internuclear distance and $a = [(8\pi^2\mu c x_e\omega_e)/h]^{\frac{1}{2}}$. The values of $x_e\omega_e$ and D_e may be obtained from the vibrational analysis but r_e, since there is no rotational analysis, can be estimated only by using the empirical fact that the product $r_e^3\omega_e$ is practically a constant for most molecules. The constant usually adopted is 3000×10^{-24}, an average value for several of the lighter symmetrical molecules. For the heaviest molecules known, however, (K_2, Br_2, I_2) the constant seems to be nearer 4000×10^{-24}. Bi_2 is, of course, much heavier than these but this constant was adopted in the hope that it would lead, at the least, to a consistent set of values of r_e for the four attractive states. Thus the values of r_e used here, in 10^{-8} cm, are, for state A, 2.85; for B, 3.10; for C, 2.95; for D, 3.15.

The heats of dissociation of the various states were obtained from the rates of convergence of the vibrational levels and the possible atomic energies of the products of dissociation. To begin with it was assumed that the lowest state (A) dissociated into two normal $^4S_{3/2}$ Bi atoms, in analogy with the lowest states of N_2 and P_2, the atoms of which have similar electronic configurations. Then state B was extrapolated to convergence, since the vibrational difference is more nearly linear (with increasing v) than in state A. The value of D_e obtained for state B was 11,516 cm^{-1}. This was added to the electronic frequency 17,742 cm^{-1} and the most likely atomic energy difference, 15,437 cm^{-1} (see Fig. 2) subtracted to give 13,821 cm^{-1} as the heat of dissociation of the lowest state A. This is equivalent to about 1.71 volts. As a check, direct extrapolation of state A gave 14,900 cm^{-1} as its heat of dissociation.

Since the Morse formula assumes a linear rate of convergence of ω_v, a value of $x_e\omega_e$ was determined from the mean slope of the curves A and B in Fig. 3 for v less than 30, rather than from the least squares calculation. This gave for A, $x_e\omega_e=0.41$; and for B, $x_e\omega_e=0.33$. With these constants, the potential energy curves for states A and B were calculated with the results shown in Fig. 4. These curves were used to locate the theoretical Franck-Condon parabola drawn in Fig. 2. While the fit is by no means perfect it indicates that the potential energy curves as drawn have considerable significance.

For state C the value of the heat of dissociation obtained by extrapolation is 2500 cm^{-1}, while the nearest available atomic levels $^2D_{3/2}+^2D_{5/2}$ indicate a dissociation energy of 4300 cm^{-1}. It is very likely that there is another curve such as N crossing C and perturbing it because, first, the vibrational levels of state C become diffuse and end prematurely and, second, such a perturbation would probably indicate an apparent heat of dissociation lower than the actual, as is the case here. It appears futile, then, to apply any particular form of potential energy expression. Assuming that dissociation occurs into the first available atomic states, the curve in Fig. 4 is a reasonable one passing through two known points, one at the minimum, one at dissociation. Its curvature near the minimum was obtained

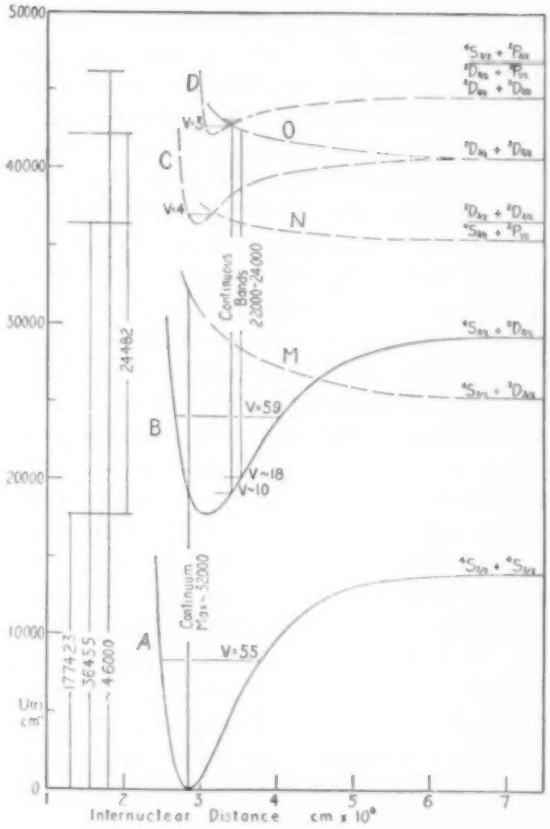

FIG. 4. Potential energy curves for states of Bi_2 molecule. A is the lower state of the visible, ultraviolet and far ultraviolet systems (electronic wave numbers shown at left). B is the upper state of the visible system and the lower state of the violet system. Curves C and D represent the upper states of the ultraviolet and violet systems, respectively. The continuous bands in the violet are supposed to be due to the transition from B to the repulsive state O. N is introduced to explain what appears to be predissociation in the ultraviolet system ($C\leftarrow A$). M would account for a broad continuum appearing around 3100A. The list of pairs of atomic states of Bi at the right contains all possible combinations of known states arising from the $6p^3$ atomic configuration. The dashed curves are less certain than the solid curves.

by using $x_e\omega_e=2.3$ (from Fig. 3) and $D=2500$ cm^{-1} in the Morse formula. The relative positions of A and C indicate, upon application of the Franck principle, a distribution of intensity like that actually found in the ultraviolet system, as described in Table II.

In state D the heat of dissociation from Fig. 3 appears to be only 400 cm^{-1}. The first available atomic energy, $^2D_{5/2}+^2D_{5/2}$, requires a heat of dissociation of about 2500 cm^{-1}. As in the case of state C, a reasonable curve is drawn in for state D. The curvature near the minimum lies between

that to be expected if D_e were 400 cm^{-1} and that if D_e were 2500 cm^{-1}. There is again qualitative agreement between the positions of the curves B and D and the distribution of intensity in the violet system (Table IV).

The premature breaking off of the upper levels of the violet system and the apparent depression of the heat of dissociation strongly suggests a crossing perturbing state such as O. Such a repulsive state as O provides, moreover, a satisfactory explanation of the closely-spaced diffuse bands between 4000A and 4050A and the continuous bands appearing above 4200A. The first group (4000A–4050A) may arise from the formation of a narrow attractive state formed above the crossing of states O and D. Such an explanation has been offered by Brown and Gibson[9] and by Brown[10] for similar bands observed in iodine chloride and iodine bromide. The continuous bands may well be due to transitions from B to O for, if O is not steep, and if the Franck principle of small change of internuclear distance in a transition is enforced each transition would give a narrow continuum. The width of each continuous band is of the order of magnitude of 200 cm^{-1} which is also about the width of one branch of the parabola in the square array of the visible system. The length of the vertical line from B to O near the crossing of D and O corresponds closely to the observed frequency of the first continuous band. Finally, the slope of this curve O was estimated by subtracting from the successive intervals between the continuous bands the proper vibrational intervals of state B. Extrapolation of state O indicates that it should approach infinity some 1000 cm^{-1} below the crossing of D and O. The first available atomic energy ($^2D_{3/2}+{}^2D_{5/2}$) is about 2000 cm^{-1} below the crossing point, which is satisfactory agreement since any error in the extrapolation of state B, the point of departure in locating the dissociation ends of the curves, would appear here. Thus if the extrapolated value of D_e (14,900 cm^{-1}) for state A is used to fix the starting point, the state O would extrapolate exactly into $^2D_{3/2}+{}^2D_{5/2}$.

There is what appears to be a similar set of continuous bands, though much weaker, in the far ultraviolet. These may arise from a similar transition to a repulsive curve above any of the curves in Fig. 4.

State M is drawn in to provide for the origin of the intense extended continuum in the near ultraviolet (about 3100A) which begins to appear at 900°C. The difference in character of this continuum and those just described is probably due to the steepness of curve M as compared with O. Any continuum is a series of overlapping continuous bands. The steeper the repulsive curve, the greater the overlapping.

There is not much basis for speculation on the kind of molecular states found in Bi_2. Assuming that the lowest state dissociates into two ^4S atoms and that Λ is a real quantum number in molecules of this weight the lowest state is probably $^1\Sigma$, in analogy with N_2 and P_2. However, transitions occur from state A to state B and B must dissociate into ^4S and ^2D atoms (if state A goes into two ^4S atoms), which atoms would ordinarily combine to form a triplet state. A triplet-singlet transition would not be surprising in such a heavy molecule. It is possible that further information about states A and B may be obtained from rotational analysis of high dispersion photographs of the visible system. There appears to be some resolution of fine structure on our plates.

There have been at least two determinations of the heat of dissociation of bismuth by molecular ray methods. The first, by Leu,[11] led, when corrected by Fraser,[12] to the result 1.15 ± 0.5 volts. The second determination, recently announced by Cheng Chuan Ko,[13] who used presumably a more accurate method, gave a much higher value, 3.21 ± 0.14 volts. Now our most probable value of the heat of dissociation of the lowest state of Bi_2 (state A) is 1.71 volts obtained

[9] W. G. Brown and G. E. Gibson, Phys. Rev. **40**, 529 (1932).

[10] W. G. Brown, Phys. Rev. **42**, 355 (1932).

[11] A. Leu, Zeits. f. Physik **49**, 504 (1928).

[12] R. G. J. Fraser, *Molecular Rays*, Cambridge (1931).

[13] Cheng Chuan Ko, Bull. Amer. Phys. Soc. **8**, No. 3, June 1, 1933. While we are not certain what bearing it has on Ko's result, it seems worth while to point out that at the temperatures used in his experiment (827°C to 947°C) many Bi_2 molecules are in the excited state B. At 1000°C the vapor is distinctly luminous, emitting the visible band system. In the molecular beam, then, there must be two kinds of Bi_2 molecules, differing in electronic energy by more than two volts.

by extrapolation of the upper state of the visible system and subtracting the proper atomic energy. The levels of state A were observed to extend above the nonvibrating state 1.0 volt (at $v=55$, where ΔG has dropped from 173 cm^{-1} to 126 cm^{-1}). Direct extrapolation of state A gave 1.84 volts for D_e; this process usually gives too high a value. It seems to us, therefore, extremely unlikely that the heat of dissociation of Bi_2 should be more than 2 volts or less than 1.5 volts.

The Absorption Spectrum of Chlorine Dioxide

Z. W. Ku, *Physical Laboratory, University of Michigan*

(Received May 22, 1933)

The spectrum of the visible and ultraviolet absorption bands of ClO_2 has been studied under various dispersions. The band heads were measured with high precision. The result of the vibrational analysis shows that the bands may be represented by

$$\nu = 20957.2 + 302.9(v_1' + \tfrac{1}{2}) - 2.3(v_1' + \tfrac{1}{2})^2 + 721.68(v_2' + \tfrac{1}{2}) - 2.797(v_2' + \tfrac{1}{2})^2 + 271.2(v_3' + \tfrac{1}{2}) - 4.42(v_1' + \tfrac{1}{2})(v_2' + \tfrac{1}{2}) - 3.9(v_1' + \tfrac{1}{2})(v_3' + \tfrac{1}{2}) - 5.9(v_2' + \tfrac{1}{2})(v_3' + \tfrac{1}{2}) - 529.0(v_1'' + \tfrac{1}{2}) - 1104.8(v_2'' + \tfrac{1}{2}) - 954.4(v_3'' + \tfrac{1}{2}) + 4.8(v_2'' + \tfrac{1}{2})^2,$$

yielding three normal frequencies for each upper and lower electronic state. The essential difference between the present analysis and that of the previous investigators is discussed. Rotational lines are partially resolved on the plates taken in the second order with a 21-foot grating. Two fundamental and one combination bands in the region 4–11μ were located with a self-recording spectrometer, and these are compared with the recent observation of Bailey and Cassie. Molecular constants have been calculated from a characteristic determinant given by Yates. They are found to be consistent with the observed isotope effect of chlorine.

THE absorption spectrum of chlorine dioxide has lately been studied by a number of investigators,[1, 2, 3] but the work of Urey and Johnston has been the most extensive. They have measured the bands in the region 5042–3226A. Their analysis of the vibrational structure yields three normal frequencies in the lower, and two in the upper electronic state. The observed intensity distribution has been found to be consistent with an extension of the Franck-Condon principle to polyatomic molecules.

Some time ago, as a preliminary for our study of intensity distribution in a band system of a triatomic molecule, the writer also examined the absorption spectrum of ClO_2 under various dispersions. In general, our measurements check well with those of Finkelnburg and Schumacher who photographed the spectrum with a two-meter grating, but they are more complete and extend into a higher frequency region. The rotational lines are partially resolved on our grating plates and reveal some interesting features. With a self-recording spectrometer,[4] the fundamental and combination bands in the region 4 to 11μ were found. Our observation has been confirmed by the recent work of Bailey and Cassie.[5] It is the purpose of this paper to present our experimental results, to propose a new interpretation of the origin of the various progressions in the band system based on their relative intensities and the infrared data, and to deduce certain molecular constants from the results of the present analysis.

Experimental

As a source of illumination in the visible region, a Phillips lamp was employed with a glass or quartz spectrograph, and a 500-watt tungsten lamp with a grating spectrograph. In the ultraviolet region a water-cooled hydrogen discharge tube of the Bay and Steiner type,[6] was used. Chlorine dioxide was prepared by reduction of Baker-analyzed potassium chlorate with oxalic crystals in the presence of a small amount of water as recommended by Bray.[7] The gas was dried, fractionated, and frozen into crystals which could be kept for some time.

Two absorption cells of 20 cm and 1 meter length were made of Pyrex with fused quartz

[1] Goodeve and Stein, Trans. Faraday Soc. **25**, 738 (1929).

[2] Finkelnburg and Schumacher, Zeits. f. physik. Chemie Bodenstein-Festband, 704 (1931).

[3] Urey and Johnston, Phys. Rev. **38**, 2131 (1931).

[4] Randall and Strong, Rev. Sci. Inst. **2**, 585 (1931).

[5] Bailey and Cassie, Nature **129**, 652 (1932). Proc. Roy. Soc. **A137**, 622 (1932).

[6] Bay and Steiner, Zeits. f. Physik **45**, 337 (1927); **59**, 48 (1929).

[7] Bray, Zeits. f. physik. Chemie **54**, 574 (1905).

plates cemented on both ends. The system was arranged for evacuation and circulation of the sample under observation. The pressure of the gas ranged from a few mm in the short cell to 1 atmosphere in the long cell. The best development of individual bands was found to be quite critical as to pressure, so it was not feasible to take a series of plates at once when working with the grating spectrograph.

The vibrational structure in the visible region was studied with the Michigan large glass spectrograph giving a dispersion of 9.0A per mm at 5000A, and in the ultraviolet region with a Hilger E1 quartz spectrograph. The rotational structure was photographed in the visible region with a 21-foot Rowland concave grating in a Paschen mounting giving a dispersion of 1.1A per mm at 4600A in the second order. Cramer's contrast and spectrum plates were used, and the time of exposure varied from fifteen to thirty minutes with a glass or quartz spectrograph, and two to four hours with a grating spectrograph. All the plates were taken at room temperature.

The plates were measured on a precision comparator. The wave-lengths were determined by comparison with the standard iron arc lines taken on the same plate. It is hoped that the wave numbers are correct within 1 cm^{-1} for the band heads. The precision of measurements for the bands with wave-length shorter than 3330A was comparatively low because from there on the bands are no longer sharp and it was found difficult to make proper settings. The intensities were estimated by eye and checked with microphotometer records.

Description of Spectrum

Fig. 1 is an enlarged reproduction of the spectrograms taken with a Hilger E1 spectrograph, and Fig. 2 is reprinted from the grating plates. An examination of the spectrograms reveals four or five well developed progressions indicated by the relative positions of the band heads, their intensities, and the similarity in the appearance of the rotational structure. The isotope effect of chlorine is prominent in certain bands, but ob-

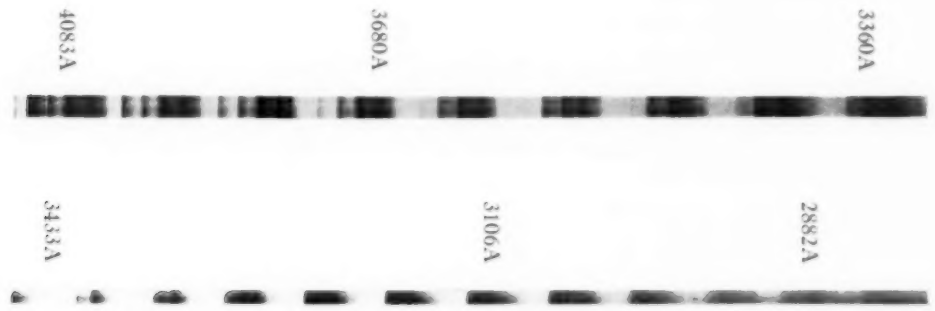

FIG. 1. Band system of ClO_2.

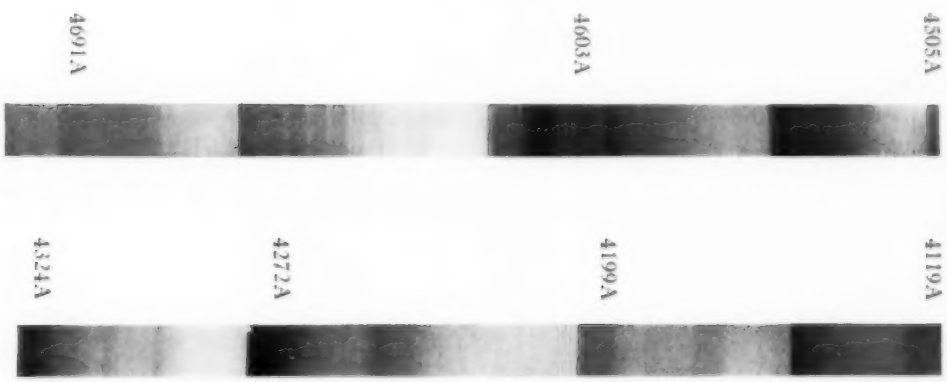

FIG. 2. Rotational structure of ClO_2 absorption bands.

TABLE I. *Wave numbers in vacuum.*

19,850.0	22,431.0	23,967.1	25,939.2	28,007.0	30,100	32,584
20,070.3	450.6	24,079.0	974.0	063.9	154	683
125.7	537.4	228.4	26,060.4	137.8	378	718
318.6	558.4	313.3	095.9	187.9	422	764
335.2	600.0	464.1	195.7	268.9	459	33,066
360.8	671.1	488.1	232.3	469.9	510	165
568.4	704.5	568.3	312.9	530.8	543	265
779.7	710.0	612.0	502.4	586.4	601	323
784.6	861.0	636.6	595.0	660.6	700	383
829.8	874.9	733.9	635.2	710.9	767	753
21,018.1	906.7	756.8	718.6	792.9	930	851
066.1	943.7	907.6	758.0	839.8	992	930
142.2	23,119.1	986.7	851.9	905.9	31,059	34,238
278.8	124.2	25,136.3	889.1	29,113.9	127	261
306.1	133.4	164.4	967.3	164.3	215	337
480.1	222.4	242.4	27,164.1	223.8	299	772
485.0	282.2	276.8	247.4	292.6	362	851
724.2	381.5	307.7	290.9	350.8	527	35,301
729.6	396.0	397.8	414.2	472.2	594	804
760.9	543.9	429.1	496.1	533.1	737	36,283
844.2	553.4	540.1	541.0	752.7	826	750
979.1	632.2	571.7	616.0	846.7	894	180
22,009.5	806.9	616.6	818.8	889.1	949	580
173.5	814.0	646.0	834.8	924.6	32,114	
177.7	900.0	836.0	893.6	980.6	183	
425.5	960.6	905.2	940.6	30,057.0	477	

scure in many others because of the high intensity near the band heads and the superposition of one band upon another. The relative intensity of various progressions and the isotope separation are seen in Fig. 3, which represents a part of the

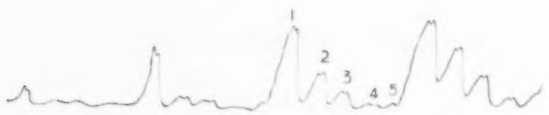

FIG. 3. 1. (0,8,0)←(0,0,0); 2. (0,9,0)←(1,0,0); 3. (1,8,0)←(0,0,0); 4. (0,10,0)←(0,0,1); 5. (1,8,1)←(0,0,0).

microphotometer records. The intensity of bands in each progression attains a maximum at about 3360A and decreases uniformly on either side of the maximum. All bands lying below 3000A fade away before their heads are reached. Several bands reported by the previous observers have not been confirmed, while additional ones have been found. In all we have measured 179 bands. The wave numbers in vacuum are given in Table I.

The great complexity of the rotational structure is evident. Each band consists of a few hundred lines of which many are unresolved. In general, the intensity of the band lines is highest near the head, decreasing rapidly toward the red till the lines merge into the head of a neighboring band. It is interesting to notice that in nearly all the bands certain intense lines show up in groups at almost regular intervals on the wave-length scale. This feature is very prominent in the most intense progression and may be seen in Fig. 2. We have measured the lines in a few bands in the visible region, but have not been able to make an analysis. For further study of the rotational structure it will be necessary to examine the spectrum under higher dispersion.

Near infrared absorption bands were found to exist in three regions. There is a doublet with maxima at 10.78μ and 10.44μ respectively; a broad, intense absorption region extends between 9.26–8.88μ; and a weaker band appears at 4.94μ. Weak absorption was also observed at 14.96μ and 4.28μ, but these are probably due to the presence of carbon dioxide as impurity. Two independent runs covering the region 1–19μ were made, and both records gave the same results.* The results of Bailey and Cassie[5] are compared with these in Table II. The first half of each double column gives their measurements and the second ours.

ANALYSIS OF BAND STRUCTURE

The analysis of Urey and Johnston[3] assumes the existence of three fundamental frequencies

* I should like to thank Professor W. W. Sleator for helping me to obtain these records.

TABLE II. *Infrared absorption bands.*

Band center (μ)		Maxima (cm^{-1})			Intensity	Identification†	
	14.96		668		weak		CO_2
		932	928				
10.57	10.61	963	958	20	medium	ν_3	ν_3
		1095	1080				
9.017	9.07	1106		50	intense	ν_1	ν_2
		1123	1126				
		1870					
5.307		1884?		2		$2\nu_3$	
		1900					
4.916	4.94	2034	2024	4	weak	$\nu_1+\nu_3$	$\nu_2+\nu_3$
	4.28		2336		weak		CO_2

† It should be pointed out that the assignment of ν_1 and ν_2 is quite arbitrary and an interchange of the subscripts introduces no change in the molecular constants.

which are not found in the infrared absorption. On the other hand, we are now quite sure that two of them are 1103 cm^{-1} and 943 cm^{-1} approximately, and we would expect them to be observable in the ultraviolet absorption. For according to the Boltzmann distribution law, molecules of a gas at ordinary temperatures will be present in appreciable numbers in all those higher states the energy of which does not differ from that of the lowest state by an amount of a higher order of magnitude than kT, while the majority of the molecules will be in the zero vibrational state. With the notation $(v_1', v_2', v_3') \leftarrow (v_1'', v_2'', v_3'')$ to represent a transition in absorption, and by taking the most intense v_2' progression to be $(0, v_2', 0) \leftarrow (0, 0, 0)$, we may look for those progressions originating from $(0, v_2', 0) \leftarrow (0, 1, 0)$ and $(0, v_2', 0) \leftarrow (0, 0, 1)$. These are found to be present. Among the bands in the long wavelength region a few members representing $(0, v_2', 0) \leftarrow (0, 0, 2)$ are also found. The third most intense v_2' progression may be regarded as arising from $(1, v_2', 0) \leftarrow (0, 0, 0)$. The assignment of bands to $(1, v_2', 0) \leftarrow (0, 0, 1)$ and $(1, v_2', 0) \leftarrow (0, 0, 2)$ then readily follows. We further note that of the remaining progressions three may be best accounted for as originating from the lowest level of the normal state to $(0, v_2', 0)$, $(1, v_2', 1)$, and $(2, v_2', 1)$ levels of the excited state. There remains but one well developed intense progression which probably originates from a first vibrational level of the normal state with a vibrational energy 529 cm^{-1}. We shall, with the previous investigators, regard it as representing $(0, v_2', 0) \leftarrow (1, 0, 0)$.

If this assignment of the origin of these progressions be adopted, their relative quantum numbers are fixed. The bands are thus arranged in Table III. Up to $\nu = 30{,}378$ cm^{-1} all but a few bands are included.

It has been found that the measurements can be represented by the following expression:

$$\begin{aligned}\nu = {} & 20{,}957.2 + 302.9(v_1'+\tfrac{1}{2}) - 2.3(v_1'+\tfrac{1}{2})^2 \\ & + 721.68(v_2'+\tfrac{1}{2}) - 2.797(v_2'+\tfrac{1}{2})^2 \\ & + 271.2(v_3'+\tfrac{1}{2}) - 4.42(v_1'+\tfrac{1}{2})(v_2'+\tfrac{1}{2}) \\ & - 3.9(v_1'+\tfrac{1}{2})(v_3'+\tfrac{1}{2}) - 5.9(v_2'+\tfrac{1}{2})(v_3'+\tfrac{1}{2}) \\ & - 529.0(v_1''+\tfrac{1}{2}) - 1104.8(v_2''+\tfrac{1}{2}) \\ & - \begin{cases} 954.4 \\ 940.6 \end{cases} (v_3''+\tfrac{1}{2}) + 4.8(v_2''+\tfrac{1}{2})^2.\end{aligned}$$

This formula applies only to bands with v_2' equal to or less than 15. The members in the $(0, v_2', 0) \leftarrow (0, 0, 1)$ progression follow $\omega_3'' = 954.5$ for $v_2' \leqq 7$ and $\omega_3'' = 940.6$ for $v_2' > 7$. The $\nu_{obs.} - \nu_{calc.}$ values are given in parentheses in Table III.

While several of these progressions extend far into the high frequency region no satisfactory formula has been obtained to represent this part of the spectrum. This is chiefly due to the irregularity in the $\omega_v : v^*$ relation. We shall return to this point later.

Knowing the three normal frequencies of vibration, we may proceed to calculate the force constants and the half-angle α at the apex of the triangular model XY_2. On the assumption that the forces are central about each atom, Dennison has obtained a characteristic equation[8] which enables us to express the force constants and the half-angle in terms of the frequencies of mechanical vibration of infinitesimal amplitudes. We find that with these two particular sets of observed frequencies his equation yields no consistent solutions. Yates,[9] on the other hand, as-

* Mulliken (Rev. Mod. Phys. **2**, 506 (1930)) defines $\Delta G(v+\frac{1}{2}) = G(v+1) - G(v)$. It follows that $\omega_e = \frac{1}{2}[\Delta G(v+\frac{1}{2}) + \Delta G(v-\frac{1}{2})]$.

[8] Dennison, Phil. Mag. **1**, 195 (1926).

[9] Yates, Phys. Rev. **36**, 555 (1930).

TABLE III. *Classification of bands. Values of* $\nu_{obs.}-\nu_{cal.c.}$ *are in parenthesis.*

	$(0, v_2', 0)\leftarrow(0, 0, v_3'')$			$(1, v_2', 0)\leftarrow(0, 0, v_3'')$		
v_2'	$v_3''=0$	1	2	$v_3''=0$	1	2
0	20318.6?(11.2)					
1	21018.1 (−0.2)	20070.3 (−3.2)	19134.1*(−4.2)	21306.1 (−1.9)	20360.8 (−2.4)	19424.4*(−3.6)
2	21724.2 (0.5)	20779.7 (0.8)	19841.7*(−2.0)	22009.5 (0.6)	21066.1 (2.0)	20125.7 (−3.2)
3	22425.5 (2.1)	21480.1 (1.5)	20542.3*(−1.1)	22704.5 (0.3)	21760.9 (1.5)	20829.8 (5.6)
4	23119.1 (1.6)	22173.5 (0.8)		23396.0 (2.1)	22450.6 (1.5)	
5	23806.9 (0.8)	22861.0 (−0.3)		24079.0 (0.9)	23133.4 (0.1)	
6	24488.1 (−0.9)	23543.9 (−0.3)		24756.8 (0.2)		
7	25164.4 (−2.0)	24228.4‡(6.8)		25429.1 (−0.5)		
8	25836.0 (−2.2)	24907.6 (−0.6)		26095.9 (−1.0)		
9	26502.4 (−1.9)	25571.7 (−2.6)		26758.0 (−0.6)		
10	27164.1 (−0.8)	26232.3 (−2.6)		27414.2 (−0.6)		
11	27818.8 (−1.1)	26889.1 (−0.8)		28063.9 (−1.5)		
12	28469.9 (0.6)	27541.0 (1.7)		28710.9 (0.5)		
13	29113.9 (0.8)	28187.9 (4.8)		29350.8 (1.1)		
14	29752.7 (1.4)			29980.6 (−2.9)		
15	30377.6 (−6.3)			30601.2		

v_2'	$(0, v_2', 1)$ $(0, 0, 0)$	$(0, v_2', 1)$ $(0, 0, 1)$	$(1, v_2', 1)$ $(0, 0, 0)$	$(2, v_2', 1)$ $(0, 0, 0)$	$(0, v_2', 0)$ $(1, 0, 0)$	$(0, v_2', 0)$ $(0, 1, 0)$
0	20568.4 (−5.3)	19625.4*(−3.5)		21142.2?(−7.3)		
1	21278.8 (0.1)	20335.2 (1.3)		21844.2 (−1.5)		
2	21979.1 (0.9)			22537.4 (1.1)		
3	22671.1 (−0.9)		22943.7?(−5.2)	23222.4 (1.1)		
4			23632.2 (−0.5)	23900.0 (−0.6)	22590.9 (2.4)	22009.5†(−3.2)
5			24313.3 (2.3)	24568.3 (−6.2)	23282.2 (5.1)	22704.5†(3.2)
6			24986.7 (3.1)	25242.4 (−0.3)	23960.6 (0.6)	23381.5 (−2.7)
7			25646.0 (−4.7)	25905.2 (−0.1)	24636.6 (−0.8)	24058.6*(−3.0)
8			26312.9 (0.8)	26549.5	25307.7 (−1.5)	24733.9 (0.5)
9			26967.3 (−0.6)		25974.0 (−1.3)	25397.8 (−1.7)
10			27616.0 (−2.2)		26635.2 (−0.7)	26060.4 (0.3)
11			28268.9 (6.0)		27290.9 (0.0)	26718.6 (3.5)
12			28905.9 (3.9)		27940.6 (0.3)	27368.6*(4.1)
13			29533.1 (−2.3)		28586.4 (2.3)	28007.0 (−1.3)
14			30154.2 (−9.1)		29223.8 (1.5)	
15					29846.7	

? Measured on one plate only.
* Measured by the previous observers.
† Coincidence with another band.
‡ Probably representing (1, 6, 0)←(1, 0, 0).

sumes that the force tending to restore a particle after a displacement is the sum of two types, the first acting along the line XY and obeying Hooke's law, the second, an angular restoring force acting at right angles to the first and proportional to the arc displacement of the Y's. His expression is

$$\lambda-K'[1/m+2\sin^2\alpha/M]=0,$$

$$\lambda^2-[(K'+2k)/m+2(K'\cos^2\alpha+2K\sin^2\alpha)/M]\lambda+2K'K(2/M+1/m)/m=0, \quad (1)$$

where K' and K are the force constants, m and M, the masses of the Y and X atoms respectively; α is the half-angle between the bonds and $\nu_i=\lambda_i^{\frac{1}{2}}/2\pi$, λ_i being the roots of Eqs. (1).

We have obtained two sets of solution for each electronic state. They are given in Table IV.

TABLE IV. $\omega(\text{cm}^{-1})$, $K(10^5$ dynes per cm).

	Normal state	Excited state
I	$\omega_1''=529$, $K'=6.74$	$\omega_1'=271.2$, $K'=0.56$
	$\omega_2''=1105$, $K=1.16$	$\omega_2'=721.7$, $K=1.56$
	$\omega_3''=954$, $\alpha=32°30'$	$\omega_3'=302.9$, $\alpha=49°27'$
II	$\omega_1''=954$, $K'=6.74$	$\omega_1'=302.9$, $K'=0.56$
	$\omega_2''=1105$, $K=0.87$	$\omega_2'=721.7$, $K=1.56$
	$\omega_3''=529$, $\alpha=60°40'$	$\omega_3'=271.2$, $\alpha=29°53'$

For the normal state, Bailey and Cassie[5] applying Hund's idea of chemical binding[10] and Dennison's investigation of an asymmetrical top molecule[11] consider the probable model to be an equilateral triangle, the length of the sides being approximately 1.2A. According to them the first

[10] Hund, Zeits. f. Physik **73**, 1, 565 (1932).
[11] Dennison, Rev. Mod. Phys. **3**, 280 (1931).

set of constants should be chosen. In obtaining this set of constants, we have assumed that the fundamental band 954 cm^{-1} corresponds to the unsymmetrical vibration ν_3 in which the electric moment oscillates along the axis of middle moment of inertia B, and hence there should be no zero branch. We assumed further that the fundamental band 1105 cm^{-1} is to be associated with a symmetrical vibration in which the electric moment oscillates along the axis of least moment of inertia A—in the present case, along the bisector of the angle between the bonds—and, therefore, a zero branch would be expected ($A/B \cong 0.8$). Now the envelopes of these bands appear to be in good accord with these characteristics. Thus we are led to the conclusion that the second set of constants is very improbable.

Now the doublet separation 30 cm^{-1} corresponds to a moment of inertia 52×10^{-40} g cm^2. This value may be associated with either the least or the largest moment of inertia. In the first case, we obtain 1.84×10^{-8} cm for the distance between O–Cl; in the second case, 1.22×10^{-8} cm. The model chosen ($\alpha = 32°30'$) is definitely in favor of the lower value.

In making a choice between the two sets of constants for the excited state, we shall turn to the theory of the isotope effect. Referring to Eqs. (1), we find that the calculated values of the isotope shift are somewhat too large compared with the observed values if the first set of constants (see Table IV) be used. On the other hand, from the second set we obtain a general agreement.

To a first approximation, the isotope shift is given by

$$\nu_2 - \nu_1 = \sum[(\rho_i' - 1)\omega_i'(v_i' + \tfrac{1}{2}) - (\rho_i'' - 1)\omega_i''(v_i'' + \tfrac{1}{2})],$$

where the subscripts 1 and 2 refer to the more and less abundant isotopes respectively, and ρ stands for the square root of the equivalent reduced masses, or $\rho = (\mu_1/\mu_2)^{\frac{1}{2}}$.

Using the second set of constants we obtain the following expressions for the isotope displacement:

$$(0, v_2', 0) \leftarrow (0, 0, 0), \quad \nu_2 - \nu_1 = 5.4 - 4.3v_2';$$

$$(1, v_2', 0) \leftarrow (0, 0, 0), \quad \nu_2 - \nu_1 = 3.1 - 4.3v_2';$$

$$(0, v_2', 0) \leftarrow (1, 0, 0), \quad \nu_2 - \nu_1 = 6.1 - 4.3v_2';$$

$$(0, v_2', 0) \leftarrow (0, 0, 1), \quad \nu_2 - \nu_1 = 10.6 - 4.3v_2'.$$

For the reasons already mentioned the isotope bands could be measured only with difficulty. In many cases the displacements turn out to be quite irregular; in others, our measurements do not check with those of previous observers. The observed and calculated values are compared in Table V. Perhaps without a knowledge of the band centers and the rotational structure a closer agreement can hardly be expected.

TABLE V. *Isotope bands.*

	$(0, v_2', 0) \leftarrow (0, 0, 0)$		$(1, v_2', 0) \leftarrow (0, 0, 0)$		$(0, v_2', 0) \leftarrow (1, 0, 0)$		$(0, v_2', 0) \leftarrow (0, 0, 1)$	
v_2'	Obs.	Calc.	Obs.	Calc.	Obs.	Calc.	Obs.	Calc.
4	−11.5*	−11.7	−14.5	−14.0				
5	−17.2*	−16.0	−20.4*	−18.3				
6	−24.0	−20.3	−22.9	−22.6	−22.4*	−19.6		
7	−28.1	−24.6	−31.3	−26.9	−24.6	−23.9		
8			−35.5	−31.2	−30.9	−28.2		
9			−38.3	−35.5	−34.8	−32.5	−31.6	−28.0
10				−39.8	−40.2	−36.8	−36.6	−32.3
11				−44.1	−43.5	−41.1	−37.2	−36.6
12			−50.3	−48.4	−47.0	−45.4	−44.9	−40.9
13				−52.7				
14			−56.0	−57.0				

* Measured by the previous observers.

Goodeve and Stein[1] have pointed out that there is a discontinuity in the curve when ω_v is plotted against v. The break in the curve occurs between $v_2' = 14$ and $v_2' = 15$, and has been accounted for as an indication of predissociation. From our measurements of the $(0, v_2', 0) \leftarrow (0,0,0)$ progression we have plotted this curve and is shown in Fig. 4. The curve is evidently nonlinear throughout its extent.

As has been pointed out by Birge[12] this feature is quite common with diatomic molecules, so

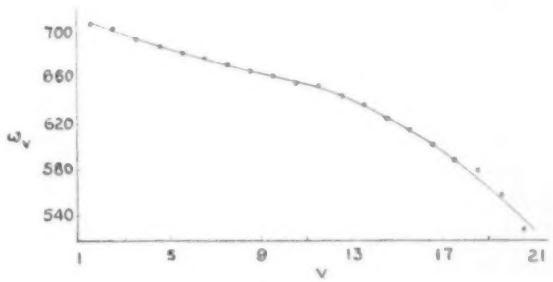

FIG. 4.

[12] Birge, Trans. Faraday Soc. **25**, 707 (1931).

presumably it must also exist with more complicated ones. Unfortunately, we have not been able to trace the curve beyond $v=20$ with certainty, although we have measured 30 members in this progression and there is every indication that it extends far beyond the limit of observation. In view of this nonlinear relationship between ω_v and v, and the limited extent of our observation, any extrapolation to determine the heat of dissociation will be untrustworthy.

Discussion of Results

It should be pointed out that the members forming the $(0, v_2', 0)\leftarrow(0, 0, 1)$ progression lie in regions where the $(1, v_2', 0)\leftarrow(1, 0, 0)$ progression should appear, and that the members representing the $(0, v_2', 0)\leftarrow(0, 1, 0)$ progression occupy the places where the isotope bands of the $(1, v_2', 0)\leftarrow(0, 0, 0)$ would be expected. This superposition effect very probably makes the intensity of these progressions higher than that estimated from the Boltzmann temperature factor $e^{-W/KT}$.

The present analysis yields three normal frequencies. There seems to be no obvious reason why no more bands forming a v_1' or v_3' progression could be found. As has been pointed out in an early paragraph, the intensity in the most intense v_2' progression increases rapidly at first with the vibrational quantum number, reaches a maximum at about $v_2'=15$, and then decreases gradually. This most favored transition is connected with the change in the molecular configuration due to the electronic transition and is discussed in the following paper.

It is seen that the constants calculated from the electronic band spectrum data are in good agreement with the values deduced by Bailey and Cassie[5] from the infrared band spectrum. This seems to support the results of the present analysis. However, in evaluating the molecular constants for the normal state we have assumed the existence of a fundamental band $\nu_1=529$ cm^{-1} which has not been observed in the infrared absorption. This band, if it really exists, should lie approximately at 19μ which was the limit of our observation.

I wish to thank Professor D. M. Dennison for the guidance of this work, Professor W. F. Colby for helpful suggestions and discussions, and Professor R. A. Sawyer for kind help and advice during the course of experimentation.

Intensity Distribution in a Band System of Symmetrical Triatomic Molecules

Z. W. Ku, *Physical Laboratory, University of Michigan*

(Received May 22, 1933)

The Franck-Condon theory has been extended to a study of band intensities of a triatomic molecule of the general type XY_2. The most probable transitions are found to be

$$v_1' = \begin{cases} A_1 \pm B_1 v_1^{\frac{1}{2}} \pm C_1 v_2^{\frac{1}{2}} + D_1 v_1 + E_1 v_2 - F_1 v_1 - G_1 v_2 + H_1 (v_1 v_2)^{\frac{1}{2}} \\ A_1 \pm B_1 v_1^{\frac{1}{2}} \mp C_1 v_2^{\frac{1}{2}} + D_1 v_1 + E_1 v_2 - F_1 v_1 - G_1 v_2 - H_1 (v_1 v_2)^{\frac{1}{2}} \end{cases}$$

$$v_2' = \begin{cases} A_2 \pm B_2 v_1^{\frac{1}{2}} \pm C_2 v_2^{\frac{1}{2}} + D_2 v_1 + E_2 v_2 - F_2 v_1 - G_2 v_2 + H_2 (v_1 v_2)^{\frac{1}{2}} \\ A_2 \pm B_2 v_1^{\frac{1}{2}} \mp C_2 v_2^{\frac{1}{2}} + D_2 v_1 + E_2 v_2 - F_2 v_1 - G_2 v_2 - H_2 (v_1 v_2)^{\frac{1}{2}} \end{cases}$$

$$v_3' = \begin{cases} (\nu_3/\nu_3') v_3 \\ (\nu_3'/\nu_3) v_3 \end{cases}$$

where the v's with and without a prime refer to the vibrational quantum numbers of the upper and lower states, respectively, and the values of the coefficients depend on the atomic masses, normal frequencies, force constants, and molecular dimensions. Two special cases which occur when the three atoms become equal and when the three atoms lie along a straight line are also considered. A wave mechanical treatment is outlined. It is found that for a triangular model the integrals, which measure the transition probabilities, corresponding to the $(v_3', 0)$ transitions when v_3' is an odd integer all vanish, and that for a linear model, in addition to these, all integrals pertaining to the $(v_2', 0)$ transitions when v_2' is an odd integer become zero. These results are, however, not to be interpreted as selection rules; they are simply consequences of the assumption of particular force fields. The results have been discussed in connection with the band intensities of ClO_2. It is shown that a knowledge of the structure of the excited molecule is essential to test quantitatively the results of the present work.

Introduction

As is well known, the relative intensities of bands in a band system are determined jointly by the initial distribution of molecules among the vibrational states and by the transition probabilities. The first factor depends, in emission, on experimental conditions such as temperature, pressure, mode of excitation, etc., and, in absorption, on the Boltzmann factor. In the following work we shall primarily be concerned with the transition probabilities in the absorption process at ordinary temperatures.

Based on Franck's theory of photochemical activity of molecules, Condon[1] has shown that the intensity distribution is definitely connected with the relative forms of $U'(r)$ and $U''(r)$ curves, and that in general there will be two or more most probable transitions for a given value of v' and v''. He has also shown how the wave mechanics predicts the small but nonvanishing values of the transition probabilities outside the classical motion.

While many applications have been made to spectra of diatomic molecules, particularly absorption spectra, this principle has not as yet been applied in detail to polyatomic molecules. Recently Urey and Johnston[2] have found that the intensity distribution in the band system of ClO_2 satisfies qualitatively the Franck-Condon rule, but, as the writer has elsewhere[3] pointed out, their analysis cannot be entirely correct and any improper correlation of the fundamental frequencies with the characteristic vibrations might vitiate their conclusions.

Despite our meager knowledge as regards the theory of electronic band spectra of polyatomic molecules and the acutal forces that govern the nuclear motion of a complicated molecule, it might be of interest to question what sort of intensity distribution is to be expected from an extension of the Franck-Condon principle. In the present paper, we shall consider only molecules of the general type XY_2 and two special cases which occur when the three atoms are equal and when the three atoms lie along a straight line.

[1] Condon, Phys. Rev. **28**, 1182 (1926); Proc. Nat. Acad. Sci. **13**, 462 (1927); Phys. Rev. **32**, 858 (1928).

[2] Urey and Johnston, Phys. Rev. **38**, 2131 (1931).

[3] The preceding paper, Ku, Phys. Rev. **44**, 376 (1933).

An Extension of the Franck-Condon Theory

For simplicity we shall assume that the atoms lie in a plane in the form of an isosceles triangle with the X atom at the apex. Let us introduce a set of coordinates q, x, y, and α to specify the molecular configuration, q being the relative displacement of the two Y atoms, x and y, the displacements of the X atom relative to the center of gravity of the Y atoms, and α the half angle at the apex of the isosceles triangle. To a first approximation, when the forces are assumed to be central about each atom* and the amplitudes of vibration are taken to be infinitesimal compared to the nuclear distances in equilibrium, the potential and kinetic energies expressed in the normal coordinates take the following simple form:

$$V=\tfrac{1}{2}(\lambda_1\xi_1^2+\lambda_2\xi_2^2+\lambda_3\xi_3^2), \qquad T=\tfrac{1}{2}(\dot{\xi}_1^2+\dot{\xi}_2^2+\dot{\xi}_3^2),$$

in which the ξ's are obtained from the following transformation:

$$q=a_1\xi_1+a_2\xi_2, \qquad y=b_1\xi_1+b_2\xi_2, \qquad x=c\xi_3, \tag{1}$$

and the coefficients are given by

$$a_1=\frac{2}{m}\left(\frac{K+\tfrac{1}{2}K'\sin^2\alpha-\tfrac{1}{2}m\lambda_2}{\lambda_1-\lambda_2}\right)^{\frac{1}{2}}, \qquad a_2=\frac{2}{m}\left(\frac{\tfrac{1}{2}m\lambda_1-K-\tfrac{1}{2}K'\sin^2\alpha}{\lambda_1-\lambda_2}\right)^{\frac{1}{2}},$$

$$b_1=-\frac{1}{m\mu^{\frac{1}{2}}}\left(\frac{\tfrac{1}{2}m\lambda_1-K-\tfrac{1}{2}K'\sin^2\alpha}{\lambda_1-\lambda_2}\right)^{\frac{1}{2}}, \qquad b_2=\frac{1}{m\mu^{\frac{1}{2}}}\left(\frac{K+\tfrac{1}{2}K'\sin^2\alpha-\tfrac{1}{2}m\lambda_2}{\lambda_1-\lambda_2}\right)^{\frac{1}{2}},$$

$$c=[2m\mu(1+\mu\cot^2\alpha)]^{-\frac{1}{2}},$$

where K and K' are the force constants, m and M the masses of the X and Y atoms, respectively, and λ's the three roots of the characteristic determinant[4]

$$\left[\left(\frac{m\lambda}{K'}\right)^2-2\left(\gamma+\frac{1}{2}+\frac{m}{M}\cos^2\alpha\right)\frac{m\lambda}{K'}+\frac{2\gamma}{\mu}\cos^2\alpha\right]\left[\frac{m\lambda}{K'}-1-\frac{2m}{M}\sin^2\alpha\right]=0,$$

where $\gamma=K/K'$, $\mu=M/(2m+M)$.

Evidently the vibratory motion of the system may be regarded as the motions of three independent equivalent harmonic oscillators with frequencies $\nu_i=\lambda_i^{\frac{1}{2}}/2\pi$. Now the motion of the ith simple harmonic oscillator expressed in the action and angle variables is given by

$$P_i=(2\mu_i\nu_iJ_i)^{\frac{1}{2}}\cos 2\pi W_i, \qquad \xi_i=(1/2\pi)(2J_i/\mu_i\nu_i)^{\frac{1}{2}}\sin 2\pi W_i.$$

---

[4] Dennison, Phil. Mag. **1**, 195 (1926).

* This restriction is in fact not necessary, for if we, with Yates[5] assume that the force tending to restore a particle after a displacement is the sum of two types, the first acting along the line XY and obeying Hooke's law, the second, an angular restoring force, acting at right angles to the first and proportional to the arc displacement of the Y's the characteristic determinant now takes the following form:

$$\left[\frac{\lambda m}{k'}-1-\frac{2m}{M}\sin^2\alpha\right]\left[\left(\frac{\lambda m}{k'}\right)^2-2\left(\frac{1}{2}+\frac{m}{M}\cos^2\alpha+\frac{\gamma}{\mu}\sin^2\alpha\right)\frac{\lambda m}{k}+\frac{2\gamma}{\mu}\right]=0$$

and the coefficients in Eqs. (1) become

$$a_1=\frac{2}{m}\left(\frac{K\cos^2\alpha+\tfrac{1}{2}K'\sin^2\alpha-\tfrac{1}{2}m\lambda_2}{\lambda_1-\lambda_2}\right)^{\frac{1}{2}},$$

$$a_2=\frac{2}{m}\left(\frac{\tfrac{1}{2}m\lambda_1-K\cos^2\alpha-\tfrac{1}{2}K'\sin^2\alpha}{\lambda_1-\lambda_2}\right)^{\frac{1}{2}},$$

$$b_1=-\frac{1}{m\mu^{\frac{1}{2}}}\left(\frac{\tfrac{1}{2}m\lambda_1-K\cos^2\alpha-\tfrac{1}{2}K'\sin^2\alpha}{\lambda_1-\lambda_2}\right)^{\frac{1}{2}},$$

$$b_2=\frac{1}{m\mu^{\frac{1}{2}}}\left(\frac{K\cos^2\alpha+\tfrac{1}{2}K'\sin^2\alpha-\tfrac{1}{2}m\lambda_2}{\lambda_1-\lambda_2}\right)^{\frac{1}{2}},$$

$$c=\frac{1}{[2m\mu(1+\mu\cot^2\alpha)]^{\frac{1}{2}}}.$$

[5] Yates, Phys. Rev. **36**, 555 (1930).

Following Condon we shall assume that the transition occurs instantaneously and that the motion of the massive nuclei is unaffected during the transition, then the following conditions must be satisfied:

$$q'=q''+q_0,\quad y'=y''+y_0,\quad x'=x'',\quad p_q'=p_q'',\quad p_y'=p_y'',\quad p_x'=p_x'',$$

where q_0 and y_0 denote the change in the nuclear distances of the normal configuration. Referring to Eqs. (1) we can immediately write down the following set of equations:

$$\frac{a_1'}{2\pi}\left(\frac{2J_1'}{\nu_1'}\right)^{\frac{1}{2}}\sin 2\pi W_1'+\frac{a_2'}{2\pi}\left(\frac{2J_2'}{\nu_2'}\right)^{\frac{1}{2}}\sin 2\pi W_2'=q_0+\frac{a_1}{2\pi}\left(\frac{2J_1}{\nu_1}\right)^{\frac{1}{2}}\sin 2\pi W_1+\frac{a_2}{2\pi}\left(\frac{2J_2}{\nu_2}\right)^{\frac{1}{2}}\sin 2\pi W_2,$$

$$a_1'(2\nu_1'J_1')^{\frac{1}{2}}\cos 2\pi W_1'+a_2'(2\nu_2'J_2')^{\frac{1}{2}}\cos 2\pi W_2'=a_1(2\nu_1J_1)^{\frac{1}{2}}\cos 2\pi W_1+a_2(2\nu_2J_2)^{\frac{1}{2}}\cos 2\pi W_2,\text{ etc.},$$

all double primes which refer to the lower state being dropped for the sake of convenience.* Solving for J_i' in terms of J_i and W_i by eliminating W_i', writing θ_i for $2\pi W_i$ and replacing J_i by v_ih, we obtain

$$\begin{aligned}
v_1' &= A_1+B_1\sin\theta_1(v_1)^{\frac{1}{2}}+C_1\sin\theta_2(v_2)^{\frac{1}{2}}+D_1v_1+E_1v_2+F_1\cos 2\theta_1v_1+G_1\cos 2\theta_2v_2\\
&\qquad +H_1\sin\theta_1\sin\theta_2(v_1v_2)^{\frac{1}{2}}+I_1\cos\theta_1\cos\theta_2(v_1v_2)^{\frac{1}{2}},\\
v_2' &= A_2+B_2\sin\theta_1(v_2)^{\frac{1}{2}}+C_2\sin\theta_2(v_2)^{\frac{1}{2}}+D_2v_1+E_2v_2+F_2\cos 2\theta_2v_2+G_2\cos 2\theta_2v_2\\
&\qquad +H_2\sin\theta_1\sin\theta_2(v_1v_2)^{\frac{1}{2}}+I_2\cos\theta_1\cos\theta_2(v_1v_2)^{\frac{1}{2}},\\
v_3' &= D_3v_3+F_3\cos 2\theta_3v_3,
\end{aligned}\qquad (2)$$

where

$$\begin{aligned}
A_1&=(2\pi^2\nu_1'/ha^2)(b_2'q_0-a_2'y_0)^2, \qquad A_2=(2\pi^2\nu_2'/ha^2)(b_1'q_0-a_1'y_0)^2,\\
B_1&=(2/a^2)(b_2'q_0-a_2'y_0)(a_1b_2'-b_1a_2')(2\pi^2\nu_1'^2/h\nu_1)^{\frac{1}{2}},\\
B_2&=(2/a^2)(b_1'q_0-a_1'y_0)(a_1b_1'-b_1a_1')(2\pi^2\nu_2'^2/h\nu_1)^{\frac{1}{2}},\\
C_1&=(2/a^2)(b_2'q_0-a_2'y_0)(a_2b_2'-b_2a_2')(2\pi^2\nu_1'^2/h\nu_2)^{\frac{1}{2}},\\
C_2&=(2/a^2)(b_1'q_0-a_1'y_0)(a_2b_1'-b_2a_1')(2\pi^2\nu_2'^2/h\nu_2)^{\frac{1}{2}},\\
D_1&=(1/2a^2)(a_1b_2'-b_1a_2')^2(\nu_1/\nu_1'+\nu_1'/\nu_1),\\
D_2&=(1/2a^2)(a_1b_1'-b_1a_1')^2(\nu_1/\nu_2'+\nu_2'/\nu_1),\\
D_3&=\tfrac{1}{2}(\nu_3/\nu_3'+\nu_3'/\nu_3),\\
E_1&=(1/2a^2)(a_2b_2'-b_2a_2')^2(\nu_2/\nu_1'+\nu_1'/\nu_2),\\
E_2&=(1/2a^2)(a_2b_1'-b_2a_1')^2(\nu_2/\nu_2'+\nu_2'/\nu_2),\\
F_1&=(1/2a^2)(a_1b_2'-b_1a_2')^2(\nu_1/\nu_1'-\nu_1'/\nu_1),\\
F_2&=(1/2a^2)(a_1b_1'-b_1a_1')^2(\nu_1/\nu_2'-\nu_2'/\nu_1),\\
F_3&=\tfrac{1}{2}(\nu_3/\nu_3'-\nu_3'/\nu_3),\\
G_1&=(1/2a^2)(a_2b_2'-b_2a_2')^2(\nu_2/\nu_1'-\nu_1'/\nu_2),\\
G_2&=(1/2a^2)(a_2b_1'-b_2a_1')^2(\nu_2/\nu_2'-\nu_2'/\nu_2),\\
H_1&=(2/a^2)(a_1b_2'-b_1a_2')(a_2b_2'-b_2a_2')(\nu_1'^2/\nu_1\nu_2)^{\frac{1}{2}},\\
H_2&=(2/a^2)(a_1b_1'-b_1a_1')(a_2b_1'-b_2a_1')(\nu_2'^2/\nu_1\nu_2)^{\frac{1}{2}},
\end{aligned}$$

* For the same reason all double primes shall be omitted throughout the following discussion.

$$I_1=(2/a^2)(a_1b_2'-b_1a_2')(a_2b_2'-b_2a_2')(\nu_1\nu_2/\nu_1'^2)^{\frac{1}{2}},$$

$$I_2=(2/a^2)(a_1b_1'-b_1a_1')(a_2b_1'-b_2a_1')(\nu_1\nu_2/\nu_2'^2)^{\frac{1}{2}},$$

$$a^2=(a_1'b_2'-a_2'b_1')=1/m^2\mu.$$

Supposing the electronic transition to be independent of the phase of motion, it is easy to see that the values of v_i' corresponding to the small values of $\partial v_i/\partial\theta_i$ will be strongly weighted. Consequently, the most probable values of v_i' are obtained by substituting in Eqs. (2) the values of θ_i satisfying

$$\partial v_1'/\partial\theta_1=\partial v_1'/\partial\theta_2=\partial v_2'/\partial\theta_1=\partial v_2'/\partial\theta_2=\partial v_3'/\partial\theta_3=0.$$

We finally obtain

$$\begin{aligned}
v_1' &= \begin{cases} A_1\pm B_1(v_1)^{\frac{1}{2}}\pm C_1(v_2)^{\frac{1}{2}}+D_1v_1+E_1v_2-F_1v_1-G_1v_2+H_1(v_1v_2)^{\frac{1}{2}} \\ A_1\pm B_1(v_1)^{\frac{1}{2}}\mp C_1(v_2)^{\frac{1}{2}}+D_1v_1+E_1v_2-F_1v_1-G_1v_2-H_1(v_1v_2)^{\frac{1}{2}} \end{cases} \\
v_2' &= \begin{cases} A_2\pm B_2(v_1)^{\frac{1}{2}}\pm C_2(v_2)^{\frac{1}{2}}+D_2v_1+E_2v_2-F_2v_1-G_2v_2+H_2(v_1v_2)^{\frac{1}{2}} \\ A_2\pm B_2(v_1)^{\frac{1}{2}}\mp C_2(v_2)^{\frac{1}{2}}+D_2v_1+E_2v_2-F_2v_1-G_2v_2-H_2(v_1v_2)^{\frac{1}{2}} \end{cases} \\
v_3' &= \begin{cases} (\nu_3/\nu_3')v_3 \\ (\nu_3'/\nu_3)v_3. \end{cases}
\end{aligned} \tag{3}$$

We notice that there are, in general, four most probable values of v_1' and v_2' corresponding to any set of v_1 and v_2. This interdependence is one of the consequences of the character of vibration, the coordinates q and y being functions of ξ_1 and ξ_2. On the other hand, x is a function of ξ_3 alone and hence v_3' varies independently. We further notice that in the absorption process when $v_1=v_2=v_3=0$, Eqs. (3) are reduced to $v_1'=A_1$, $v_2'=A_2$, $v_3'=0$. While the values of A_1 and A_2 are explicitly given on page 385, it is more convenient for later discussion to write

$$v_1'=\tfrac{1}{2}m^2\mu\alpha_1'(b_2'q_0-a_2'y_0)^2, \qquad v_2'=\tfrac{1}{2}m^2\mu\alpha_2'(b_1'q_0-a_1'y_0)^2, \tag{4}$$

where

$$\alpha_1'=4\pi^2\nu_1'/h, \qquad \alpha_2'=4\pi^2\nu_2'/h.$$

Here the α's may be regarded as the amplitudes of the nuclear vibration in terms of the normal frequencies, and the a's and b's the amplitude of the component displacements of the nuclei. It has been found that there exists a simple relation between the most probable values of v_1' and v_2' given by

$$v_1'/\nu_1'+v_2'/\nu_2'=(2m/h)(q_0^2+4\mu y_0^2). \tag{5}$$

We may then conclude that in the absorption process at ordinary temperatures the strongest bands in the v_1' and v_2' progressions will be $(v_1', 0)$ and $(v_2', 0)$ where v_1' and v_2' are associated with the quantized states in the neighborhood of the unquantized ones determined by A_1 and A_2. It is clear that if there be small change in the normal moment of inertia caused by the electron jump approaching the case $q_0=y_0=0$, the most probable transitions would be the (0, 0) bands. The strongest band in the v_3' progression is, however, always (0, 0).

Consider a special case which occurs when the three atoms become equal. Referring to the characteristic determinant on page 384 we obtain

$$\nu_1=(1/2\pi)(3K'/m)^{\frac{1}{2}}, \qquad \nu_2=\nu_3=\nu_1/2^{\frac{1}{2}}.$$

The coefficients in Eqs. (1) now become

$$a_1=a_2=1/m^{\frac{1}{2}}, \qquad b_1=b_2=-(3/4m)^{\frac{1}{2}}, \qquad c=(3/4m)^{\frac{1}{2}}.$$

The most probable transitions are found to be

$$v_i' = A_i \pm B_i(v_i)^{\frac{1}{2}} + (D_i - F_i)v_i, \quad \text{for} \quad |B_i/(4F(v_i)^{\frac{1}{2}})| > 1,$$

and in addition to these

$$v_i' = A_i + B_i^2/8F_i + (D_i + F_i)v_i, \quad \text{for} \quad |B_i/(4F_i(v_i)^{\frac{1}{2}})| < 1, \qquad i = 1, 2 \quad (6)$$

$$v_3' = \begin{cases} (\nu_3/\nu_3')v_3, \\ (\nu_3'/\nu_3)v_3, \end{cases}$$

where

$$A_1 = (\pi^2 m\nu_1'/18h)q_0^2, \qquad A_2 = (25\pi m\nu_2'/18h)q_0^2,$$

$$B_1 = (\pi/3)(2m/h\nu_1)^{\frac{1}{2}}\nu_1' q_0, \qquad B_2 = (5\pi/3)(2m/h\nu_2)^{\frac{1}{2}}\nu_2' q_0,$$

$$D_1 = \tfrac{1}{2}(\nu_1/\nu_1' + \nu_1'/\nu_1), \qquad D_2 = \tfrac{1}{2}(\nu_2/\nu_2' + \nu_2'/\nu_2),$$

$$F_1 = \tfrac{1}{2}(\nu_1/\nu_1' - \nu_1'/\nu_1), \qquad F_2 = \tfrac{1}{2}(\nu_2/\nu_2' - \nu_2'/\nu_2).$$

The distinction between v_2' and v_3' vanishes because of the degeneracy.

The vibrations of a collinear model have been discussed fully by Dennison.[6] The method of finding the transition probabilities are very much the same as has already been sketched above and need not be repeated here. We shall simply give the most probable values of the v's as follows:

$$v_1' = a_1 + (b_1 - d_1)v_1 - c_1(v_1)^{\frac{1}{2}}, \quad \text{when} \quad |c_1/(4d_1(v_1)^{\frac{1}{2}})| > 1,$$

and in addition to these

$$v_1' = a_1 + c_1/8d_1 + (b_1 + d_1)v_1, \quad \text{when} \quad |c_1/(4d_1(v_1)^{\frac{1}{2}})| < 1,$$

where

$$a_1 = (\pi^2 m\nu_1'/h)q_0^2, \qquad b_1 = \tfrac{1}{2}(\nu_1/\nu_1' + \nu_1'/\nu_1),$$

$$c_1 = 2\pi\nu_1'(m/h\nu_1)^{\frac{1}{2}}q_0, \qquad d_1 = \tfrac{1}{2}(\nu_1/\nu_1' + \nu_1'/\nu_1);$$

$$v_2' = \tfrac{1}{2}(\nu_2/\nu_2' + \nu_2'/\nu_2)v_2 \pm K(\nu_2/\nu_2' - \nu_2'/\nu_2);$$

where K stands for $\cos 2\pi(\delta_z - \delta_y)$, δ_z and δ_y being the phase angle of the component harmonic vibrations of the isotropic plane oscillator. A special case occurs when the component harmonic vibrations are in phase ($\delta_z = \delta_y$), Eqs. (7) are reduced to

$$v_2' = \begin{cases} 3/2(\nu_2/\nu_2')v_2 \\ 3/2(\nu_2'/\nu_2)v_2; \end{cases} \qquad v_3' = \begin{cases} (\nu_3/\nu_3')v_3 \\ (\nu_3'/\nu_3)v_3. \end{cases}$$

The above analysis leads to the following conclusions: In the absorption process at ordinary temperatures the most intense band in the v_1' progression will be $v_1' = a_1$; the larger the change in the normal equilibrium distance between the Y's the higher will be the value of v_1'. The strongest band in the v_2' progression depends on the phase difference of the component harmonic vibrations as well as the characteristic frequencies in both states. The most intense band in the v_3' progression will again be (0, 0).

Intensity Distribution According to Wave Mechanics

The same problem will now be considered from the wave mechanical standpoint. According to the usual method for calculating transition probabilities, the matrix component of the electric moment of the molecule corresponding to the transition in question must be computed. Born and Oppenheimer[7] have shown how the general wave equation can be handled. On account of the heavy mass of the nuclei as compared with that of the electrons the complete wave function of a

[6] Dennison, Rev. Mod. Phys. **3**, 280 (1931).

[7] Born and Oppenheimer, Ann. d. Physik **84**, 457 (1927).

molecule in a state characterized by the electronic quantum number e and the vibrational quantum number v may be approximately written

$$\psi_{ev}(x, \xi) = \phi_e(x, \xi) u_{ev}(\xi),$$

where ϕ_e is the wave function of electronic motion, and u_{ev} is that of nuclear vibration, x and ξ being the collective coordinates of the electrons and nuclei respectively.

Since the nuclear motion of a symmetrical triatomic molecule may be resolved into that of three independent equivalent oscillators the vibrational factor of the wave function, to a first approximation, can be written

$$u_{ev}(\xi) = \Pi u_{ev}(\xi_i).$$

The electric moment $M(x, \xi)$ of the molecule is a linear function of the electronic and nuclear coordinates, and the matrix component of electric moment whose square measures the transition probability of an electronic transition (e', e) and vibrational transition (v', v) is

$$M\begin{pmatrix} e' & e \\ v' & v \end{pmatrix} = \int M(x, \xi) \psi_{e'v'}(x, \xi) \psi_{ev}(x, \xi) d\xi.$$

When studying the intensity distribution in a band system we shall deal with the same electronic transition. Suppose we integrate over the electronic coordinates, then we have

$$M_{v'v} = \int M_{e'e}(\xi) u_{v'}(\xi) u_v(\xi) d\xi.$$

As ordinarily the wave functions vary with the nuclear coordinates much more rapidly than does the electric moment and the latter does not change very much over the region in which the wave functions have appreciable values, it becomes clear that for low values of v all but the constant term in $M_{e'e}(\xi)$ may be neglected. Writing $M_{e'e}(\xi) = A$ we have

$$M_{v'v} = a \Pi \int u_{v_i'}(\xi_i) u_{v_i}(\xi_i) d\xi_i.$$

If $u_{v_i'}(\xi_i) = (1/N_{v_i'}) H_{v_i'}(\eta_i') e^{-\eta_i'^2}$ is taken to be the wave function of the nuclear motion for the upper state,

$$u_{v_i}(\xi_i) = (1/N_{v_i}) H_{v_i}(\beta_i \eta_i' + \zeta_i) e^{-\frac{1}{2}(\beta_i \eta_i' + \zeta_i)^2}$$

then represents that for the lower state, where

$$\eta_i = \alpha_i^{\frac{1}{2}} \xi_i, \quad \alpha_i = 2\pi(\lambda_i)^{\frac{1}{2}}/h, \quad \beta_i = (\nu_i/\nu_i')^{\frac{1}{2}},$$

$$\zeta_i = \alpha_i^{\frac{1}{2}}(\xi_{ei}' - \xi_{ei}), \quad N_{v_i} = \pi^{\frac{1}{2}} 2^{v_i/2} (v_i!)^{\frac{1}{2}}$$

ξ_i being the normal coordinates of nuclei in the equilibrium configuration, H_{v_i} the Hermitian functions associated with the state specified.

The portion contributed by the ith oscillator will be

$$M_{v_i'v_i} = \frac{1}{N_{v_i'} N_{v_i}} \int H_{v_i'}(\eta_i') e^{-\eta_i'^2/2} H_{v_i}(\beta_i \eta_i' + \zeta_i) e^{-\frac{1}{2}(\beta_i \eta_i' + \zeta_i)^2} d\eta_i'. \tag{7}$$

If we study the absorption spectrum at a room temperature we shall primarily be interested in transition probabilities associated with bands originating from the lowest state, i.e., $v_i = 0$. For these transitions the integral may be evaluated quite easily. It may be shown that the matrix elements corresponding to the transitions $(v_3', 0)$ when v_3' is an odd integer all vanish, while all others take on values depending on the ratio of the normal frequencies and molecular constants characteristic for the transition in question. The same statement holds for the case in which the three atoms become equal.

For a collinear model the integral which measures the transition probability is approximately

$$M_{v'v} = B \int u_{e'v'_1}(q) u_{ev_1}(q) u_{e'v'_2}(r, \phi) u_{ev_2}(r, \phi) u_{e'v'_3}(x) u_{ev_3}(x) dq dr d\phi dx,$$

where B is a constant representing the effective electric moment of the molecule for the electronic transition in question and

$$u_{v_1} = (1/N_{v_1}) H_{v_1}(\rho_1) e^{-\rho_1^2/2},$$

$$u_{v_2} = \rho_2^{|m|} \sum_{k=0}^{v_2-m} a_k \rho_2^k e^{-\rho_2^2/2} e^{+im\phi},$$

$$u_{v_3} = (1/N_{v_3}) H_{v_3}(\rho_3) e^{-\rho_3^2/2},$$

$$\rho_1 = \pi\overline{(2m\nu_1/h)}^{\frac{1}{2}} q, \qquad \rho_2 = 2\pi\overline{(\mu\nu_2/h)}^{\frac{1}{2}} r,$$

$$\rho_3 = 2\pi\overline{(\mu\nu_3/h)}^{\frac{1}{2}} x, \qquad a_{k+2} = \frac{2k+2m-2v_2}{(k+2)(k+2m+2)} a_k.$$

It can be shown that the integrals corresponding to the transitions $(v_2', 0)$ or $(v_3', 0)$ when v_2' or v_3' is an odd integer all vanish and all other integrals may be expressed in terms of the normal frequencies and molecular constants.

Perhaps it should be emphasized that the vanishing of the matrix components representing transition probabilities as mentioned above is not to be interpreted as rigid selection rules. We have shown that on the assumption of any particular force fields—whether it be central or valence forces—we are led to deal with wave functions (e.g., Hermitian polynomials, functions containing a factor $e^{im\phi}$ where m is an integer positive or negative, etc.) whose properties are directly responsible for the vanishing integrals. As in an actual molecule, particularly when transitions to some high vibrational states are involved, the force fields might deviate considerably from what has been assumed, we would, therefore, rather expect some of the forbidden transitions to appear in the spectrum.

The Intensities of the ClO_2 Bands

In the preceding paper[3] we have mentioned the remarkable uniformity in the intensity distribution of the ClO_2 bands. In practically all the progressions there are central maxima which occur in the neighborhood of 3360A. This general feature was reported by Urey and Johnston[2] who have plotted curves showing the distribution of intensities in the four most prominent v_2' progressions. The overlapping of bands makes the intensity measurement rather difficult. We have estimated the relative intensities from the microphotometer records. These estimates have been made at points of maximum intensity in the unresolved bands and no corrections have been attempted for the variations of the dispersion of the instrument and of the plate sensitivity with the wave-length. The results are shown in Figs. 1 and 2 where the intensities in arbitrary unit are plotted against v_2'.

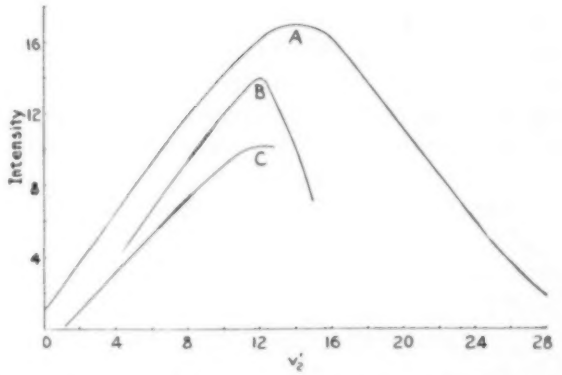

FIG. 1. A. $(0, v_2', 0) \leftarrow (0, 0, 0)$; B. $(0, v_2', 0) \leftarrow (1, 0, 0)$; C. $(0, v_2', 0) \leftarrow (0, 0, 1)$.

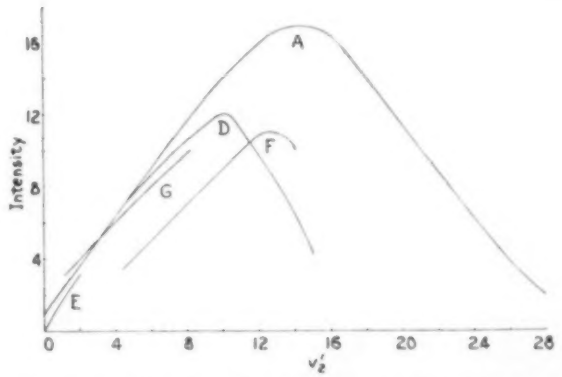

FIG. 2. A. $(0, v_2', 0) \leftarrow (0, 0, 0)$; D. $(1, v_2', 0) \leftarrow (0, 0, 0)$; E. $(0, v_2', 1) \leftarrow (0, 0, 0)$; F. $(1, v_2', 1) \leftarrow (0, 0, 0)$; G. $(2, v_2', 1) \leftarrow (0, 0, 0)$.

We are now ready to discuss how far the observed intensities agree with the results of the present analysis. On the whole, because of the Boltzmann factor, we would expect the bands originating from the (0, 0, 0) level to be much stronger than the corresponding bands arising from any of the higher levels, and this has been found to be consistent with the vibrational analysis to which reference has been made. Let us assume, for the moment, our vibrational analysis to be correct and let us examine each mode of vibration independently. The absence of all bands associated with transitions to v_3' higher

than 1 and the fact that the corresponding members of (1, 0) are considerably weaker than those of (0, 0) seem to support the theoretical prediction that the (0, 0) transition in the (v_3', 0) progression is most favorable. On the other hand, the nonvanishing intensity of the (1, 0) transition would mean that our wave mechanical treatment is inadequate and that higher orders of approximation must be employed in order to account for the observed intensity.

The intensities in the v_1' progression may be examined by comparing the corresponding members of (0, v_2', 0) with those of (1, v_2', 0) or (0, v_2', 1) with (1, v_2', 1), and (2, v_2', 0), all originating from the ground state. Here too all transitions to v_1' higher than 2 are absent. We notice that, for $v_3'=0$, the corresponding members of the (1, 0) bands are much less intense than those of the (0, 0) bands; for $v_3'=1$, this becomes less obvious. The most probable value of v_1' therefore remains uncertain.

If we substitute in Eqs. (4) the value of the molecular constants as given in Table V of the preceding paper we obtain

$$v_1' = 8.93\times10^{16}(1.25q_0 - 2.08y_0)^2,$$

$$v_2' = 23.8\times10^{16}(-1.44q_0 - 1.81y_0)^2.$$

With a knowledge of the most probable values of v_1 and v_2 it would seem possible to solve for q_0 and y_0—the change in the nuclear distances in the normal equilibrium configuration—and consequently to calculate the dimensions of the excited molecule. We have seen in Fig. 1 that the most intense band in the (0, v_2, 0) (0, 0, 0) progression is $v_2'=14$ or 15. Unfortunately the most probable value of v_1' is not precisely known. Until we have known the values of y_0 and q_0 we cannot make use of Eqs. (3)–(6) to test quantitatively the results of the present work.

I wish to express my gratitude to Professor D. M. Dennison for his continued interest in the work and frequent discussions throughout the investigation.

The Far Infrared Absorption Spectra of Ammonia and Phosphine Gases under High Resolving Power

NORMAN WRIGHT AND H. M. RANDALL, *University of Michigan*

(Received June 27, 1933)

A spectrometer of large aperture employing a reflection grating of the echelette type ruled to concentrate radiation in the region of the 1st order of 90μ has been applied in the spectral range from 60 to 125μ. The resolving power was several times that hitherto obtained in this region. The pure rotation absorption spectra of water vapor and of the gases NH_3 and PH_3 have been investigated. In the case of NH_3 the absorption lines shown as single in the observations of Badger and Cartwright have been found under the higher resolution of the present work to be doublets with a doublet separation of 1.33 cm^{-1}. Despite the similarity of structure of the molecules PH_3 and NH_3 the pure rotation lines of PH_3 exhibit no trace of a doubling. The frequencies of the PH_3 lines and the mid-frequencies of the NH_3 doublets have been shown to agree very accurately with formulas of the type $\nu_J{}^{J-1} = BJ - DJ^3$. Determinations of the moments of inertia A of NH_3 and PH_3 have been made and in the case of NH_3 the measurement of the doublet separation has led to a slight revision of the values for the moment of inertia C and for the molecular dimensions obtained by Dennison and Uhlenbeck.

INTRODUCTION

THE spectra dealt with in this work are of the pure rotation type having their origin in changes in the rotational states of molecules possessing permanent electric moments. In general these spectra have their maximum intensities in the far infrared ($\lambda > 30\mu$) and although they are of special interest because of the simplicity of their structure, the experimental difficulties of the far infrared have prevented a development similar to that of the near infrared.

The most important examples of observations of pure rotation spectra are those of Czerny[1] on the hydrogen halides and of Badger and Cartwright[2] on ammonia. While these measurements are of very great value they are nevertheless subject to the experimental limitation of small resolving power.

The present work was undertaken with the purpose of developing a technique for the application of echelette gratings in the far infrared and employing these gratings in a spectrometer of large aperture to bring a high resolving power to bear in this spectral region. High resolving power here refers to frequency difference and means ability to resolve absorption lines as close together as 1 cm^{-1}, an amount comparable with the best achieved in the near infrared.

Dennison and Hardy[3] in a recent work on the 3μ fundamental vibration band of NH_3 observed a splitting of the rotation-vibration lines into doublets with doublet separation of 1.6 cm^{-1}. From considerations set forth it was predicted in that work that the far infrared spectrum should also consist of doublets of about the same separation. The work of Badger and Cartwright because of insufficient resolving power showed no trace of this doubling.

The far infrared spectrum of NH_3 therefore furnished an excellent opportunity both to verify the theory and to demonstrate the resolving power attained by the apparatus. The similar structure of the phosphine molecule (PH_3) made it desirable to investigate this gas also.

EXPERIMENTAL

The spectrometer used for this investigation has been previously described by Randall.[4] An important feature is its large aperture, the principal mirror having a diameter of 61 cm (24 inches) and a focal length of 81.4 cm (36

[1] M. Czerny, Zeits. f. Physik **44**, 235 (1927).

[2] R. M. Badger and C. H. Cartwright, Phys. Rev. **33**, 692 (1929).

[3] D. M. Dennison and J. D. Hardy, Phys. Rev. **39**, 938 (1932).

[4] H. M. Randall, Rev. Sci. Inst. **3**, 196 (1932).

inches). In this case a 10×10 inch area of grating surface containing around 1200 lines was utilized.

Reflection gratings of the echelette type having cross sections as shown in Fig. 1 were employed.

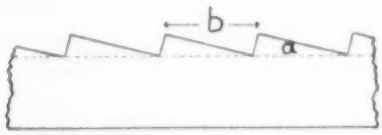

FIG. 1.

The grating used for most of the present work had the characteristics: $b = 190.50\mu$, $\alpha = 13°\ 40'$ and blaze at 90.0μ. The constants of the gratings were obtained from the ruling engine screw which was sufficiently well calibrated to justify wave-length measurements to five significant figures.

The radiation was detected by means of a vacuum thermopile of the Pfund type having two junctions in series. The receivers consisted of silver or tin foil, 0.6×3.0 mm, coated with aquadag (graphite). Tests showed that aquadag in layers of the thickness used on the receivers is opaque to radiation of the wave-lengths studied in the present case but the relative amounts reflected and absorbed have not been determined. The thermopile current was amplified about 150 times by means of a Moll thermorelay and the galvanometer deflections were read on a scale 4 meters distant. Under these conditions the Brownian movements were discernible and amounted to 2 or 3 mm scale deflection.

All optical parts of the spectrometer were enclosed in a gas-tight case of sheet metal the outside of which was covered with a layer of Celotex $\frac{1}{2}$ inch thick. Vessels of P_2O_5 were introduced for drying the air of the interior. The source of radiation, a Welsbach gas mantle which was partly surrounded by a water jacket, was placed directly in front of the entrance slit at a distance of 8 cm. This small space between source and slit was readily accessible for inserting the filters, cell and radiation shutters.

The elimination of overlapping orders of spectra, the greatest problem connected with the use of gratings, had to be accomplished in this case entirely by means of radiation filters and selective reflection, since no orders are suppressed in the blaze of the echelette grating. In all of the work described here a filter of crystal quartz of at least 5 mm thickness was present in the radiation path. It has been found in agreement with the results of Barnes[5] that a plate of this thickness absorbs all radiation from 4 to about 45μ beyond which transmission begins and has a general increase, becoming roughly 50 percent at 90μ. The radiation of wave-length less than 4μ was partially eliminated by using one or two filters of thin tissue paper or lacquer covered with a layer of soot. Its effect was further decreased by using as shutters a plate of NaCl crystal which transmits all but about 9 percent of the short wave-length radiation but is opaque beyond 25μ. Finally this 9 percent was corrected for by taking deflections both with the NaCl shutter and with one of metal. As this method of eliminating the short wave-length radiation was employed in all cases no further mention of it will be made. The last step in the elimination of higher orders consisted of a single reflection of the radiation from a residual ray plate.

The methods of purification of the spectrum for the various wave-length regions were as follows: from 70 to 80μ, a 5 mm crystal quartz filter only; from 80 to 90μ, a 5 mm quartz filter and reflection from KBr; from 90 to 105μ, 5 mm quartz and reflection from KI; from 100 to 125μ, 5 mm quartz and reflection from a plate of pressed TlBr powder.

Despite the fact that all parts of the thermopile circuit were protected by both copper and iron shieldings, all work had to be done at night to avoid electromagnetic disturbances arising in nearby laboratories. Because the thermopile was of the uncompensated type it was necessary to use the utmost care in preventing temperature fluctuations in the surroundings.

The procedure involved in making observations was as follows. The room containing the apparatus was allowed several hours to come to thermal equilibrium after the gas mantle source had been started. The observer took his place at the side of the spectrometer a half hour before taking readings. The steady drift which was usually present was corrected for by averaging the two deflections produced on opening the radiation shutter and on closing it. Also, a

[5] R. B. Barnes, Phys. Rev. **39**, 562 (1932).

metronome was used to give the proper intervals between readings. Since the total time of response of the system was 20 seconds, this time was allowed to elapse between opening and closing the shutter. Often as many as six or more of these double deflections were taken at a single setting of the grating and under the best conditions the mean deviation from the average of these was 2 or 3 mm, making the probable error in the neighborhood of 1 mm. The size of the deflections throughout the spectrum varied from 20 to 150 mm as may be seen from the energy curves of Fig. 3.

The absorption spectra of the gases were obtained by placing the cell between the source and slit. The cell consisted of a rectangular glass tube with crystal quartz plates, 2 mm thick, cemented to the ground ends. Because of the strong absorption of the gases observed and the high resolving power of the spectrometer the length of the cell, i.e., internal distance between windows, was made but 1 cm. All observations were made with the gases under reduced pressures, the cell being of sufficient strength to permit evacuation.

The irregular absorption produced throughout the spectrum by the small amount of water vapor, principally in the 8 cm exterior radiation path, necessitated in all cases the taking of two sets of observations, one with the gas in the cell and another with the cell evacuated. This irregularity of the energy distribution introduces an error in the wave-length determinations but no correction was made since it appears of the same order of magnitude as that caused by errors in the deflection measurements.

Results

The curves shown in Fig. 2 and Fig. 3 give the galvanometer deflections obtained throughout the spectrum. Readings were taken in steps of 2.5′ on the grating circle, an interval corresponding to 0.27μ at 95μ. The curves are in effect water vapor absorption curves, the numerous deep minima being due to absorption by the water vapor present in that part of the radiation path passing through undried room air. The envelopes of the curves are determined by the emission characteristics of the gas mantle, the absorption of the quartz filter, characteristics of the grating and reflecting powers of the reststrahlen plates. Curves *A* and *B* were obtained with a 5 mm crystal quartz filter only. Curves *C* and *D* were obtained with the 5 mm quartz filter and in addition by reflecting the radiation from a plate of KI crystal in the case of *C* and from TlBr in *D*. Since the quartz begins to transmit at 45μ, second order radiation might be expected to appear in curves *A* and *B* at around 90μ and, in fact, comparison of these curves with *C* and *D*, in which the second order is removed, shows this to be the case. The frequent occurrence of strong water vapor absorption lines, or groups of lines, reducing the deflections nearly to zero, was used as an indication of spectral purity, the presence of second orders as in curve *B* preventing the deflections from coming to zero. A grating ruled for the region of 150μ was used for curve *E*; here the 5 mm quartz filter was used and although the radiation was reflected from TlBr, the spectral purity is somewhat doubtful.

For all the curves of Fig. 2 the radiation passed through 80 cm of undried air, a focussing mirror having been used outside the spectrometer case. The source was then moved to its final position 8 cm in front of the entrance slit and curves *F*, *G*, and *H* of Fig. 3 were obtained. The extent to which water vapor absorption has been reduced in these curves may be seen by comparing them with *A* and *C*, portions of which are reproduced in this figure. It will be noticed that, in some cases, broad absorption regions have been resolved into two or more sharp lines.

Table I. *Water vapor.*

Wave-length (μ)	Frequency (cm^{-1})	Wave-length (μ)	Frequency (cm^{-1})
134.7	74.22	92.662	107.92
132.3	75.59	89.919	111.21
127.8	78.26	88.520	112.97
126.5	79.02	85.662	116.74
125.6	79.59	84.690	118.08
121.7	87.44	83.196	120.20
113.1	88.42	81.988	121.97
111.7	89.53	78.63	127.2
108.1	92.51	77.66	128.8
104.03	96.125	75.32	132.8
100.96	99.045	71.79	139.3
99.415	100.59	70.98	140.9
98.559	101.46	66.62	150.1
95.613	104.59	65.14	153.5
94.541	105.78	63.34	157.9
93.199	107.30	60.01	166.6

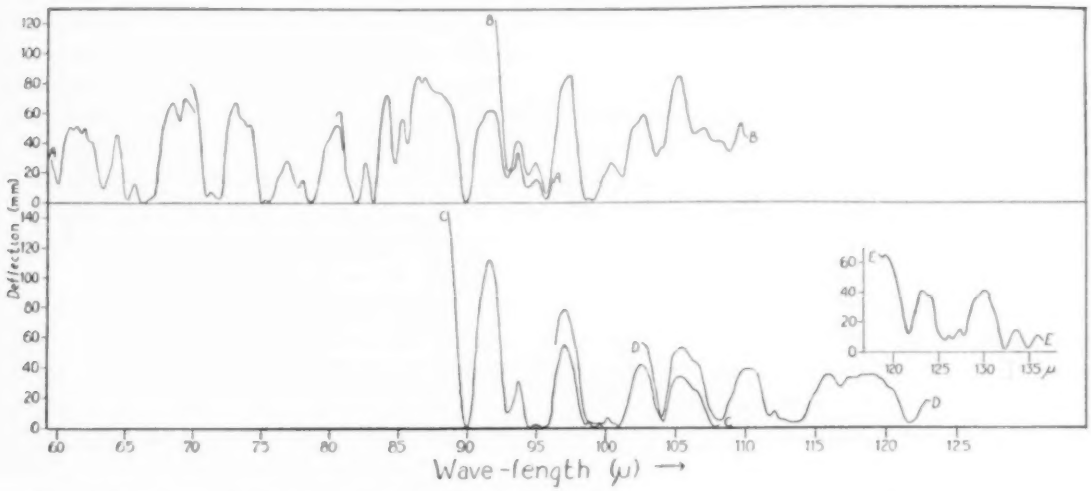

FIG. 2. H_2O vapor: Curve *A*—2mm slits, 6 mm quartz; *B*—3 mm slits, 6 mm quartz; *C*—3 mm slits, 6 mm quartz, reflection from KI; *D*—3 mm slits, 6 mm quartz, refl. from TlBr; grating with blaze at 90μ in all cases; Curve *E*—3 mm slits, 6 mm quartz, refl. from TlBr; 150μ grating.

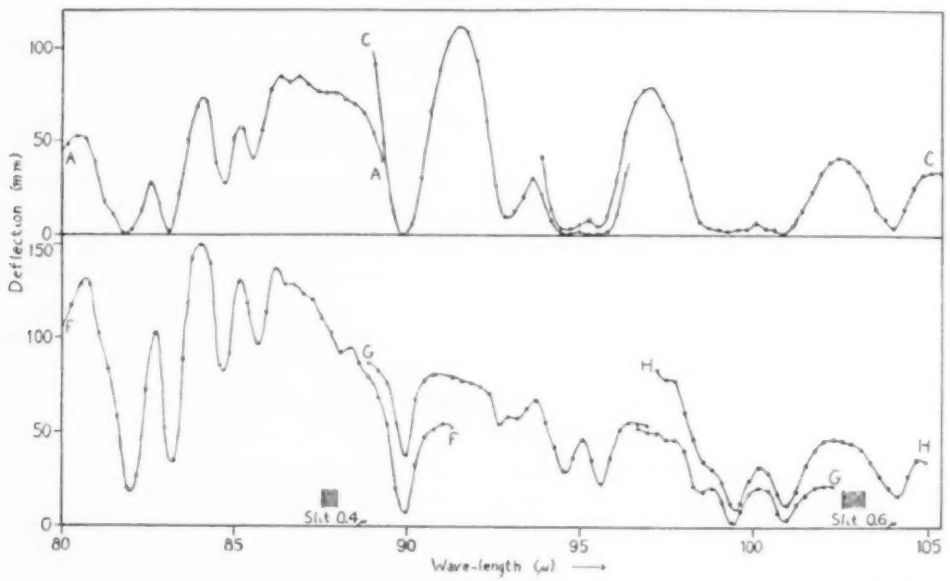

FIG. 3. H_2O vapor: Curves *A* and *C* same as in Fig. 2; undried air path 80 cm; Curve *F*—2 mm slits, 5 mm quartz, refl. from KBr; *G*—2 mm slits, 5 mm quartz, refl. from KI; *H*—3 mm slits, 5 mm quartz, refl. from KI; undried air path 8 cm. 90μ grating in all cases.

The high practical resolving power attained by the spectrometer is demonstrated by these water vapor absorption curves. That the resolution of lines as close together as 1 cm^{-1} has been achieved may be seen by consulting Table I which contains a list of the wave-lengths and corresponding frequencies.

In agreement with the prediction of Dennison[3] the pure rotation spectrum of NH_3 was found to consist of doublets with doublet separation 1.33 cm^{-1}. The doublets of ordinal number 5, 6 and 7 were observed and are plotted to a frequency scale in Fig. 4. The precision of the measurements is indicated by the extent to which the experimental points fall on smooth curves. Table II gives a list of the wave-lengths and frequencies of the doublets. The frequencies of the doublets 5 and 6 as measured unresolved by Badger and

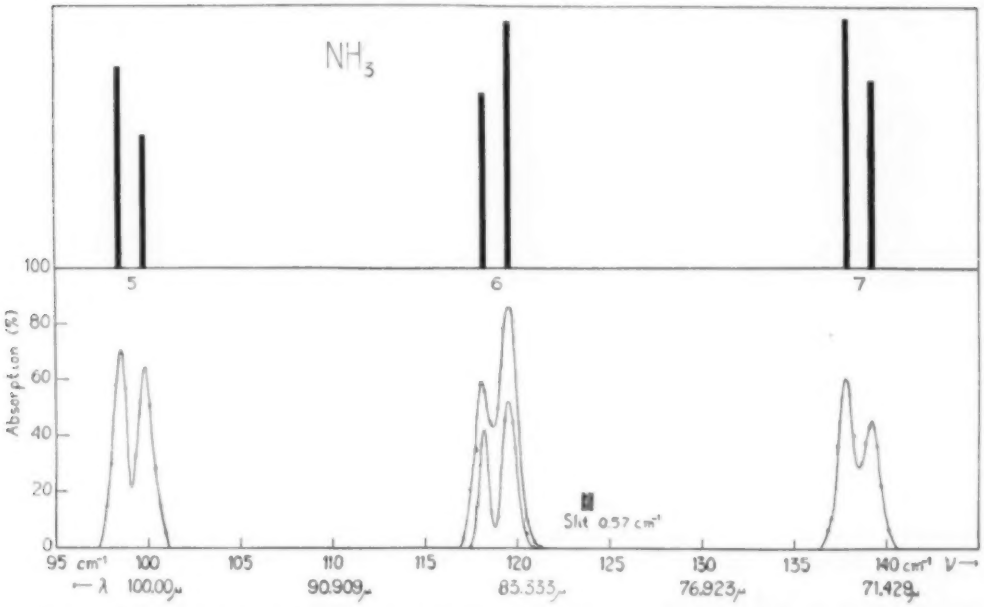

FIG. 4. NH_3 gas: No. 5—3 mm slits (0.60 cm^{-1}), 5 mm quartz, refl. from KI, gas pressure 8 cm Hg; No. 6—2 mm slits (0.57 cm^{-1}), 5 mm quartz, refl. from KBr, pressures 6.5 and 10 cm; No. 7—1.5 mm slits (0.58 cm^{-1}), 5 mm quartz only, pressure 7.3 cm; 90μ grating.

TABLE II. *Pure rotation lines of NH_3.*

Final J	Wave-length (μ)	Frequency (cm^{-1})	$\Delta\nu$	$\bar{\nu}_J{}^{J-1}$ (Obs.)	$\bar{\nu}_J{}^{J-1}$ (Calc.)	Δ	ν (Badger and Cartwright)
5	101.49	98.529	1.30	99.180	99.178	−0.002	99.06
	100.17	99.832					
6	84.591	118.22	1.36	118.90	118.90	0.00	118.60
	83.628	119.58					
7	72.525	137.88	1.33	138.54	138.55	0.01	——
	71.836	139.21					

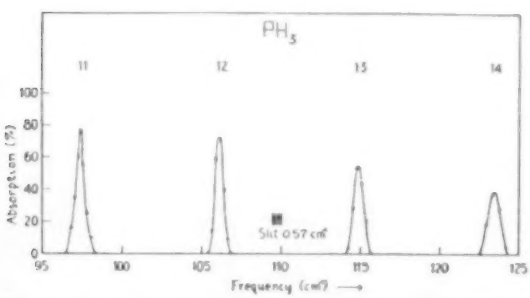

FIG. 5. PH_3 gas: No. 11—3 mm slits, 5 mm quartz, refl. from KI; No. 12—2 mm slits, 5 mm quartz, refl. from KI; No. 13—2 mm slits, 5 mm quartz, refl. from KBr; No. 14—2 mm slits, 5 mm quartz, refl. from KBr; gas pressure in all cases 30 cm; 90μ grating.

Cartwright[2] are included for comparison in this table; the 7th doublet was not measured by them due to lack of energy in the 72μ region.

TABLE III. *Pure rotation lines of PH_3.*

Final J	Wave-length (μ)	Frequency (cm^{-1})	Frequency (Calc.)	Δ
11	102.72	97.355	97.35	0.00
12	94.255	106.10	106.10	0.00
13	87.073	114.84	114.83	−0.01
14	80.951	123.53	123.53	0.00

The pure rotation spectrum of PH_3, unlike that of NH_3, was found to consist of single lines. The lines of ordinal number 11, 12, 13 and 14 were observed and are plotted on a frequency scale in Fig. 5. A list of the observed wave-lengths and frequencies is given in Table III.

Discussion

The molecule H_2O is of the asymmetrical type, and exhibits a rotation spectrum of great complexity as, indeed, is required for the asymmetrical rotator in the wave-mechanical treatments given by Kramers and Ittmann,[6] Klein,[7] and Dennison.[8] In the last-mentioned treatment a diagrammatical representation of the spectrum in terms of the three unknown moments of inertia has been made. Because, however, of the increasing complexity of the spectrum with higher J values the transitions depicted in the diagram involve only levels for which $J \lesssim 4$. In the present investigation the absorption of water vapor has been observed throughout the region from 60 to 125μ under varying degrees of resolution. This region, however, is not adequate to permit a correlation with Dennison's diagram. In fact, an examination of the rotational structure of the fundamental vibration bands of H_2O observed by Plyler and Sleator[9] indicates that the pure rotation lines involving the lower levels for which $J \lesssim 4$ lie for the most part at greater wavelengths than those observed in this work.

Ammonia

The molecule NH_3 is an example of the symmetrical type, consisting of a triangular pyramid with the nitrogen atom at the apex. As is well known, the frequencies in the pure rotation spectra of symmetrical rigid molecules are given by $\nu_J{}^{J-1} = (h/4\pi^2 A)J$, where A is the moment of inertia about an axis perpendicular to the axis of symmetry. For actual molecules, however, there is a correction to be applied because of the fact that centrifugal forces set up by the rotation cause a slight deformation. When this effect is taken into account the expression for the frequencies becomes

$$\nu_J{}^{J-1} = BJ - DJ^3 \qquad (1)$$

where B is but negligibly different from $h/4\pi^2 A$ and D is a small constant depending on the two moments of inertia of the normal molecule and on various constants involved in the potential energy expression.

In the case of NH_3 a modification of the spectrum is introduced through the fact that the nitrogen atom can make transitions between equivalent positions of equilibrium on opposite sides of the plane of the hydrogen atoms. The potential energy associated with the distance of the N atom from the plane of the H atoms thus has two minima, one at each position of equilibrium. A discussion of the results of this fact is contained in the papers of Dennison,[8] of Dennison and Hardy[3] and of Dennison and Uhlenbeck.[10]

It is shown that the energy levels are split into pairs with constant separation as illustrated in Fig. 6 which represents levels of the 0th vibrational state. The states designated α have wave functions of which the part depending on the vibrational coordinates alone is symmetrical for an interchange of any two of the hydrogen nuclei. The states β are antisymmetrical for this interchange. The selection rules for both the parallel vibration bands and the pure rotation spectrum allow transitions only from α to β-states and *vice versa*. As a consequence the spectral lines also occur in pairs, the doublet difference being the sum of the separations in the initial and final pairs of levels.

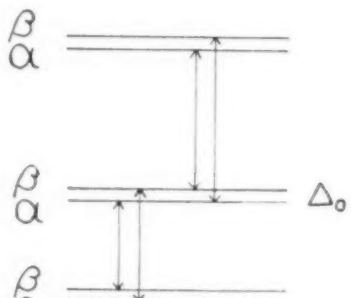

Fig. 6.

The theoretical intensities of the pure rotation doublets of NH_3 derived by using the weights of the states as given by Dennison[8, 3] are plotted

[6] H. A. Kramers and G. P. Ittmann, Zeits. f. Physik **53**, 553 (1929); Zeits. f. Physik **58**, 217 (1929) and Zeits. f. Physik **60**, 663 (1930).

[7] O. Klein, Zeits. f. Physik **58**, 730 (1929).

[8] D. M. Dennison, Rev. Mod. Phys. **3**, 317 (1931).

[9] E. K. Plyler and W. W. Sleator, Phys. Rev. **37**, 1493 (1931).

[10] D. M. Dennison and G. E. Uhlenbeck, Phys. Rev. **41**, 313 (1932).

in Fig. 4 immediately above the corresponding observed lines. Owing to the fact that the various doublets were observed under different gas pressures the intensities of one doublet relative to another have not been determined. It will be noticed, however, that the observed relative intensities of the doublet components possess the alternating character of the theoretical values.

Quantitative expressions for the doublet separations have been derived in the paper of Dennison and Uhlenbeck.[10] The energy level separations, Δ_0 in the 0th vibrational state and Δ_1 in the 1st excited state of the vibration ν_3, are given by the two simultaneous equations:

$$\Delta_0/h\nu_3=(2\alpha/\pi^{\frac{1}{2}})\times\exp\left[-\alpha^2-2(x_0-\alpha)(\alpha^2-1)^{\frac{1}{2}}\right], \quad (2)$$

$$\Delta_1/h\nu_3=\left[(4\alpha^3-4\alpha)/\pi^{\frac{1}{2}}\right]\times\exp\left[-\alpha^2-2(x_0-\alpha)(\alpha^2-3)^{\frac{1}{2}}\right], \quad (3)$$

in which $x_0=[h/4\pi^2\mu\nu_3]^{-\frac{1}{2}}q_0$, q_0 is the normal distance of the N atom from the plane of the H atoms, and α is a parameter of the potential energy curve. From the measurements of the present work the doublet separation $2\Delta_0$ of the pure rotation doublets is 1.33 cm^{-1}, hence $\Delta_0=0.67$ cm^{-1}. The fundamental vibration band ν_3 observed by Barker[11] yields the values $\nu_3=948$ cm^{-1} and the doublet separation $\Delta_0+\Delta_1=31.6$ cm^{-1}. Hence $\Delta_1=30.9$ cm^{-1}. Substituting these values in the above equations and solving for q_0, we obtain

$$q_0=0.388\times10^{-8}\text{ cm}.$$

(This value is a few percent different from that obtained by Dennison and Uhlenbeck using older data on the ν_3 band and assuming $\Delta_0=0.8$ cm^{-1}.)

Since the pure rotation lines of NH_3 occur in pairs, the expression (1) for the frequencies now refers to the mid-frequency of each pair. Fitting this expression to the observed values (Table II) results in the formula

$$\bar{\nu}_J{}^{J-1}=19.880J-0.00178J^3,$$

where $\bar{\nu}_J{}^{J-1}$ is the mid-frequency (cm^{-1}) of the Jth doublet. Table II shows the very close agreement of the observed frequencies and those calculated from the above equation. The relation $h/4\pi^2cA=19.880$ determines the moment of inertia

$$A=2.782\times10^{-40}\text{ g cm}^2.$$

This is in good agreement with the values obtained in the following investigations:

Barker[11]	
Band ν_3	2.80×10^{-40}
Dennison and Hardy[2]	
Band ν_1	2.82
Badger and Cartwright[2]	
Pure rot. spectrum	2.77
Dickinson, Dillon, and Rasetti[12]	
Raman spectrum	2.79

The values of A and q_0 yield the following determinations:

C(moment of inertia about the axis of symmetry) $=4.33\times10^{-40}$ g cm^2

N–H (normal distance between N and H nuclei) $=1.01\times10^{-8}$ cm

H–H (normal distance between H nuclei) $=1.61\times10^{-8}$ cm.

It is interesting to note that the combination principle affords a test of the accuracy of the frequency measurements. From a consideration of the energy levels of the 0th vibrational state of the molecule and of the 1st excited states of the parallel vibrations ν_1 and ν_3, it is readily seen that certain relationships exist among the pure rotation frequencies and the rotation-vibration frequencies in the bands ν_1 and ν_3. If the rotational levels of the 0th vibrational state are termed $R_{\alpha\text{ or }\beta}^{J,K}$ and those of the 1st excited states of ν_1 and ν_3 are termed $V_{1\alpha\text{ or }\beta}^{J,K}$ and $V_{3\alpha\text{ or }\beta}^{J,K}$, respectively, the relationships with which the present work is concerned may be expressed:

$$\begin{aligned}(R_\beta{}^{5,K}-R_\alpha{}^{4,K})+(R_\alpha{}^{6,K}-R_\beta{}^{5,K})&=(V_{1\beta}{}^{5,K}-R_\alpha{}^{4,K})-(V_{1\beta}{}^{5,K}-R_\alpha{}^{6,K})\\&=(V_{3\beta}{}^{5,K}-R_\alpha{}^{4,K})-(V_{3\beta}{}^{5,K}-R_\alpha{}^{6,K}),\end{aligned} \quad (4)$$

$$\begin{aligned}(R_\alpha{}^{5,K}-R_\beta{}^{4,K})+(R_\beta{}^{6,K}-R_\alpha{}^{5,K})&=(V_{1\alpha}{}^{5,K}-R_\beta{}^{4,K})-(V_{1\alpha}{}^{5,K}-R_\beta{}^{6,K})\\&=(V_{3\alpha}{}^{5,K}-R_\beta{}^{4,K})-(V_{3\alpha}{}^{5,K}-R_\beta{}^{6,K}).\end{aligned} \quad (5)$$

[11] E. F. Barker, Phys. Rev. **33**, 684 (1929). (The data quoted here are from unpublished measurements of ν_3 made recently by Dr. Barker.)

[12] R. B. Dickinson, R. T. Dillon and F. Rasetti, Phys. Rev. **34**, 582 (1929).

The frequencies indicated on the left sides of the equations are those of the pure rotation doublets, Nos. 5 and 6, measured in this work. The other frequencies are of band ν_3, measured by Barker[11] and of band ν_1, measured by Dennison and Hardy.[3] Table IV shows the close agreement of the experimental values.

TABLE IV.

Pure rotation	Band ν_1	Band ν_2
Eq. (4)		
99.83+118.22	3436.0−3217.5	1065.83−847.68
=218.05	= 218.5	=218.15
Eq. (5)		
98.53+119.58	3434.3−3216.1	1034.16−816.25
=218.11	= 218.2	=217.91

Phosphine

As has been mentioned the pure rotation lines of PH_3, unlike those of NH_3, do not exhibit a doubling but are as sharp, for example, as the component lines of the NH_3 doublets. The four observed PH_3 lines (Table III) yield the frequency formula:

$$\nu_J{}^{J-1} = 8.892J - 0.000348J^3.$$

Here again there is accurate agreement of the observed frequencies and those calculated from the formula. From the relation $h/4\pi^2 cA = 8.892$ we find for the moment of inertia A of PH_3

$$A = 6.221 \times 10^{-40} \text{ g cm}^2.$$

The fact that no trace of a doubling of the PH_3 lines is observed may be accounted for qualitatively by assuming that q_0 is larger for this molecule than for NH_3, an assumption supported by the larger moment of inertia A of PH_3. Eq. (2) shows that the level separation Δ_0 is extremely sensitive to x_0 (hence to q_0) and that a small increase in the latter could easily lead to a doublet separation far too small for spectroscopic resolution.

Dispersion of the Kerr Electro-Optic Effect in the Short Infrared Spectrum

L. R. INGERSOLL AND WESLEY R. WINCH, *University of Wisconsin*

(Received July 10, 1933)

Measurements of the Kerr electro-optic effect have been made on carbon disulphide, nitrobenzene, *o*-nitrotoluene, chlorobenzene, and halowax oil over a spectral region extending from the sodium lines to beyond 1.6μ (2.1μ for CS_2), or some three times the wave-length range previously investigated by other observers. A spectro-radiometric method was used, involving effectively the measurement of the minor axis of the ellipse into which the plane polarized radiation is converted by the electrostatic stress in the Kerr cell. The potentials across the cell of 3300 to 31,000 volts were furnished by a kenotron and condenser equipment. The Havelock formula for electro-optic dispersion $K=C(n^2-1)^2/n\lambda$ and two others have been tested in connection with the results. In most cases the agreement with the Havelock formula is somewhat better than with the others and for CS_2 this law fits the observed dispersion almost within the limits of experimental error throughout the spectral range investigated. Beyond 1μ the dispersion of all the liquids is much the same and the agreement with all these formulas reasonably good. In fact, for this region the Kerr effect is very nearly proportional to the inverse wave-length.

THE dispersion of the Kerr electro-optic effect (birefringence produced by high electrostatic field) has been extensively investigated for the visible spectrum.[1] In the ultraviolet, Szivessy and Dierkesmann[2] have applied photographic means to the study of a number of liquids in this connection. Apparently no previous investigators, however, have experimented with this effect in the infrared. In this paper[3] we shall describe the method and results of a study of the electro-optic dispersion of five liquids in the wave-length range from that of the sodium lines to about 2μ, together with a comparison of the results with theory.

Dispersion Formulas

If n_p and n_s are the refractive indices for the components of the light vibrating parallel and perpendicular, respectively, to the lines of force, the phase difference D after passing through l cm of the substance in an electric field of E e.s.u. is

$$D=2\pi l(n_p-n_s)/\lambda=2\pi KlE^2 \text{ radians}, \quad (1)$$

where λ is the wave-length of the light. K is called the Kerr constant.

Three dispersion formulas will be tested in connection with the present work; they are (a) the well-known Havelock law[4]

$$K=C_1(n^2-1)^2/n\lambda, \quad (2)$$

(b) a development on the basis of the Born[5] classical theory,

$$K=C_2(n^2+2)(n^2-1)/n\lambda \quad (3)$$

and (c) one recently developed by Serber[6] on a quantum basis which, on approximation, simplifies to

$$K=C_3\frac{(n^2+2)(n^2-1)}{n\lambda}\left\{1+C_4\frac{1+\nu^2/\nu_1^2}{1-\nu^2/\nu_1^2}\right\}, \quad (4)$$

where ν_1 is the main ultraviolet absorption frequency, really the centroid frequency. The latter two formulas apply primarily to the case of gases, where the mutual influence of the molecules is small, but they should also hold

[1] For general references see J. W. Beams, Rev. Mod. Phys. **4**, 133–172 (1932); G. Szivessy, Handb. d. Physik **21**, 724–884, Julius Springer (1929).

[2] G. Szivessy and A. Dierkesmann, Ann. d. Physik **3**, 507 (1929).

[3] The following brief accounts have been published: L. R. Ingersoll, Phys. Rev. **37**, 1184 (1931); L. R. Ingersoll and W. R. Winch, Phys. Rev. **42**, 909 (1932).

[4] T. H. Havelock, Proc. Roy. Soc. **A80**, 28 (1907), **A84**, 492 (1911); Phys. Rev. **28**, 136 (1909).

[5] M. Born, Ann. d. Physik **55**, 177 (1918). See also H. A. Stuart, Zeits. f. Physik **55**, 358 (1929); Ergebnisse d. Exacten Naturwiss. **10**, 159, Julius Springer (1931); C. V. Raman and K. S. Krishnan, Phil. Mag. **3**, 713 (1927); Proc. Roy. Soc. **A117**, 1, 589 (1928).

[6] R. Serber, Phys. Rev. **43**, 1011 (1933).

approximately for liquids, although in the case of (b) only for nonpolar molecules.

Experimental Method

The method and apparatus are partly the outgrowth of investigations carried out some years ago by one[7] of us on the Faraday and Kerr magneto-optic effects in the infrared. Fig. 1

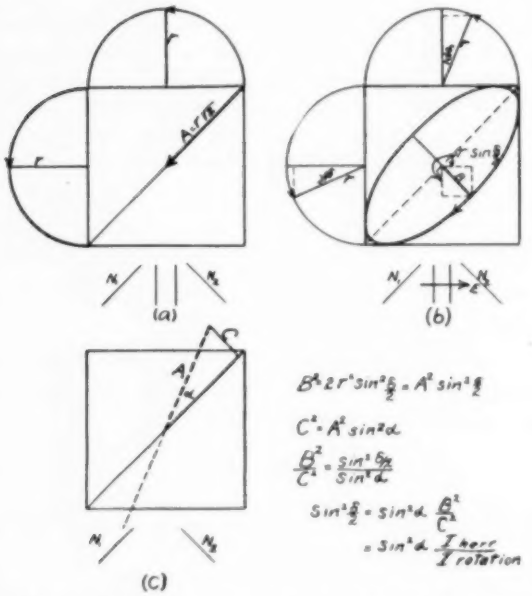

Fig. 1. Diagram illustrating the principles involved in the measurements.

illustrates the method. As indicated in (a), light vibrating at 45° with the plane of the Kerr cell comes from the polarizer whose azimuth is indicated at N_1. It is obvious that none of this radiation will pass the analyzer of azimuth N_2, at right angles to this, until a potential is applied across the cell as in (b). This produces a difference of velocity of the two component beams, which results in the Kerr phase difference D (or δ as we have called it, measured in degrees) and the consequent elliptical vibration. If A represents the amplitude of the original vibration and B the semi-minor axis of the ellipse, then, as is clear from the figure, the relation is

$$\sin^2(\delta/2) = B^2/A^2. \tag{5}$$

While it would be possible to measure the ratio of B^2 to A^2 directly, it is simpler to get at it by means of a rotation α of the original plane of polarization as shown in (c). This results in a beam of intensity C^2 being transmitted by the analyzer and this is easily compared with the intensity B^2 which results from the excitation of the Kerr cell, being of the same order of magnitude. The equation, as indicated in Fig. 1, is

$$\sin^2(\delta/2) = \sin^2\alpha\, B^2/C^2. \tag{6}$$

Apparatus

Fig. 2 shows the general arrangement of the apparatus. Light from the special strip-filament

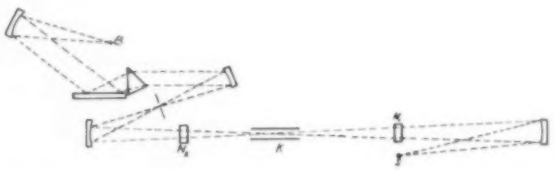

Fig. 2. General arrangement of the apparatus. S, strip filament tungsten lamp; N_1, N_2, double image (or nicol) prisms, crossed; K, Kerr cell; and B, bolometer or thermopile.

lamp was focussed by a silvered concave mirror and, after passing through the polarizer, was converged in a narrow conical beam between the plates of the Kerr cell. It then went on to the analyzer which was crossed so that no light passed until the Kerr cell was excited, in which case the transmitted radiation was focussed on the slit of the spectrometer and, after dispersion into a spectrum, fell on the receiver. It may be remarked that both polarizer and analyzer were really double-image prisms instead of nicols, but they were used in exactly the same way, for the second image, being turned aside at a small angle, was readily cut off. The polarizer was mounted in a large conical bearing so that it could be rotated between stops by the angle α, mentioned above, which in the present work was 21° 20′.

In the first work with this apparatus the radiation receiver was a bolometer used with a Thomson galvanometer. It was later replaced, however, by a sensitive bismuth-tellurium thermopile. This had a receiving surface (using a double couple—uncompensated) of 0.5 mm×10

[7] L. R. Ingersoll, Phil. Mag. **11**, 41 (1906); Phys. Rev. **23**, 490 (1906); Phil. Mag. **18**, 74 (1909); Phys. Rev. **9**, 257 (1917); J.O.S.A. and R.S.I. **6**, 663 (1922).

mm and was used in high vacuum maintained by a charcoal trap in liquid air. When connected with a Zc (Kipp and Zonen) galvanometer it gave a tenfold gain in sensitivity over the bolometric outfit, even when used with narrower slit and longer focus mirrors in the spectrometer. Since a variety of conditions—in most cases the absorption of the liquid under test was the limiting factor—confined the measurements to the short infrared, a glass prism could be used in the spectrometer. This was a large 45° prism of heavy glass, the dispersion of which was calibrated with the aid of a grating.

The high voltage was furnished by two kenotrons and condenser connected with a 140,000 volt transformer, which, in turn, was controlled by an autotransformer allowing the application of any fraction of the 220 volt primary e.m.f. in 1 percent steps. Because of the minuteness of the current the output voltage ripple was only a fraction of a percent in most cases. To measure the voltage on the Kerr cell a Wulf electrometer (Leybold) was connected across its terminals. This had a range up to 50,000 volts and was an essential part of the equipment since inevitable small voltage fluctuations were of frequent occurrence.

Four different Kerr cells were used, varying in length from 5 to 39 cm, the shorter cells being used for liquids of high Kerr constant such as nitrobenzene and the longest for carbon disulphide. They consisted in all cases of glass tubes of 6 cm or more in diameter with ends of tested plate glass cemented on, usually with water glass. The Kerr plates were of heavy brass, nearly as long as the cell, from 4 to 5 cm wide and from 4 to 13 mm apart. Drilled glass plates screwed on top and bottom kept them accurately spaced.

The making of measurements was relatively simple. With the spectrometer set at the desired wave-length the high voltage was alternately thrown on and off the Kerr cell at regular intervals of about a minute and the corresponding galvanometer deflection measured. The Wulf electrometer was also read each time the cell was excited. Then, with the voltage off, the galvanometer deflection was read as the polarizer was turned through the angle α. The Kerr effect, measured by δ, could then be calculated at once from Eq. (6). To avoid correction for errors in galvanometer proportionality it was very desirable to have the deflections for B and C as nearly equal as possible. This was accomplished by cutting down one or the other intensity by a suitable and known factor, and, after some experimentation, the best way found to do this was to place in the beam a rotating sector of accurately measured opening.

The application of the Havelock or other electro-optic dispersion equation demands a knowledge of the index of refraction n and since this is known in the infrared for only a few liquids it had to be measured specially in the present case. This was done by the method of total reflection, using two glass plates cemented together to form a very thin air cell. It rotated in a cell filled with the liquid and was mounted in a divided circle which allowed the angle to be read to 1′. The check of these measurements at the sodium wave-length with the ordinary tabulated values was very good.

Sources of Error

1. Impurities

The best available material was used and this was further purified, if necessary, by the usual chemical and physical means. The last step in purification was usually to shake up the liquid with P_2O_5, let stand for a day or two, and then distill. In most cases, however, the current drawn by the cell on the initial application of the voltage was many times that (of the order of a milliampere, sometimes much less) to which it finally settled down after perhaps an hour. This was attributed to the presence of a minute amount of water and water-soluble impurities which were electrolyzed out and held on one of the plates. Reversing the current at once released these impurities, so throughout the work the voltage was always applied in the same direction. This self-purification was an important step in the process of the measurements and no readings were taken until the current had settled down to its minimum value.

2. Lack of field uniformity, edge and end effects

The use of a slightly conical beam (necessary to secure sufficient energy) meant that parts of the beam would approach nearer the plates than

others and into a region of inevitable field non-uniformity because of the rather wide (up to 13 mm) distance necessary between the plates. This would be a vital source of error if absolute values were demanded in the measurements, but in view of the fact that only relative values are necessary for dispersion measurements it became of somewhat secondary importance. It was necessary nevertheless to see that the position of the beam in the cell did not shift in the slightest degree during any one run, i.e., series of measurements throughout the spectral range.

3. Temperature variation

A thermometer in the cell was read at occasional intervals and the cell cooled by fan, if necessary, to keep temperature variations within 1°C. The mean temperature in most cases was 24°C.

4. Voltage variations

As already explained, the Wulf electrometer was read every time the voltage was applied to the cell. Making use of the fact that the Kerr effect is proportional to the square of the field, a correction was accordingly applied to each measurement to bring it effectively to a definite mean voltage.

5. "Creep"

This was one of the most serious difficulties. In certain liquids, notably chlorobenzene, the Kerr effect, as measured, began to decrease slightly after the field had been on for a minute or more; in other cases a small increase would take place. No explanation could be found for this and it is planned to make it the object of a special study in the future. Its effect was minimized in the present case by taking readings at definite regular intervals.

6. Spectral impurity

This may be of two sorts: (1) a very small amount of general impurity due to radiation scattering in the prism-mirror system and (2) the inevitable coverage by the receiver (and slit image) of an appreciable spectral range. The first sort was taken account of by making a series of Kerr measurements in the neighborhood of the sodium wave-length with a piece of heat-absorbing glass before the slit. This cut out practically all the infrared impurity and led to a correction of the order of 0.5 percent which was applied to the results for the sodium and adjoining wave-lengths. A similar test made with a cell containing iodine in CS_2, which absorbed the visible, indicated that no such corrections were necessary in the infrared.

The second sort of error was minimized by making the receiver and slit as narrow as possible. That this error was not large enough to be taken seriously into account was indicated by a comparison of results with the bolometer and those made later with the thermopile under conditions of somewhat larger effective dispersion. These indicated that the only uncertainty is in the neighborhood of the sodium wave-length. This is as applied to the results as a whole. There is one case, however, in which this error is so serious as to render measurements almost meaningless and that is in the immediate neighborhood of an absorption band. After much time spent in fruitless investigation of this point with the use of double dispersion, we were compelled to limit our study for the present to spectral regions free of marked absorption, although we hope at some time in the future to be able to develop a means of studying in this connection the interesting phenomena which may group around an absorption line or band.

Results

The following liquids were tested:

Carbon disulphide

This was purified by treatment with mercury and filtration, then phosphorus pentoxide and distillation and used in Kerr cell with plates 37.5 cm long and 1.3 cm apart at 31,200 volts.

Nitrobenzene

Purification was by fractional freezing, followed by P_2O_5 treatment and distillation. The cell was 8.0 cm long with plates 0.6 cm apart. Voltages were 3310, 5250, and 8710.

***o*-Nitrotoluene (Eastman)**

This was dehydrated and distilled. The cell was 4.5 cm long, 0.4 cm plate separation. Voltages were 4795 and 10,020.

Chlorobenzene (Eastman)

This was dehydrated and distilled. The cell was 10.0 cm long, 0.6 cm separation. Voltages were 22,840 and 28,550.

Halowax Oil No. 1007, from the Halowax Corporation of New York

This is a chloronapthalin whose properties make it a good liquid to test in the present connection. It was used untreated. The cell was 8.0 cm long, 0.6 cm separation. Voltages were 13,590, 19,420, and 25,970.

The results are given in the table and the curves of Fig. 3. The values of δ plotted in the curves are the actual angles in degrees as measured. While it would be possible to compute the absolute values of the Kerr constant by using the voltages and cell dimensions as given, the error involved would be large because of the edge and end effects as already mentioned. These, however, in no way affect the dispersion results which are considered to have a probable error of not more than 1 percent for the spectral range 0.7μ to 1.4μ (2.0μ for CS_2). The approximate values of the Kerr constant for the sodium wave-length are, referred to CS_2 as 1: nitrobenzene, 99; o-nitrotoluene, 37; chlorobenzene, 3; halowax, 4.

While measurements were made for two or three different voltages on all liquids save CS_2 all the separate results are not given, for it was found, as might be expected, that the dispersion

TABLE I. *Relative Kerr constants.*

λ	n	Observed Kerr constants	Computed Kerr constants: Havelock	Born	Serber	$1/\lambda$
Carbon disulphide						
0.589	1.6275	1.872	1.885	1.810	1.899	1.697
0.60	1.6253	1.836	1.835	1.768	1.850	1.667
0.70	1.6138	1.515	1.510	1.476	1.514	1.428
0.80	1.6060	1.287	1.289	1.272	1.288	1.250
0.90	1.6006	1.124	1.123	1.122	1.122	1.111
1.00	1.5969	1.000	1.000	1.000	1.000	1.000
1.10	1.5942	0.896	0.899	0.903	0.899	0.909
1.20	1.5922	0.816	0.818	0.825	0.817	0.833
1.30	1.5905	0.749	0.751	0.757	0.750	0.769
1.40	1.5891	0.695	0.694	0.700	0.694	0.714
1.50	1.5880	0.647	0.645	0.653	0.646	0.667
1.60	1.5870	0.601	0.602	0.608	0.603	0.625
1.70	1.5861	0.566	0.565	0.576	0.565	0.588
1.80	1.5852	0.538	0.531	0.543	0.534	0.555
1.90	1.5845	0.510	0.503	0.511	0.503	0.526
2.00	1.5840	0.485	0.479	0.486	0.477	0.500
2.10	1.5835	0.462	0.454	0.462	0.454	0.476
Nitrobenzene						
0.589μ	1.5525	1.825	1.853	1.789	1.945	1.697
.60	1.5506	1.770	1.806	1.742	1.891	1.667
.70	1.5417	1.470	1.497	1.472	1.537	1.428
.80	1.5355	1.280	1.279	1.267	1.298	1.250
.90	1.5318	1.125	1.120	1.117	1.128	1.111
1.00	1.5296	1.000	1.000	1.000	1.000	1.000
1.10	1.5282	0.900	0.901	0.906	0.900	0.909
1.20	1.5271	0.818	0.825	0.828	0.818	0.833
1.30	1.5261	0.751	0.759	0.763	0.750	0.769
1.40	1.5253	0.697	0.702	0.707	0.693	0.714
1.50	1.5248	0.663	0.654	0.659	0.644	0.667
1.60	1.5240	0.626	0.612	0.629	0.601	0.625

λ	n	Observed Kerr constants	Computed Kerr constants: Havelock	Born	Serber	$1/\lambda$
o-Nitrotoluene						
0.589	1.5472	1.857	1.857	1.793	1.739	1.697
.60	1.5442	1.807	1.798	1.745	1.695	1.667
.70	1.5357	1.491	1.494	1.466	1.444	1.428
.80	1.5305	1.277	1.272	1.267	1.257	1.250
.90	1.5269	1.120	1.122	1.117	1.114	1.111
1.00	1.5244	1.000	1.000	1.000	1.000	1.000
1.10	1.5223	0.905	0.901	0.905	0.907	0.909
1.20	1.5208	0.823	0.822	0.827	0.827	0.833
1.30	1.5198	0.761	0.751	0.761	0.766	0.769
1.40	1.5191	0.708	0.699	0.705	0.710	0.714
1.50	1.5186	0.664	0.653	0.657	0.663	0.667
1.60	1.5181	0.618	0.610	0.616	0.621	0.625
Chlorobenzene						
0.589	1.5246	1.806	1.839	1.770	1.684	1.697
.60	1.5236	1.756	1.799	1.735	1.655	1.667
.70	1.5161	1.448	1.496	1.460	1.424	1.428
.80	1.5111	1.250	1.283	1.262	1.245	1.250
.90	1.5085	1.110	1.129	1.115	1.109	1.111
1.00	1.5069	1.000	1.000	1.000	1.000	1.000
1.10	1.5055	0.907	0.912	0.907	0.910	0.909
1.20	1.5044	0.832	0.833	0.828	0.834	0.833
1.30	1.5037	(0.772)	0.766	0.764	0.770	0.769
1.40	1.5033	(0.723)	0.710	0.708	0.716	0.714
1.50	1.5029	(0.680)	0.662	0.660	0.669	0.667
1.60	1.5025	(0.644)	0.620	0.619	0.627	0.625
Halowax						
0.589	1.6374	1.807	1.885	1.797		1.697
.60	1.6354	1.771	1.837	1.757		1.667
.70	1.6251	1.480	1.522	1.475		1.428
.80	1.6183	1.278	1.302	1.252		1.250
.90	1.6132	1.124	1.136	1.119		1.111
1.00	1.6098	1.000	1.000	1.000		1.000
1.10	1.6073	0.902	0.902	0.903		0.909
1.20	1.6054	0.827	0.821	0.826		0.833
1.30	1.6042	0.763	0.755	0.761		0.769
1.40	1.6031	0.712	0.698	0.704		0.714
1.50	1.6023	0.658	0.649	0.656		0.667
1.60	1.6015	0.617	0.607	0.614		0.625

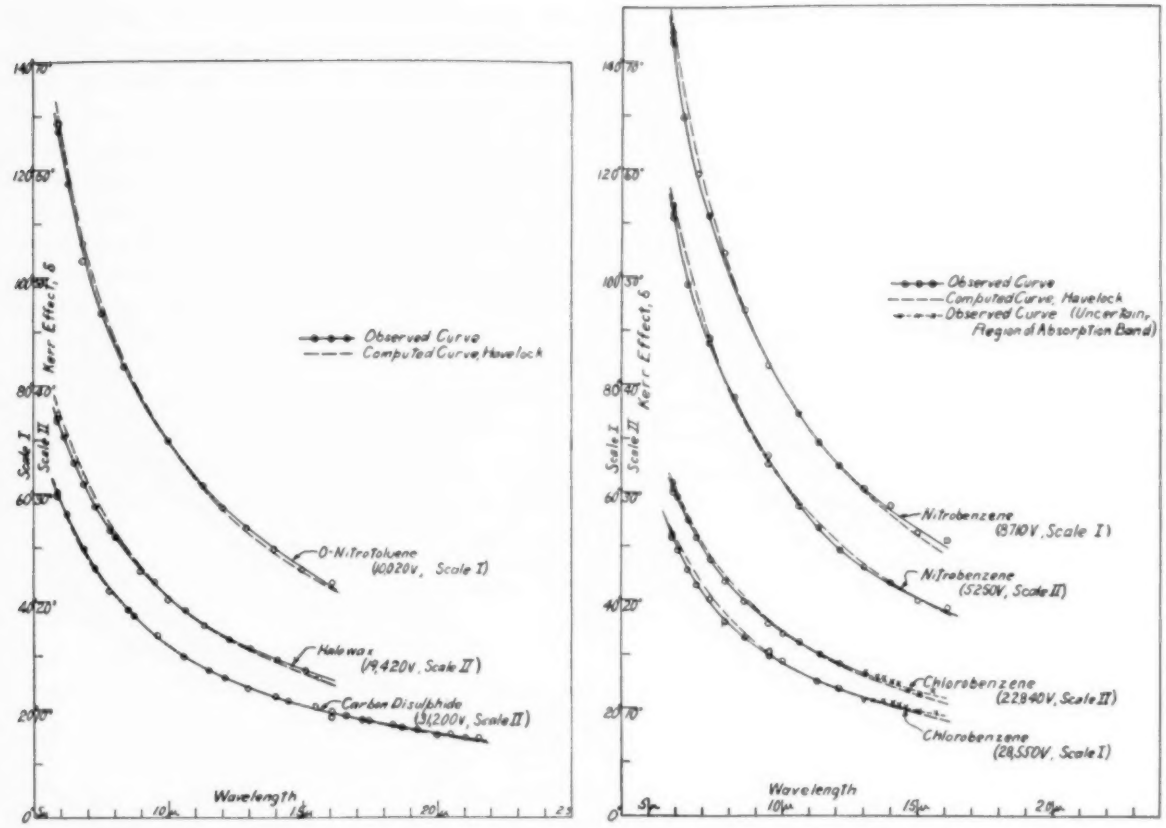

FIG. 3*a*. Kerr effect dispersion curves for *o*-nitrotoluene, halowax, and carbon disulphide; *b*, Kerr effect dispersion curves for nitrobenzene and chlorobenzene.

is not dependent on the voltage. A possible exception to this is *o*-nitrotoluene, which is to be investigated further in this connection. Two voltages are plotted in Fig. 3b to indicate the general accuracy and agreement of the results. The results for the different voltages gave a general agreement with the law of proportionality of the Kerr effect to the square of the field but, for the same general reasons as already mentioned, the suitability and accuracy of the method in this connection was not particularly good.

The observed values in Table I are a composite of the results for all the different voltages for each material. The Havelock and Born computed values need no explanation since each involves only a single constant, which is fixed by the fact that all values are referred to that at 1μ as unity. In using the Serber formula the main ultraviolet absorption wave-length for each substance was used, varying from 2000 to 2600A. The second constants were determined by fitting the observed curves at two points between 0.8 and 1.4μ.

The values listed for the refractive index are those determined (temp. 22°C) in the present work, save those for CS_2 which are from the L. and B. tables.

DISCUSSION OF RESULTS: CONCLUSIONS

Perhaps the most striking thing about the results is the fact that the simple Havelock formula, with its rather meager theoretical background, fits the facts on the whole better than either of the others. However, the Born formula really applies only to nonpolar materials so, in all strictness, its use here should be limited to CS_2. Regarding the Serber formula, it may also be explained that there is no certainty that the ultraviolet frequencies as chosen are really

the centroid frequencies which should be used. To find these by a process of fitting the observed curve, however, would require the determination of one more constant.

It will be noted from the tables that the Havelock formula gives slightly *larger* values than the observed for shorter wave-lengths and slightly *smaller* for the longer wave-lengths, i.e., a somewhat steeper dispersion curve. This was also found to be the case by Szivessy and Dierkesmann[2] for three of the five liquids they tested in the visible and ultraviolet. Only one liquid, *viz.*, chlorobenzene, was common to these two investigations. For this liquid Havelock's law fits somewhat better in the ultraviolet than in the infrared.

As a matter of fact, beyond 1μ the simple law of the inverse wave-length fits the observed values about as well as any of the more complicated formulas, particularly for the polar liquids. A little study of this point shows that a formula of the type

$$K = C[(n^2+2)^2/n\lambda]\{1+a/\lambda^2+b/\lambda^4+\cdots\},$$

which by some simplification can be read out of Serber's work[6] would fit the results best of all.

The general conclusion to be drawn from our results is that for wave-lengths beyond 1μ the electro-optic dispersion is much the same for the five liquids investigated, is in reasonably good agreement with any of the three dispersion formulas tested and, indeed, departs only slightly from the simple inverse wave-length law. For the shorter wave-lengths agreement with theory is not as good, although in some cases the Havelock formula fits very well. For carbon disulphide the deviations of our results from Havelock's law is almost within the limits of experimental error for the whole spectral region investigated.

Cosmic-Ray Positive and Negative Electrons

CARL D. ANDERSON, *California Institute of Technology*

(Received June 19, 1933)

A determination of the specific ionization of cosmic-ray particles, first, by a count of the number of drops per cm along cosmic-ray tracks on cloud-chamber photographs and, second, by measurements of the energy loss in lead has shown that the great bulk of the cosmic-ray particles of positive charge are positive electrons. The primary ionization was found to be about 31 ion-pairs per cm in air at S.T.P., but the total energy loss represents about 120 ion pairs per cm in air. Approximately the same values of specific ionization were found for the positives as for the negatives. Positive and negative electrons were found to occur in nearly equal numbers and to have similar distributions in energy. Energy distribution curves are given for the positives and negatives. A brief description of the experimental procedure is given, and several track photographs are shown. In view of the discovery that hard gamma-rays of Th *C''* give rise to positives and negatives in pairs, similar to the effects found in cosmic-ray studies, it is concluded that the absorption of the Th *C''* rays is due in part to that by free negative electrons and in part to a nuclear effect which results in the production of pairs of positive and negative electrons, the former effect accounting for the greater part of the absorption of the Th *C''* rays. The symmetry in occurrence of the positive and negative electrons found in the cosmic-ray studies shows that the nuclear effect which results in the production of positive and negative electrons in pairs represents the predominant part of the absorption for the range of energies as high as those of the cosmic rays and that the absorption by free negative electrons is relatively small.

THE Wilson cloud-chamber photographs of Skobelzyn[1] showed the existence of cosmic-ray particles of energy greater than 15×10^6 electron-volts, his limit of measurement.

Experiments[2] by the writer in collaboration with Professor R. A. Millikan making use of a vertical Wilson chamber, specially designed for a study of cosmic rays and capable of measuring energies up to 3 and 4×10^9 volts by means of a strong magnetic field up to 20,000 gauss brought to light the fact that there occur particles of negative charge and also particles of positive charge in abundance. A preliminary survey of their energies was given.

By measurements on the density of ionization along the track it was shown that in general the tracks of both positive and negative curvatures were due to particles of charge equal to that of one electron, and could not be due to particles of multiple charge.

For the purpose of studying in detail the mechanics of the interaction of the particles with matter and to help identify the particles of positive charge, a sheet of lead was inserted in the chamber so as to allow the observation of the particles before and after they penetrated the lead plate. It was then possible to study the scattering and energy loss of the particles in lead,[3] and in particular, effects were obtained which we could interpret logically on the basis of specific ionization, curvature, and range as due only to particles of positive charge and mass small compared with that of the proton.[4] These particles have been called positrons. Blackett and Occhialini, using a tube-counter controlled Wilson chamber in a magnetic field of 3000 gauss, obtained effects similar to those that we observed and confirmed our conclusion that it is necessary to call upon positive particles of mass small compared with that of the proton to explain the observed effects.[5]

The tendency of the cosmic-ray particles to occur in groups, first noticed by Skobelzyn, also

[1] Skobelzyn, Zeits. f. Physik **54**, 686 (1929).

[2] Millikan and Anderson, Phys. Rev. **40**, 325 (1932), and Anderson, Phys. Rev. **41**, 405 (1932). See Kunze, Zeits. f. Physik **80**, 559 (1933).

[3] Anderson, Phys. Rev. **43**, 381A (1933).

[4] Anderson, Science **76**, 238 (1932) and Phys. Rev. **43**, 491 (1933).

[5] Blackett and Occhialini, Proc. Roy. Soc. **A139**, 699 (1933).

a marked feature of our photographs,[6] is strongly emphasized in the photographs of Blackett and Occhialini.

Before the lead plate was inserted in the chamber we interpreted the tracks of negative curvature as due to electrons, and the tracks of positive curvature as due probably to protons, at that time the only known positive particle of unit charge. This interpretation was made with some hesitation, however, because of the fact that while protons and electrons at high energies produce about the same ionization the positive tracks of considerable curvature could only with difficulty be ascribed to protons because of the meager ionization exhibited. Fig. 2 shows in a general way the ionization of protons as compared to particles of the same charge but of a mass equal to that of the free electron as a function of the curvature in the magnetic field. Fig. 3 gives for comparison the energy of protons and electrons for various values of $H\rho$. We pointed out at that time that precise data on the specific ionization of the lower energy positive tracks were needed to distinguish protons from electrons. One of the purposes of this paper is to report the results of this work, which lead to the conclusion that the bulk of the positive particles are positrons and not protons. Additional evidence for this conclusion will be brought out in a discussion of the curvature distribution of the positive and negative tracks.

Experimental Procedure

In answer to numerous queries a brief description will be given of the experimental method employed. A vertical Wilson chamber of 16.5 cm diameter and 4 cm depth was incorporated in a large electromagnet designed to produce a uniform magnetic field over the volume of the chamber of magnitude sufficient to measure the energies to be expected for the cosmic-ray particles. The magnet contains 800 turns of copper tubing of $\frac{1}{4}$ inch inside and $\frac{3}{8}$ inch outside diameter wound in the form of 40 pies and arranged in two coils. The copper tubing serves the double purpose of carrying the electric current and the circulating water for cooling purposes, the pies in each coil being connected in series electrically and in parallel for the water circuits. For the greater part of the work a current of 1600 amperes at a potential of 275 volts was used, the two coils being connected in parallel and giving a field of 15,000 gauss. A steady flow of about 35 gallons of water per minute through the coils was maintained during operation. A schematic sketch indicating the relationship of the essential parts is shown in Fig. 1. Located at the center of

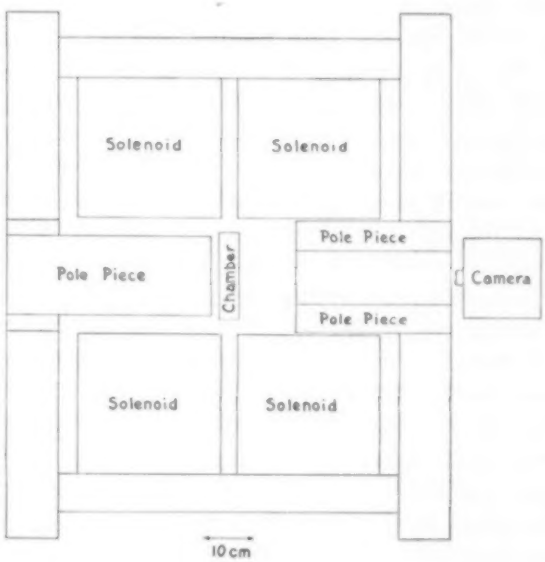

Fig. 1. Schematic diagram of apparatus.

the coils is the Wilson chamber. It is of the reciprocating piston type, a thin rubber diaphragm placed across the head of the piston sealing it air-tight. It operates automatically at the rate of one expansion every 14 seconds. The air is drawn out from behind the piston to produce the expansion. Nearly filling the space inside the piston is a solid core of Armco iron of 14.8 cm diameter. Separated from this by an air-gap of 16.5 cm is the second pole piece of 22 cm diameter which contains a square hole 11 cm×11 cm through which the tracks are photographed. The magnetic field is uniform to within 10 percent throughout the volume occupied by the chamber. The cloud chamber suffers practically no temperature increase during a run which is usually of two hours' duration, and 500 photographs are taken without an adjustment of the expansion ratio. A carbon arc light is used for illumination, and the photographs are taken

[6] Anderson, Phys. Rev. **43**, 368 (1933).

on 35 mm supersensitive panchromatic film. A beam of light collimated to a width of 1 cm was used for most of the work. A single photograph was considered sufficient to give the data desired, though by a simple arrangement provision has been made for taking stereoscopic pictures. A pair of mirrors was placed at the sides of the square hole in the iron pole piece through which the photographs were taken, and the two reflected images of the chamber along with the central direct central image were all recorded together on the one film. See for example Fig. 18.

The yield of cosmic-ray tracks is in agreement with that to be expected from the amount of ionization due to cosmic radiation as measured in ionization chambers. Including short tracks and the very diffuse tracks, about one track per five expansions is obtained. To date over 1500 photographs of cosmic-ray tracks have been obtained. Of course, only the long and sharp tracks which represent but a fraction of these are suitable for curvature measurements. For the purpose of determining the distribution in energy of the particles, given in this paper, only the long and exceedingly sharp tracks were chosen. Extreme care was taken to eliminate to a high degree all disturbing influences such as motion of the gas in the chamber, falling drops, etc. To insure against errors due to falling drops the camera shutter was opened just previous to the time of formation of the drops; thus any motion of the drops would appear on the photographs and could not escape detection. The tracks from which the energy distribution was determined were particularly free from such effects.

Specific Ionization

In order to determine the abundance of positrons as compared with protons the specific ionization was determined for a number of tracks of both positive and negative curvature by counting on diffuse tracks the number of drops per cm. (See for example Figs. 6 and 7.) By this method differences in specific ionization of 20 percent could readily be detected. The difference in specific ionization between a positron and proton amounts to about 20 percent for a value of $H\rho$ equal to 3×10^6 gauss-cm, and for curvatures greater than this the difference becomes more pronounced until at values of $H\rho$ less than 10^6 gauss-cm the ionization of positrons and protons differs in order of magnitude (see Fig. 2). Although for tracks of the degree of diffuseness used for drop-counts it is possible to measure energies only for the more curved tracks, it is these which are best suited for differentiating between positrons and protons. Those of positive curvature do not in general show a greater ionization than those of negative curvature, and the amount of ionization measured is consistent with that to be expected from particles of small mass (of the order of that of the free electron) and for the more curved tracks is definitely inconsistent with that to be expected from protons. Further, for a large number of slightly diffuse positively curved tracks where the ions are not sufficiently resolved for an exact count, but where a difference in ionization such as that to be expected between positrons and protrons could readily have been detected, positrons rather than protons were indicated for the bulk of the tracks. For individual cases of single positively curved tracks it is not possible to state definitely that the tracks represent a positive particle travelling downward through the chamber rather than a negative particle travelling upward. However, it is a safe inference based on various kinds of evi-

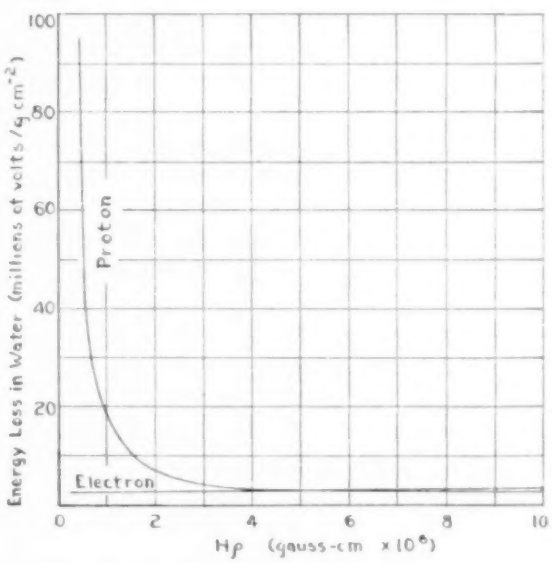

Fig. 2. Relative ionization of protons and electrons in terms of curvature in magnetic field.

dence which we have previously pointed out that the tracks of positive curvature in general represent downward positives rather than upward negatives. Professor Millikan and Dr. Neher have found that a screen of lead placed above their electroscope decreases the ionization by a considerable amount whereas the same lead screen below the electroscope produces no detectable change in ionization. This also is strong evidence that the particles are in general moving downward. The conclusion is reached, therefore, that the positives in general are positrons rather than protons, though in two cases we have found tracks which ionize too heavily to represent electrons and may represent protons. Blackett and Occhialini[5] have also reported protons but conclude that the positives in general represent positrons. Heavier positive particles may also occur but because of their relatively short range may frequently escape detection.

The drop-counts on 26 diffuse tracks lead to a mean value of 31 ion-pairs per cm in air at S.T.P. which is in fair accord with the value of 36 ion-pairs reported by Locher.[7] This must, however, represent only a lower limit to the actual specific ionization because of clusters of large numbers of ions at various points along the tracks at which the ions could not be accurately counted and were therefore not included in the count. Occasionally an electron will be removed from the *k*-shell of an atom of the gas through which the particle passes, and in returning to its normal state the atom by internal conversion of the photon may emit an electron which carries off the ionization energy. An electron of this energy would have only a very short range and the ionization would all be produced in the immediate neighborhood of the track. An electron may also receive a considerable energy by a close encounter and because of the presence of the strong magnetic field be sufficiently coiled up so as to produce ionization only in the immediate neighborhood of the track (unless the energy received is of the order of a million volts or more, an event which is relatively improbable). A study of these effects on the mean energy loss of the particles is now being made. Kolhorster and Tuwin[8] by combined electroscope and Geiger-counter determinations report a value of 135 ion-pairs per cm. This figure includes effects such as the two mentioned above, and this together with the effect of associated tracks may account for the high value they find.

Another method for determining the energy loss of the cosmic-ray particles is to measure their energies before and after they penetrate a plate of a given material of known thickness. We have reported a preliminary value of about 35×10^6 volts per cm energy loss in lead for electrons of the order of 300×10^6 volts energy.[3] The energy loss of particles in such a lead plate is subject to considerable statistical fluctuation and further measurements will be needed before an accurate mean value of energy can be given. Fig. 8 shows an electron of 113 million volts initial energy which loses 27 million volts in passing through 13.4 mm of lead. This corresponds to an energy loss close to 20 million volts per cm which is good accord with the calculated value of 19.4 million volts per cm of lead for electrons of 100 million volts energy given by Bethe.[9] The mean value for energy loss in lead on the basis of our present data is, however, greater than this and is approximately 35 million volts per cm.

For comparison with specific ionization measured in air it is interesting to compute the number of ion-pairs per cm to be expected in air on the basis of a value of 20 million volts per cm in lead. Using the values given by Bethe for the relative energy loss per g cm^{-2} in water and lead (2.90 million volts per g cm^{-2} in water as compared to 1.76 million volts per g cm^{-2} in lead for 100 million volt-electrons) and assuming the same value per g cm^{-2} for air as for water, we find an energy loss of 3900 volts per cm for air at S.T.P. If we take a mean value of 32 volts as the energy required to produce a pair of ions,[10] this leads to 122 ion-pairs per cm in air at S.T.P. It appears probable that though the *primary ionization* is 30 to 35 ion-pairs per cm in air, the *total ionization* is of the order of 120–140 ion-pairs per cm for electrons in this energy range.

Although drop-counts have shown no differ-

[7] Locher, Phys. Rev. **39**, 883 (1932).

[8] Kolhorster and Tuwin, Zeits. f. Physik **81**, 435 (1933).

[9] Bethe, Zeits. f. Physik **76**, 293 (1932). See also Carlson and Oppenheimer, Phys. Rev. **41**, 763 (1932).

[10] Kulenkampff, Phys. Zeits. **30**, 777 (1929).

ence in ionization between positives and negatives, the energy loss in lead for the positives is slightly higher than for the negatives as far as the data have been collected. This may well be a statistical fluctuation and further work is in progress.

Curvature Measurements

We have given the results of energy measurements for a number of tracks,[11] and Kunze[12] has reported energies in essential agreement with ours. Curvature measurements have now been made on a new set of very carefully selected tracks. A curvature distribution based on a relatively small number of tracks on most of which accurate measurement was possible was considered preferable to one based on a larger number of tracks which included short and diffuse tracks. Hence only very sharp tracks longer than 8 cm were chosen. Precautions were taken to reduce to a minimum all disturbing influences in the cloud chamber which might introduce errors. Figs. 13–17 are typical examples of tracks of this group. Measurements were made on the original negatives by means of a comparator, the coordinates of points 0.5 mm apart being measured and plotted. In Fig. 4 is plotted a typical set of such measurements. The units of ordinates are millimeters and the units of abscissae are hundredths of millimeters as measured on the original negative film which is 0.14 full size. A circular track plotted in this way forms a parabola and from a measurement of a and b on the graph the radius of curvature can be determined. Electron energies up to one or two billion volts were in most cases found readily measurable.

The values of the energies of these tracks, listed separately for the positives and negatives, are given in Table I on the assumption that the positives are positrons and the negatives are electrons, an assumption justified by the evidence discussed in the previous section. These criteria for the selection of the tracks, *viz.*, length and sharpness, should favor neither the low nor the high energies and should, therefore, give a fair cross section of the energies of the particles except for statistical fluctuations.

[11] Anderson, Phys. Rev. **41**, 405 (1932).
[12] Kunze, Zeits. f. Physik **80**, 559 (1933).

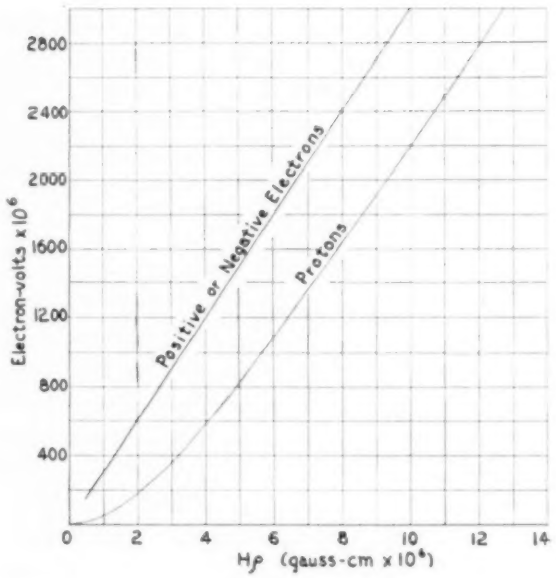

FIG. 3. Energies of fast electrons in terms of curvature in magnetic field. A curve for protons is given for comparison.

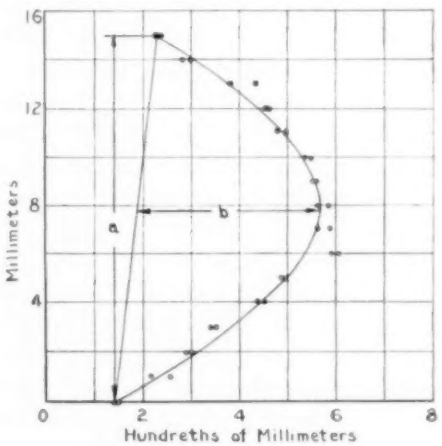

FIG. 4. Plot of the measurements of a representative high energy electron track. Radius of curvature ($R \sim a^2/8b$) reduced to full size in chamber is 498 cm. $H\rho = 7.5 \times 10^6$ gauss-cm; energy $= 2.2 \times 10^9$ electron-volts.

It is to be noted first of all that in this group the positives and negatives occur in nearly equal numbers, and as Fig. 5 shows, with quite symmetrical distributions in energy.

It is necessary to point out that this energy distribution does not characterize the main cosmic-ray beam as it is incident on the earth, but only after it has been filtered by passage through the atmosphere and the screening material around the cloud chamber. The presence

TABLE I. *Energy distribution of positive and negative electrons.* In addition to the tracks listed below there are to be included eleven tracks which showed irregularities due to mass-motion of the air in the cloud chamber and could not be accurately measured or classified as to sign of charge. The energies of the tracks in this group are all very probably greater than about one billion volts.

Positive electrons Energy (volts $\times 10^6$)	Negative electrons Energy (volts $\times 10^6$)	Positive electrons Energy (volts $\times 10^6$)	Negative electrons Energy (volts $\times 10^6$)
120	60	880	600
145	75	900	660
166	85	970	800
190	120	1000	860
200	125	1000	870
220	135	1000	930
235	140	1150	1150
260	155	1350	1250
270	230	1600	1300
310	280	1700	1800
340	300	1900	2200
340	330	2000	2400
440	360	2100	2400
480	370	2200	2600
530	480	2400	2700
540	510	2500	3000
590	540	2700	5000
640	540	2700	
750	570	2700	
770	600		

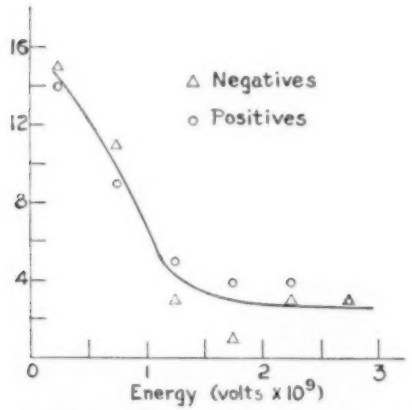

FIG. 5. Distribution in energy of the positive and negative electrons. Each point on the curve represents the number of tracks in the corresponding half-billion-volt interval.

of the large amount of heavy material, coils, pole pieces, etc., immediately surrounding the cloud chamber will also affect the energy distribution of the observed particles because of the "ubergangseffekte." Other indications point to the view that at high altitudes the cosmic-ray particles of low energies form a larger proportion than at the earth's surface.

Out of an additional group of 216 tracks which were not considered sharp enough for energy measurements but which were definitely subject to division into positive and negative curvatures, there were found 107 positives and 109 negatives indicating again approximately equal numbers of positives and negatives.

The symmetry between the positives and negatives is not maintained, however, if we consider only the low energy particles, i.e., those of curvatures corresponding to energies less than 100 million volts. For single particles of low energy because of the high degree of curvature in the magnetic field it is in general not possible to infer their sign of charge since the particles may be turned completely around by the field. Therefore a study was made only of those tracks which were associated with other tracks, where it was possible to infer their direction of motion and hence their sign of charge. In order to obtain a sufficient number with which to work it was necessary to include a number of diffuse tracks where it was not possible to determine unambiguously the direction of the curvature of the higher energy tracks, but it was always possible to determine the sign of charge and the energy of the highly curved lower energy tracks. It was here found that in 52 groups of tracks there were 64 negatives and only 5 positives in the energy range lying below 100 million volts. The excess of low energy negatives over positives associated with other tracks may well be due to close encounters between high speed particles (positive or negative) and extranuclear negative electrons in which a considerable energy transfer takes place.

The general symmetry in occurrence between the positives and negatives is in accord with the view that in the primary absorption process of the incident cosmic-ray beam positives and negatives are formed in pairs perhaps as governed by Dirac's theory of electrons.[13]

The near equality in the number of positive and negative particles shown here is of course only statistical. It will be noted, however, that there are 16 measured positives above one billion volts as compared to only 11 negatives. Though

[13] Dirac, Proc. Roy. Soc. **A126**, 360 (1930) and **A133**, 60 (1931).

The magnetic field strength was 15,000 gauss for all photographs except Fig. 18 where it was 650 gauss. The actual diameter of the portion of the chamber shown in the photographs is 14 cm.

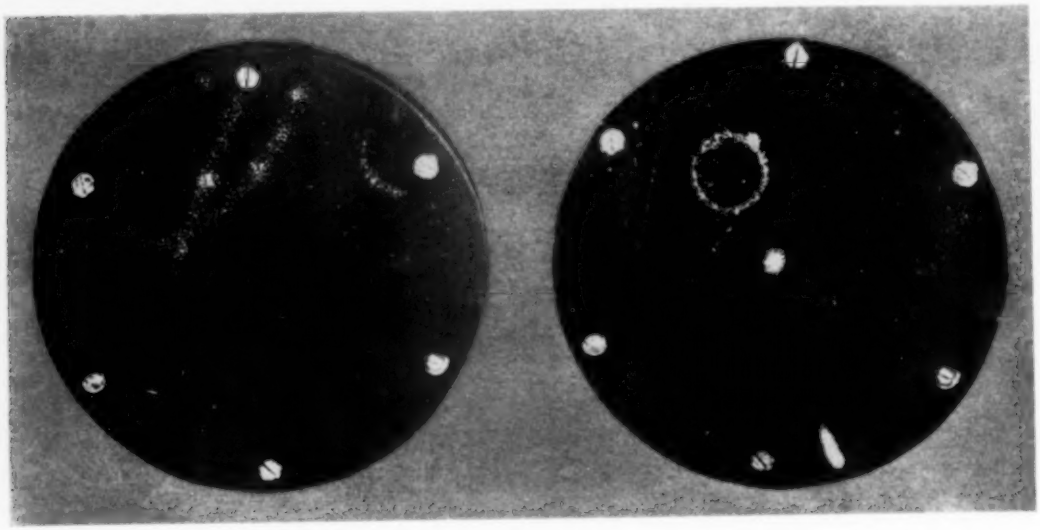

6 7

FIG. 6. A representative group of three "early" tracks suitable for an ion-count, showing drops resolved as a result of the diffusion of the ions. On the upper portion of the high energy track is a small cluster of ions.

FIG. 7. Three ages of tracks are represented: (1) a high energy very diffuse early track, (2) a later pair of tracks showing less diffusion of ions; the circular track is an electron of 4.8 million volts energy, the other one a higher energy track of uncertain sign of charge, and (3) at the left a short, sharp track produced by a particle which entered the chamber coincident with or immediately following the expansion.

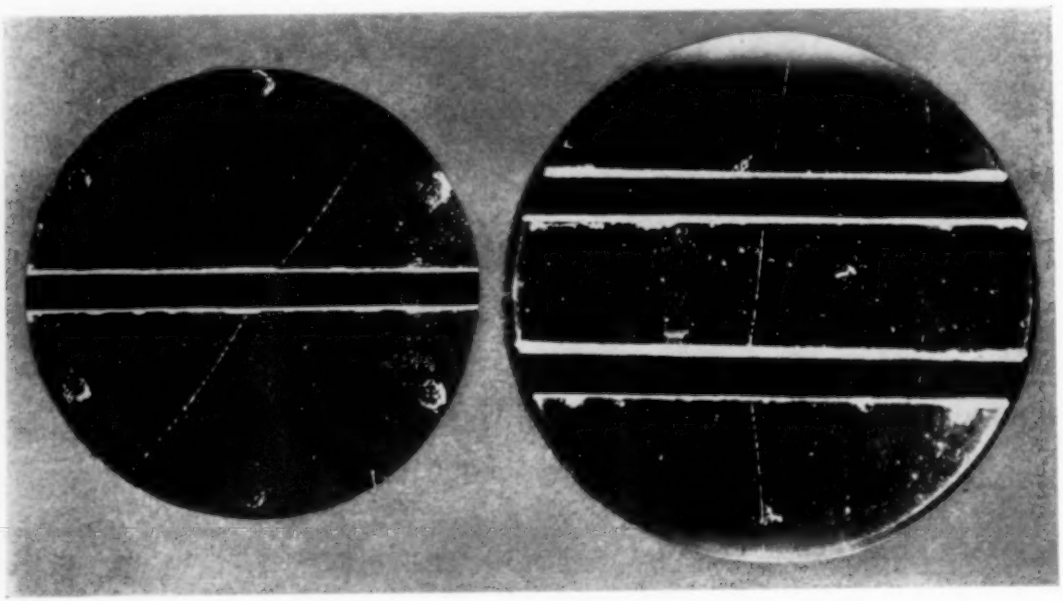

8 9

FIG. 8. A 113 million volt-electron traversed 13.4 mm of lead and emerged with an energy of 86 million volts, showing an energy loss of 20 million volts per cm of lead. Thickness of lead plate is 11 mm.

FIG. 9. An electron of 240 million volts energy lost about 20 million volts in first passage through the 11 mm lead plate and an additional 60 million volts in the lower plate.

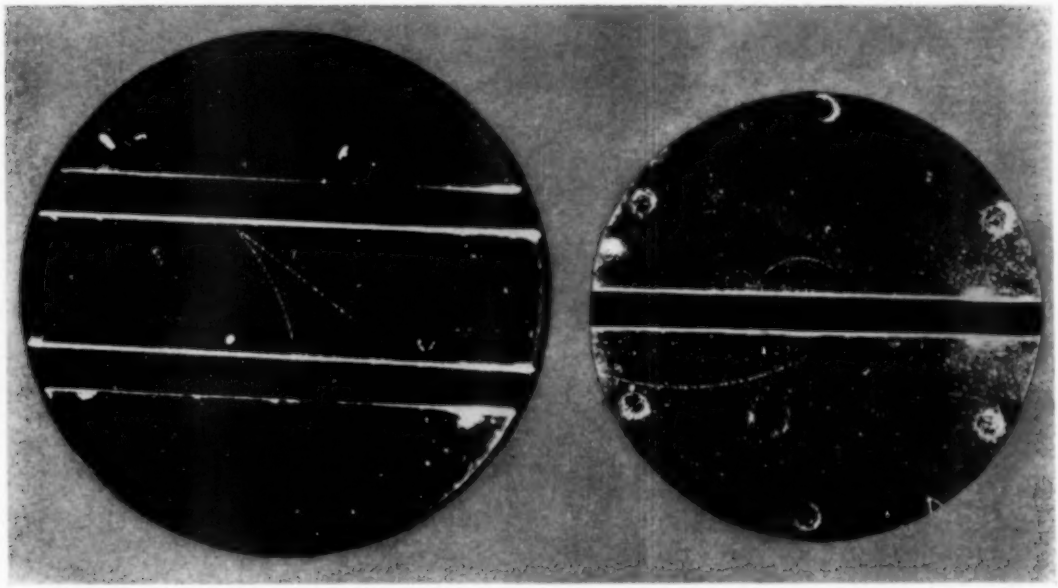

10 11

FIG. 10. A secondary electron of 32 million volts energy was ejected by a fast electron which passed through the lead plate. The angle, θ, between the directions of the primary and secondary electrons satisfies within experimental uncertainty the relation $\tan\theta=(2mc^2/E)^{\frac{1}{2}}$, where E is the energy of the secondary electron. The energy of the primary electron measured between the plates is about 800 million volts. An additional secondary electron of about 6 million volts energy was produced in the lower plate and appears just above the lower plate at the right. The frequency of occurrence of secondary electrons produced by close encounters is in close agreement with that to be expected from theoretical considerations.

FIG. 11. There are two interpretations of this photograph. The first is that a positron of 38 million volts energy penetrated the lead plate and emerged above with 6 million volts energy. It is seen to suffer a sharp deflection upon striking the upper surface of the lead plate. The second interpretation is that an electron of 38 million volts energy was ejected downward from the plate, and at the same time a positron of 6 million volts energy ejected upward and deflected by the magnetic field until it struck the plate and rebounded. Either of these two views requires the positron interpretation.

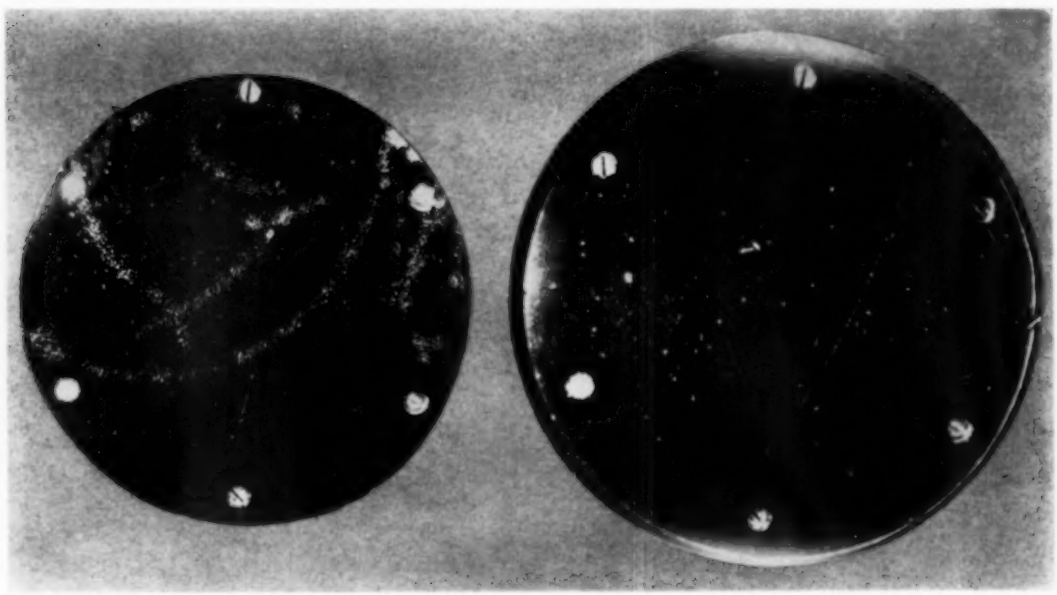

12 13

FIG. 12. A shower represented by a group of simultaneous early tracks. From the specific ionization and curvature in the magnetic field it is necessary to ascribe most of these tracks to particles of small mass, i.e., positrons or electrons.

FIG. 13. An electron of 120 million volts energy.

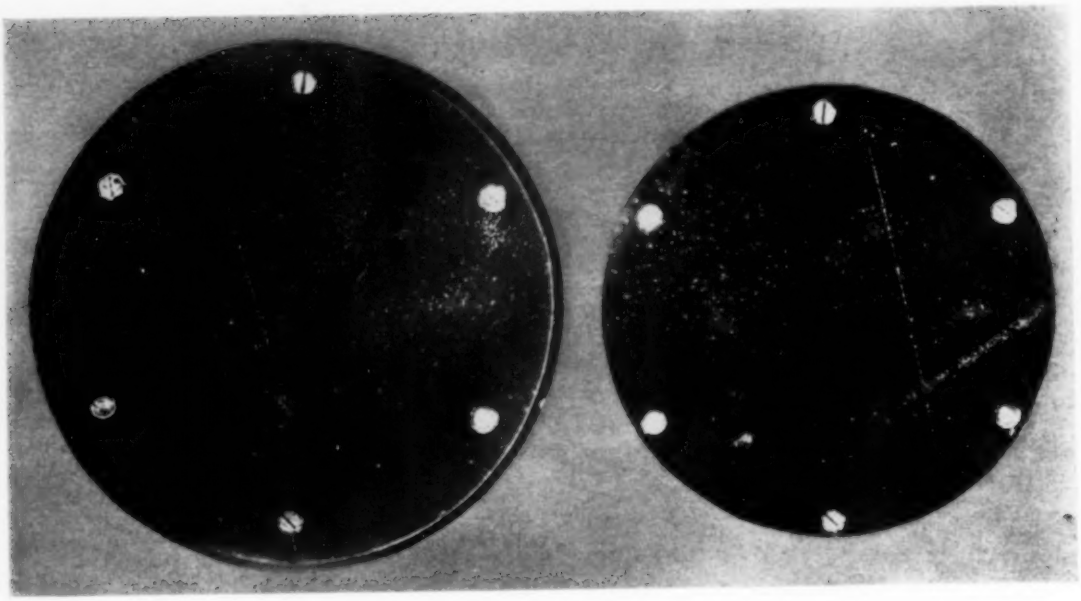

14 15

FIG. 14. A positron of 900 million volts energy.
FIG. 15. An electron of 1300 million volts energy.

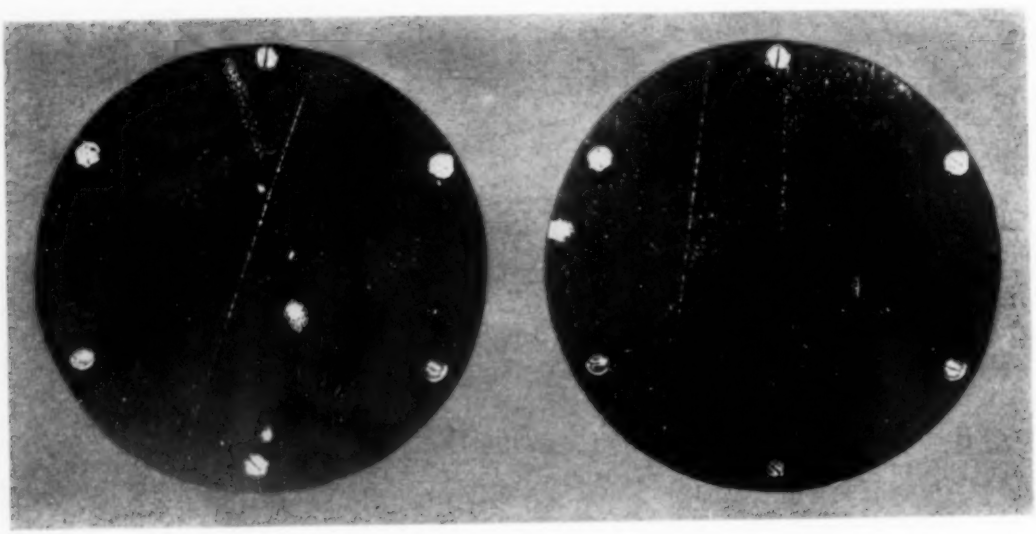

16 17

FIG. 16. A positron of 2700 million volts energy.
FIG. 17. An electron of 5000–7000 million volts energy.

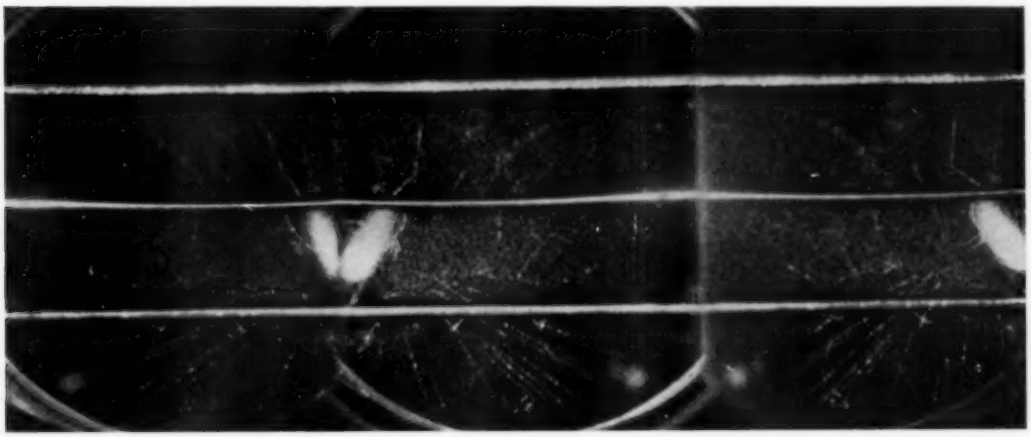

FIG. 18. A shower of more than 20 cosmic-ray particles originating in the iron of the pole piece. Three views are shown, the outer two views are mirror images of the direct central view. The outer views are equivalent to photographs taken by cameras placed on either side of the chamber with their axes inclined at 12.5 degrees to the axis of the chamber. This shower occurred during a study of the Th *C''* gamma-ray effects and the magnetic field was adjusted to the low value of 650 gauss. Although most of the tracks are essentially straight both positives and negatives occur, and their energies are all above those to be attributed to effects of the gamma-rays present. The short, thick track is very probably an alpha-particle arising from stray radioactive material in the chamber. Its high degree of diffuseness indicates that it passed through the chamber before the shower of cosmic-ray particles occurred.

our data are based on too few tracks to detect a small difference in number between positives and negatives, the excess of high energy positives over negatives agrees in a general way with the tube-counter experiments of Johnson[14] and Alvarez and Compton,[15] dealing with large numbers of particles, which show an east-west asymmetry that indicates an excess of positives over negatives.

A certain group of 815 tracks most of which were not capable of accurate measurement for energy were classified as to multiplicity of tracks with the following results: there occurred 708 singles, 82 doubles, 7 triples, 7 quartets, 3 quintets, 7 having between 6 and 10 tracks, and one with more than 10. Photographs showing more than one track were not counted as examples of multiple tracks unless the tracks were clearly associated in time as shown by an equality in diffusion of the ions on all the tracks. In most cases the multiple tracks appear to originate at a common center, but in some cases there also occur tracks definitely associated in time but apparently not coming from the same source. As a general rule in the photographs showing several tracks both positives and negatives occur.

CONCLUDING DISCUSSION

To obtain a complete description of the primary cosmic-ray beam it will of course be necessary to understand in detail the absorption processes involved. Experiments have shown that these processes are of considerable complexity and further experimental data are needed. Certain general conclusions, however, can perhaps safely be drawn from the experimental data at hand. We shall consider the primary cosmic-ray beam at sea level to consist in greater part of photons, a point of view held by Professor Millikan for several years, and now given additional support by the fact that hard gamma-rays of Th *C''* have been found to produce positrons as do the cosmic rays.[16, 17] It is apparent at once as we have already pointed out that the Klein-Nishina formula which deals only with absorption by free electrons cannot be valid for radiation as energetic as the cosmic rays.[2] To explain the presence of the large number of positrons

[14] Johnson, Phys. Rev. **43**, 834 (1933).

[15] Alvarez and Compton, Phys. Rev. **43**, 835 (1933).

[16] Anderson, Science **77**, 432 (1933).

[17] Anderson and Neddermeyer, Phys. Rev. **43**, 1034 (1933).

observed, and their frequent occurrence in groups associated with negative electrons, it is necessary to call upon a new type of absorption which must be due to nuclear effects.

The excess absorption[18] and anomalous scattering[19] effects of Th C'' gamma-rays in the heavy elements is undoubtedly due at least in part to the production and perhaps the annihilation of positrons and amounts to approximately 20 percent of the total absorption for the hard component (2.6×10^6 volts) of Th C'' gamma-rays in lead. In contrast to the approximately equal numbers of positives and negatives for the cosmic-ray particles we have observed a considerably greater number of negatives than positives ejected from lead by the Th C'' rays. This accords with the view that absorption by the free negative electrons represents the more important part of the absorption for gamma-rays of this energy. A statistical study of the positives and negatives produced by Th C'' gamma-rays is in progress.

The striking fact that in the cosmic rays positives and negatives occur in practically equal numbers and have apparently a similar energy distribution is in accord with the assumption that the nuclear effects involved give rise to the positives and negatives in pairs (in some cases several pairs as evidenced by the showers), and that this type of absorption represents nearly the whole absorption for rays in the energy range of hundreds of millions of volts, the absorption by free electrons being of relatively minor importance.

I wish to make grateful acknowledgment to the Carnegie Corporation for a grant which made this work possible and to Mr. Seth H. Neddermyer for his assistance.

[18] Chao, Proc. Nat. Acad. Sci. **16**, 431 (1930); Phys. Rev. **36**, 1519 (1930); and Meitner and Hupfield, Naturwiss. **19**, 775 (1931).

[19] Gray and Tarrant, Proc. Roy. Soc. **A136**, 662 (1932).

LETTERS TO THE EDITOR

Prompt publication of brief reports of important discoveries in physics may be secured by addressing them to this department. Closing dates for this department are, for the first issue of the month, the twentieth of the preceding month; for the second issue, the fifth of the month. The Board of Editors does not hold itself responsible for the opinions expressed by the correspondents.

Concerning W. T. Sproull's Article on "Diffraction of Low Speed Electrons by a Tungsten Single Crystal"

Sproull[1] reports intense sharp beams in the AA' azimuth (perpendicular to the cube diagonals) of the (112) plane for normal incidence. They obey a volume equation after allowing for refraction, and not the surface equation. All other beams are weak and broad. A simple interpretation of the intense beams is at hand if we make the logical assumption that due to evaporation during heat treatment of the crystal etching occurs parallel to the more densely populated (011) sets of planes which contain the atoms used for the volume equation. On this view the lines which Sproull has plotted in Fig. 2 as the volume condition (curved lines) now become the surface condition (straight lines) and *vice versa*, and θ is to be replaced by the angle of emergence measured from the normal to the (011) planes. Thus the beams in the AA' azimuth are really following the surface grating and are little affected by the depth grating. Also, the surface layer of atoms will appear more effective than for normal incidence, and the beams should continue over greater ranges in voltage and angle. This interpretation vitiates Sproull's values of the inner potential W_o, and his conclusion regarding constancy of the values, since his method does not apply when the angle of incidence is other than normal. Theoretically the observations should fall on the line representing the surface grating condition regardless of the value of W_o. That they are slightly displaced may be attributed to some other cause.[2]

Two other considerations require comment. First, Sproull concludes that the higher outgassing temperatures which could be used with tungsten compared with those which could be used by the writer with copper account for the "more consistent values" of W_o. We have previously emphasized that during the final observations on copper, the surface gas layer was reduced to such a thickness that it had no observable effect on the *intensity* of the beams due to copper, and further that even when the gas layer was thick enough to reduce appreciably the intensity of these beams, the *voltages* at which the beams attained their maximum values were not noticeably altered.

Second, Sproull states that contact potentials of over 7 volts exist in his electron gun and that their large fluctuation of 2 or 3 volts from day to day "may account for the irregular variations of W_o reported by some observers" using an oxide electron source. Since the writer has reported values of inner potential obtained when using such a source it is in order to state here that precautions have been taken and observations made which eliminate errors of the type mentioned due to spurious causes. For every type of electron gun used by the writer, preliminary investigations have been made to test the homogeneity of the electron stream and the contact potentials in the gun by an arrangement equivalent to that given in *J.O.S.A. and R.S.I.*[3] In addition, a check as to the constancy of the conditions from day to day during the course of a long series of observations has always been made by checking the voltage, colatitude angle, and intensity of a low voltage (below 100 volts) diffraction beam once or twice each day. The voltages have always checked to within the order of 0.1 volt after sufficient outgassing. We believe that these tests are sufficient to eliminate the possibility of any fluctuations as observed by Sproull, and conclude that some condition peculiar to his arrangement is responsible for his observed fluctuations.

H. E. FARNSWORTH

Brown University,
Providence, R. I.,
April 19, 1933.

[1] Sproull, Phys. Rev. **43**, 516 (1933); R.S.I. **4**, 193 (1933).

[2] Space is not available here for a discussion of this.

[3] H. E. Farnsworth, J.O.S.A. and R.S.I. **15**, 290 (1927).

Comments on W. T. Sproull's Article "Diffraction of Low Speed Electrons by a Tungsten Single Crystal"

I should like to suggest an alternative explanation of the very interesting effects in electron diffraction described by W. T. Sproull in a recent number of your journal.[1] He finds that sharp beams are obtained from a single crystal of tungsten cut to a (1–1–2) plane which do not follow the law to be expected for surface effects, but another[2] which he interprets as a condition for volume interference. This equation is, however, the condition that wavelets from atoms in a (1–0–1) plane should be in phase,

[1] W. T. Sproull, Phys. Rev. **43**, 516 (1933).

[2] Reference 1, p. 519, Eq. (2).

and I suggest that the results would be explained if this plane were actually present on the specimen as a result of the etching which the specimen underwent. I have found[3] with single crystals of copper and silver similarly cut and etched that the surface is very far from being a geometrical plane, but consists of a series of pits and pyramids formed by faces developed in the etching, the apparent surface being present, if at all, only to a slight extent. This view would also explain the relative weakness of beams diffracted in the *BC* azimuth[4] compared with those in the *AA'* azimuth, as the (1–1–0) planes in the former azimuth make a larger angle, 54½° against 30°, with the apparent surface than do the latter, and it would be harder for the diffracted beams to escape without hitting the face on the opposite side of the pit, or that of the next pyramid, as the case might be. It would also explain the low value of 5.5 volts found for the inner potential. If the effects observed are due only to the surface atoms the full inner potential, which would only be reached a finite distance inside the crystal, would not come into play.

G. P. THOMSON

Imperial College of Science
and Technology,
London, England,
June 9, 1933.

[3] G. P. Thomson, Proc. Roy. Soc. **A133**, 1 (1931).
[4] Reference 1, p. 518, Fig. 1.

The Be III $1snp\ ^1P_1 - 1s^2\ ^1S_0$ Series

Members of this series have been reported by Ericson and Edlén[1] and Edlén[2] but no accurate calculation of the series limit was made from their observations. The authors find on one of their plates, which was taken with a twenty-one-foot grazing-incidence vacuum spectrograph, two members of this series in the second order and three members in the first order. Accordingly, the second order lines were measured and their wave-lengths determined from known copper lines, which had been standardized against Edlén's oxygen standard lines. These values together with λ75.9270 Be IV $^2P - ^2S$ were used in the first order to determine the wave-length of the third member of the series. The results are given in Table I.

TABLE I. *Lines of the Be III series* $1snp\ ^1P_1 - 1s^2\ ^1S_0$.

Int.	λ	cm^{-1}
50	100.2535A	977,471
25	88.3738	1,131,557
5	84.8408	1,178,678

If one calculates the limit of the series from the second and third members in the usual way, one gets 1,239,752 cm^{-1} as a value for the limit. This value can be improved by using the relation

$$(D_1 - D_2)/(D_2 - D_3) = (T_1 - T_2)/(T_2 - T_3)$$

which can be derived from the Ritz term formula and where $D_1 - D_2$ is the difference of the fractional parts of the Rydberg denominators of the terms and $T_1 - T_2$ = the difference between the term values. This calculation gives the term values in Table II.

TABLE II. *Term values of Be III* $1snp\ ^1P_1$ *and* $1s^2\ ^1S_0$.

Designation	Term value	Rydberg denominator
$1s^2\ ^1S_0$	1,239,703 cm^{-1}	0.89254
$1s2p\ ^1P_1$	242,232	2.01915
$1s3p\ ^1P_1$	108,146	3.02190
$1s4p\ ^1P_1$	61,024	4.02286

This gives a value of the ionization potential of Be III of 153.012 volts.

P. GERALD KRUGER
F. S. COOPER

Department of Physics,
University of Illinois,
August 8, 1933.

[1] Ericson and Edlén, Zeits. f. Physik **56**, 656 (1930).
[2] Edlén, Nature **127**, 406 (1931).

The Isotope Shift of Tl

In a recent communication Schüler and Westmeyer[1] discuss a paper by the writer[2] in which it was attempted to explain the isotope shifts of the Hg, Tl, Pb arc and spark spectra as a result of a difference in the nuclear radii of the isotopes. Since this paper was written the material on Tl I has been improved on and it appears certain that the shifts are appreciable only for $6p_{1/2}$ and $6p_{3/2}$ and are nearly the same for these two terms. Schüler and Westmeyer find difficulty in accounting for this fact because according to the writer's paper one would expect the valence electron to produce the largest shift for the $7s$ term, a smaller shift for $6p_{1/2}$ and no shift for $6p_{3/2}$. This difficulty, however, is only apparent. It has been explained in the above paper that the $(6s)^2$ subgroup and perhaps other subgroups must be taken into account as well. Thus the shifts in Pb I, II could be brought into agreement only after the screening effect of the valence electrons on this subgroup was taken into account and it was pointed out[2] that the lack of relative shifts between $7s$Tl I and the higher terms could be explained by a similar

[1] H. Schüler and H. Westmeyer, Zeits. f. Physik **83**, 270 (1933).
[2] G. Breit, Phys. Rev. **42**, 348 (1932).

screening effect. The approximate equality of the shifts of the two $6p$ terms can be explained in the same way. The $6p_{1/2}$ term is the more penetrating but it also has the larger screening effect on the $6s$ subgroup. The observed shifts indicate that the main effect is that of screening the $6s$ subgroup by the valence electron which is such that $\psi^2(0)$ for the $6s$ electrons is largest when the valence electron approaches ionization and which produces a relatively tighter binding for the lighter isotope in the higher energy terms. This is equivalent to considering the high energy terms as undisplaced and to assigning a tighter binding to the heavier isotope in the low energy terms as is done by Jackson[3] and by Schüler and Keyston.[4]

The above explanation is only qualitative and presumably it can be made quantitative only by means of calculations with self-consistent fields, which have not as yet been made for Tl, as well as by considering perturbations by other configurations. Thus the spin splittings of the $6p$ terms of Tl I are brought into agreement with theory by Fermi and Segrè[5] by taking into account the perturbation by $6s6p7s$. The effect of this perturbation on the isotope shift is qualitatively the same as that of screening of the $6s$ subgroup by the $6p$ electron. Supposing that the linear combination which describes the wave function contains the $6s6p7s$ function with the coefficient 0.2 and disregarding the effect of cross product terms, the shift would be of the order of 0.04 times the shift of a single $6s$ electron or roughly 0.02 cm^{-1} which is sufficiently great to be considered. The screening effect can be also estimated as to order of magnitude either by means of numerical calculations of radial functions, with central fields adjusted to fit observed term values,[6] or by analogy with $\overline{1/r^3}$ of p electrons as determined from the gross multiplet structure. Changes in $\psi^2(0)$ and in $\overline{1/r^3}$ depend on very similar effects and it will be seen in a forthcoming paper by L. A. Wills and the writer that in different configurations of Pb, Tl, Bi the $\overline{1/r^3}$ of the same $6p$ electron varies by at least 5 percent. Since the isotope shift due to both $6s$ electrons is expected to be of the order of 1 cm^{-1} such a change in screening may be held responsible for the observed shifts in Tl I.

G. Breit

Department of Physics,
New York University,
University Heights, New York, N. Y.
August 15, 1933.

[3] D. A. Jackson, Zeits. f. Physik **75**, 223 (1932).

[4] H. A. Schüler and J. E. Keyston, Zeits. f. Physik **70**, 1 (1931); H. Kallmann and H. Schüler, Ergebnisse der Exakten Naturwissenschaften **XI**, 134–175 (1932), especially p. 167.

[5] E. Fermi and E. Segrè, Zeits. f. Physik **82**, 729 (1933).

[6] G. Breit, Phys. Rev. **38**, 463 (1931).

Isotopes of Chlorine

The magneto-optic method[1] has proved very useful in the study of isotopes of cations because of its extreme sensitivity which is increased even more for isotopes because of their mutual influence on each other.[2] Chlorine, however, is normally found as the anion of the compound and hence does not show its isotopes. Every compound that has been examined, however, produces its characteristic minimum or minima regardless of the type of bonding in the compound. The location of these minima on the wire path scale is a function of the equivalent weight of each constituent for both inorganic[1] and organic[3] compounds. Therefore, it seemed possible that the diatomic molecule of chlorine dissolved in water might give minima appropriate to chlorine chloride. A search of the appropriate region of the scale showed three minima as given in Table I. Hydrofluoric acid was added and three minima appropriate to chlorine fluoride were found. Upon the addition of phosphoric acid, three minima of chlorine phosphate were seen. Potassium bromide was added and minima of bromine chloride were obtained but no minima in the region of the scale for chlorine bromide were found.

The order of abundance of the chlorine isotopes was determined by the nicol rotation method[4] in each of the three compounds. All solutions used were saturated with chlorine. The angles read are the same within experimental error as were found with mixtures of calcium compounds. Assigning a mass of 35 to the most abundant and 37 to the second, the third which has the smallest scale reading would be heaviest, probably 39. The difference in nicol rotation between Cl^{35} and Cl^{39} is abnormally large for

[1] Allison and Murphy, J. Am. Chem. Soc. **52**, 3796 (1930).

[2] Allison, Ind. Eng. Chem., Anal. Ed. **4**, 9 (1932); Allison, Science **77**, 494 (1933).

[3] McGhee and Lawrenz, J. Am. Chem. Soc. **55**, 2614 (1933).

[4] Bishop, Dollins and Otto, J. Am. Chem. Soc. In press.

Table I. *Scale readings of minima and nicol rotation for chlorine isotopes.*

Probable atomic mass	Order of abundance	*Chlorine chloride* Scale reading	Nicol rotation	*Chlorine fluoride* Scale reading	Nicol rotation	*Chlorine phosphate* Scale reading	Nicol rotation
35	1	22.67	13° 40′	24.68	13° 50′	31.25	13° 37′
37	2	22.48	13° 27′	24.55	13° 37′	31.07	13° 27′
39	3	22.31	12° 22′	24.41	12° 28′	30.88	12° 33′

isotopes indicating a very small amount of Cl^{39}. This difference is of the same order as that between beryllium isotopes and slightly less than that between the hydrogen isotopes. But since the nicol rotation at which these minima can be seen differ by only a little more than a degree, the minima must either be due to isotopes which become visible in close succession because of mutual influence, or to a contamination that is consistently present at approximately the same concentration as the chlorine. The latter seems highly improbable. To test this point, perchloric acid was added to the solution being studied and all minima ascribed to chlorine compounds disappeared. Fresh solutions were placed in a cell and sulfur dioxide added; again the minima ascribed to chlorine compounds disappeared. It seems impossible that any contamination of such weight as to give minima in the scale region of these three chlorine compounds and that would undergo both oxidation and reduction could be present. Therefore, the minima observed must be due to three isotopes of chlorine.

EDNA R. BISHOP
FRED ALLISON

Department of Physics,
Alabama Polytechnic Institute,
July 29, 1933.

A Combination Relation in the Absorption Spectrum of Liquid Oxygen

We have investigated the absorption spectrum of liquid oxygen between the wave-length limits 27,500 and 3400A. The electronic $^1\Delta$ term predicted for the O_2 molecule in the infrared by Mulliken lies at 7930 cm^{-1}. Two vibrational terms follow at intervals of about 1480 cm^{-1}, which is approximately the magnitude of the vibrational terms of the well-known $^1\Sigma$ and normal $^3\Sigma$ states. All of the bands in the wave-length range given above can be assigned to five v' progressions, although intensity considerations require a slightly different arrangement than that of McLennan, Smith and Wilhelm.[1] The three, four, or five members of each of these progressions have approximately constant frequency separations.

If we designate the term values of the $^1\Delta$ and $^1\Sigma$ states by ν_1 and ν_2, respectively, the electronic terms of the five progressions are given within the limits of accuracy of measurement (<0.4 percent) by ν_1, ν_2, $2\nu_1$, $\nu_1+\nu_2$ and $2\nu_2$. Inasmuch as there is other evidence for the existence of loosely bound $[O_2]_2$ molecules in liquid oxygen, the most natural interpretation of this combination relationship is the following. The frequencies $2\nu_1$, $\nu_1+\nu_2$ and $2\nu_2$ are associated with an absorption act in $[O_2]_2$ molecules resulting in an excitation of both of the O_2 pairs. Either excitation of but one pair of the $[O_2]_2$ molecule or absorption by unassociated O_2 molecules in the liquid would account for the ν_1 and ν_2 frequencies.

A fuller account of this work will be submitted soon to the *Zeitschrift für Physik* for publication.

JOSEPH W. ELLIS
University of California at Los Angeles
HANS O. KNESER*
University of California, Berkeley

August 7, 1933.

[1] McLennan, Smith and Wilhelm, Trans. Roy. Soc. Can. **3**, 24, 1–22 (1930).

* Fellow of the Rockefeller Foundation.

Lead Isotopes by the Mangeto-Optic Method

Bishop, Lawrenz and Dollins,[1] and Piggot,[2] have reported sixteen isotopes of lead. Their evidence for these isotopes is based upon light minima obtained when working with water solutions of various lead salts in the Allison magneto-optic apparatus described[3] in the *Journal of the American Chemical Society*, and elsewhere during the past three years. These 16 minima are not shown by pure water. Recently we have located 16 light minima between 36 and 38 Allison units when using an aqueous solution of $PbCl_2$ in the magneto-optic apparatus. Although we had read the papers by Bishop, *et al.*, and by Piggot shortly after their publication last January, we did not remember any of their scale readings for the lead isotopes and purposely did not look them up until our observations had been completed. We only knew that they had found 16 readings (minima) between 36 and 38 Allison units. Our readings, each the average of 4 to 8 independent settings in good agreement, are as follows: 36.10, 36.18, 36.29, 36.40, 36.49, 36.60, 36.70, 36.79, 36.90, 37.09, 37.30, 37.43, 37.52, 37.65, 37.81, 37.90. Readings recorded by Bishop, *et al.*, are: 36.10, 36.19, 36.28, 36.40, 36.50, 36.59, 36.68, 36.78, 36.90, 37.08, 37.30, 37.40, 37.50, 37.68, 37.79, 37.90. A comparison of these two sets of readings shows 5 minima identical, 6 differing by ±0.01, 3 by ±0.02, and 2 with ±0.03 deviation.

We wish to acknowledge the kindness of Dr. Fred Allison for the use of his laboratory and magneto-optic apparatus.

JOHN H. YOE

Cobb Chemical Laboratory,
University of Virginia,
University, Virginia,
August 14, 1933.

[1] Bishop, Lawrenz and Dollins, Phys. Rev. **43**, 43 (1933).
[2] Piggot, Phys. Rev. **43**, 51 (1933).
[3] J. Am. Chem. Soc. **52**, 3796 (1930).

A Magnetostatic Oscillator for the Generation of 1 to 3 cm Waves

Continuous waves have been produced by tubes, of the split anode type,[1, 2] of very small dimensions. A simple grating spectrometer consisting of two parabolic brass mirrors, about one meter in diameter, and an echelette grating was used to measure the wave-length. The grating consisted of 18 elements of sheet aluminum each 7.4 cm wide and 70 cm long. The angle between the plane of the grating and the elements may be changed from zero to the largest angle at which the grating may be used without reducing the effective width of the beam of radiation. In use, the elements were automatically adjusted to give maximum energy at any position of the grating. The receiver was completely shielded except for an opening at the focus of the receiving mirror.

The reading on the grating circle is plotted against the galvanometer deflection in Fig. 1. Six orders are shown and also the direct image. The tube used for this curve had an anode diameter of 0.070 cm and operated with 910 volts on the anode and in a magnetic field of 9700 gauss. The wave-length as measured by the spectrometer is given in Table I.

TABLE I.

Order:	1	2	3	4	5	6
λ (cm):	1.233	1.229	1.224	1.227	1.230	1.232

A small hump appears on the long wave-length side of the peaks. As the magnetic field is decreased this hump disappears and then reappears on the opposite side. At a field of 7500 gauss the peaks become double. The tube must be operating at two slightly different frequencies, the weaker characteristic of the geometry of the tube and the other characteristic of the fields applied. Although both frequencies vary with the field, the former does not vary as rapidly as the latter. When in proper adjustment

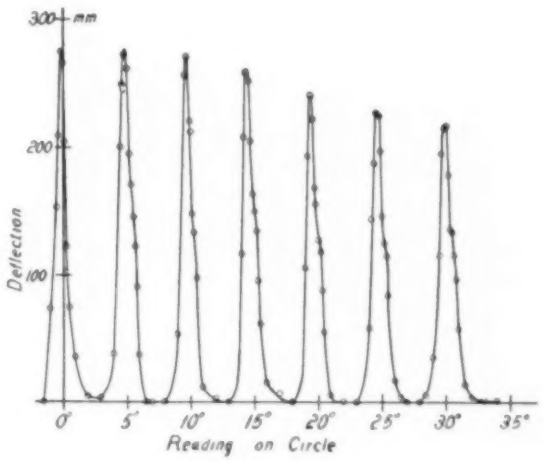

FIG. 1. Six orders at λ1.23 cm as given by the echelette grating.

the two merge into one and the oscillations are much stronger.

With a tube of somewhat smaller dimensions waves of 1.05 cm length were obtained. The oscillations were very stable in all cases except when the adjustments were such as to give peaks that were decidedly double.

C. E. CLEETON
N. H. WILLIAMS

Department of Physics,
University of Michigan,
August 21, 1933.

[1] H. Yagi, Proc. I. R. E. **16**, 715 (1928).
[2] K. Okabe, Proc. I. R. E. **18**, 1748 (1930).